Techno-economic and Sensitivity Analysis of Microalgae-based Biorefinery

A THESIS

SUBMITTED TO THE FACULTY OF THE GRADUATE SCHOOL

OF THE UNIVERSITY OF MINNESOTA

BY

SUDHANYA BANERJEE

IN PARTIAL FULFILLMENT OF THE REQUIREMENTS

FOR THE DEGREE OF

DOCTOR OF PHILOSOPHY

SHRI RAMASWAMY, Adviser

DECEMBER, 2019

Acknowledgements

I am deeply grateful to my advisor, Dr. Shri Ramaswamy, whose guidance, encouragement, and unwavering support has made this dissertation possible. His immense knowledge, enthusiasm and composure in the face of difficulties has always been a source of motivation for me and has helped me become a better researcher.

I would also like to express my sincere gratitude towards Dr. Anu Ramaswami, Dr. Bo Hu, and Dr. Jason Hill, for their advice, guidance, and support throughout my time at the University of Minnesota.

I would also like to thank members of Ramaswamy lab who were always ready to share helpful suggestions and ideas, and have made this experience an enjoyable one.

I would like to acknowledge my friends, Agnivo, Sourav, Saikat, Sai, Gourav, Sandeep, and others who were always there for me, and have given me some wonderful memories. I am indebted to my parents, Sunandita and Dhananjoy Banerjee, for their constant encouragement and unconditional support throughout the course of my study. Finally, I want to thank Rebecca Chowdhury who has always believed in me, has made me a better person and without whom none of this could have been accomplished.

I am also grateful to the Buckman Graduate Fellowship and Doctoral Dissertation Fellowship from the University of Minnesota for supporting this work.

Abstract

Microalgae possess tremendous potential to meet the ever-increasing demand for food, feed, energy and fuels in a sustainable manner. However, to be commercially viable, the entire supply chain of microalgae production including harvesting and conversion needs to be thoroughly investigated and better understood. To this end, a comprehensive theoretical approach was used in the present study involving first-principles based detailed modeling, simulation and analysis. Mathematical models were developed to quantify microalgae productivity potential and the associated feed stock costs in commercial scale biorefineries. In addition, detailed process modeling of the conversion of algae to multiple value-added products and the associated technical and economic feasibility and environmental assessment were conducted for the different geospatial locations. Using a first principles-based approach, algae growth and productivity were modeled considering an open raceway pond reactor and a flat panel photobioreactor to understand the implications of reactor geometry on microalgae growth and harvesting. Economic analysis was also conducted to determine algae production costs in the two different reactor systems, and across several geographic locations, thereby offering direct comparisons to facilitate selection of the most productive algae reactor system and the location. Then process models were developed for the conversion of microalgae to natural astaxanthin and eicosapentanoic acid (EPA) and docosahexanoic acid (DHA). These process models were used to assess the cost of production of the above products using different bioreactor systems and at various geospatial locations. In addition to value-added products, utilization of the residual algae biomass was also included in the overall techno-economic analysis to understand the economic competitiveness of microalgae-derived natural products and algal biorefinery in a fossil fuel-dominated market. The results obtained here suggest that microalgae productivity potential as well as production costs are heavily

influenced by geographic location. Predicted yields and corresponding costs for astaxanthin and EPA and DHA suggest that the production of these high-value products may be more successful in locations characterized by favorable environmental profiles that are more conducive to algae growth. While the costs of production in algal biorefineries were found to be higher than those of their petroleum-based counterparts, with further research and development the commercial production of microalgae-based natural products is highly promising for future industrial applications.

Contents

List of Tables

List of Figures

Chapter 1. Introduction

The global increase in population, accompanied by a mounting demand for energy, food, feed and fiber has prompted the need to identify sustainable natural resources, resulting in a world-wide transition from a fossil fuel-based economy to a rapidly growing bio-based economy. In 2010, bioproducts accounted for an estimated 8.45% of the economy in the United States, 6.4% in Canada, and 5% in the European Union (EU) [1–3]. Biomass-based products and energy harbor the potential not only to meet the growing demands for human consumption but also to curtail greenhouse gas (GHG) emissions in the atmosphere, thereby helping to mitigate climate change. As part of the efforts to combat climate change, the United States has set a carbon dioxide (CO_2) emissions reduction goal of 17% by 2020 in comparison to 2005 levels [4]. However, at the current rate, emissions will be reduced only by 9% relative to 2005, signaling the immediate need for more conscious active efforts and implementation of renewable energy projects across different spheres of the economy [4].

In a bioproducts-based economy, biomass resources are valorized and utilized for production of food, feed, energy and fuels in a sustainable manner [5]. However, scientific research efforts have generally concentrated on the sole production of biofuels from biorenewable resources [6,7]. Despite these efforts, biofuel production from biomass remains inadequate. For example, the EU produced only 1.6 million ton of biofuel per year which is merely about 0.1% of total fuel consumption [8]. The last several decades have seen microalgae researchers focus primarily on its utilization as a renewable fuel source. The Aquatic Species Program, an undertaking of the National Renewable Energy Laboratory in Colorado, USA was conceived with the goal of assessing the feasibility of microalgae of as an energy source [9]. However, the program was discontinued in 1996

after finding that fuel prices based on microalgae as a feedstock was more than twice the price of fossil fuels despite using aggressive assumptions [9]. High capital costs have made it challenging to construct microalgae-based renewable energy plants on industrial scales. While there has been significant progress in performing techno-economic and life-cycle assessment of microalgae-based products taking into consideration various assumptions [10,11,20–24,12–19], a lack of detailed comprehensive data regarding microalgae cultivation, harvesting, conversion and associated costs presents a major hurdle in the commercialization of microalgae products. To realize the full potential of biorenewable resources, it is essential to combine and optimize performances of different bio-based feedstocks, conversion pathways and production routes in large-scale biorefineries [5,25].

Biorefineries are essentially similar to fossil-fuel based refineries except for the utilization of biorenewable resources as the primary feedstock to produce a plethora of products [26]. In a biorefinery, one or more bio-based feedstocks may be subjected to different conversion and production routes to manufacture a wide variety of bio-based products, thus helping to meet human consumption demands as well as acting as suitable fossil fuel substitutes in the market. Generally, biorenewable-based resources can be differentiated into three product categories – 1) first generation feedstock, 2) second generation feedstock, and 3) third generation feedstock [5]. First generation biorenewable feedstocks refer mainly to different types of woods, grasses, starches and oil crops. Bio-feedstock in the second-generation category commonly includes agricultural residues, as well as waste such as sewage and manure. Third generation feedstock include microalgae and macroalgae which are emerging biobased feedstock that may be utilized to produce various value-added products [22,27,28].

Microalgae are a versatile form of feedstock composed primarily of lipids, proteins, carbohydrates, and pigments, components which may further yield a diverse range of bioproducts [29,30]. Advantages of using microalgae as feedstock include high lipid yields, rapid growth rates, utilization of less arable lands and poor quality water, and ease of integration of carbon dioxide from point sources (for example, coal fired power plants) [30–32]. Besides biofuel production, microalgae also have the potential to be utilized as source of food, feed, pharmaceuticals and nutraceuticals [33–36]. Different algae components and their potential conversions and applications in the market is given in Figure 1.1.

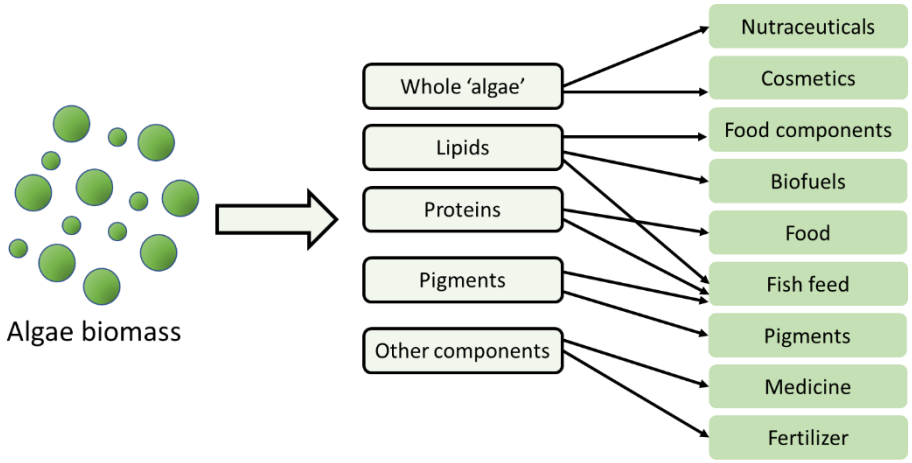

Figure 1. 1. Algae-based biorefinery and product applications [37]

To determine the feasibility of microalgae-based biorefineries, the entire supply chain of microalgae cultivation, harvesting, and conversion to bioproducts needs to be considered. In an algae-based biorefinery supply chain, the algal production step is often considered to be the most important element [11,27]; however, a more holistic approach is needed to realize the full potential of microalgae-based biorefineries. Although significant progress has been made in the last decade, the focus has mainly been on laboratory or pilot scale projects, where algae cultivation is performed under highly controlled conditions thereby generating significant uncertainties regarding commercial

scale algae cultivation. Much work still needs to be done to ultimately ascertain the overall implications of large-scale microalgae-biorefineries [30,38,39].

1.1 Estimating algae productivity on a commercial scale and under ambient conditions

Microalgae cultivation on a commercial scale is mainly conducted in two different types of reactor systems, namely open raceway ponds and photobioreactors [40]. Open raceway ponds are the simplest of the bioreactors used for algae growth. They are often uncomplicated in operation and relatively easy to construct. The light path in open raceway ponds is generally between 0.2 – 0.3 m for optimal microalgae growth [41]. On the other hand, closed bioreactors or photobioreactors are often relatively sophisticated in design and operationally more complex. The most common types of photobioreactors used for algae cultivation are horizontal tube, vertical tube, and flat panel photobioreactors [37]. Vertical and horizontal tube photobioreactors are thus named depending on the position and layout of microalgae growth tubes, which may have the tubes vertically or horizontally stacked. Flat panel photobioreactors are generally rectangular in shape and the path of light is generally between 0.02 – 0.10 m [42]. The design and shape of bioreactors heavily influence microalgae productivity, and optimal design of growth reactors is critical for maximizing algae productivity.

Studies investigating algae cultivation and productivity in outdoor systems are quite limited in literature. Even among these, there is a wide variability in reported microalgae productivity, possibly stemming from differences in location, reactor systems, and microalgae species. For example, Thomas *et al*. and Ansell *et al*. reported productivity of *Phaeodactylum tricornutum* in open raceway ponds to be 59.1 and 10.6 – 27.3 t ha^{-1} $year^{-1}$ in La Jolla, California and Poole, England respectively [43,44]. Similarly, there is a huge productivity difference for *Spirulina platensis* cultivation varying from 20 – 91 t ha^{-1}

year^{-1}, for locations in Florence, Italy and Australia [45,46]. Furthermore, choice of species plays a critical role in algae productivity as well. For example in Tuscon, Arizona, the reported productivity for *Nannocholoropsis salina* is 12.2 – 12.7 ton ha^{-1} year^{-1} [47], whereas productivity of Spirulina in western Australia, with similar weather and climate patterns as Arizona, is determined to be 91 ton ha^{-1} year^{-1} [46]. This wide variability in the reported productivity values together with the limited information focusing on algae cultivation in outdoor systems, leads to inherent uncertainties and creates difficulties in quantifying microalgae productivity in commercial systems and analyzing the implications of factors like bioreactor design, choice of species, and geospatial variation. Consequently, computational modeling and simulation are indispensable techniques for determining and comparing algal productivity and incorporating relevant factors like local weather, bioreactor design, design and operating conditions, as well as species characteristics.

A small number of microalgae productivity models based on different parameters and operating conditions have been described previously. For example, Quinn *et al*. developed an algae growth model and experimentally validated it by taking into account effects of light intensity, temperature of the culture medium and carbon assimilation in algae [48]. However, there is not much information regarding the derivation of light intensity in the reactor medium, thereby, rendering it less useful in designing other bioreactor systems. Bosma *et al*. developed a regression based model to determine algal volumetric productivity cultivated in bubble column reactors [49]. For algae cultivation in photobioreactors, researchers have developed models incorporating average light intensity and coupling it with algae growth model based in literature [50–52]. However, using average light intensities was ultimately found to underestimate algal growth in Spain [53,54]. The different models that currently exist only considered few of the parameters,

single algae species, and a single location. Furthermore, these models did not perform detailed process modeling of algal carbon or nutrients assimilation during growth phase. Thus, currently, there is a significant research gap which may be addressed by developing a framework/model capable of predicting algal growth in different reactor systems considering geospatial variabilities and other process parameters. The development and implementation of such a bottom-up model has been addressed in this work.

Development of algae productivity models for outdoor cultivation systems is important to elucidate the implications on resources at commercial scale. Land, water, CO_2, and nutrients are essential for microalgae production. Past studies have investigated the requirements of land, water, carbon dioxide and nutrients (mainly phosphorus and nitrogen) for microalgae processing pathways [10,55–63]. Evaluation of the different resource requirements helps to understand the feasibility of scaling up microalgae-based biorefineries and can also be compared with the resources that are currently available. Results from literature [31,58,63] demonstrate that water availability, CO_2 supply, nitrogen and phosphorus requirements could be limiting factors in scaling up of microalgae production systems to commercially relevant scales, whereas availability of land appears to be mostly non-restrictive. One of the biggest advantage of microalgae is the ability to grow in marginal lands or less arable lands unfit for agriculture. Several studies have investigated the potential limitations of land resources in scaling up microalgae production [57–59]. Researchers have also found that land availability for microalgae production is significantly higher than the present United States Department of Energy (DOE) goal of replacing 30% transportation fuels by 2030 [64]. Thus, availability of land resources does not pose a significant challenge to the scale-up of microalgae-based fuels and products. However, it is imperative to select suitable locations for microalgae cultivation to maximize resource use. Water requirements for microalgae growth are very much dependent on the

location, reactor geometry and configuration, and vary significantly among different geographic locations due to differences in rate of evaporation [65,66]. Microalgae growth in open raceway ponds requires a huge amount of water in comparison to tubular or flat plate photobioreactors as there is significant evaporative loss from open ponds [67,68]. Thus, water requirement may be an essential limiting factor in algae cultivation. As microalgae can grow in saline water or nutrient-rich waste water, the integration of non-fresh water to microalgae production systems is crucial for their success [31,69–73]**.** Carbon dioxide is another important raw material associated with microalgae growth [31,58,63]. Several challenges exist with respect to the capture and economical delivery of carbon dioxide and its efficient utilization by microalgae that are often neglected in technoeconomic analyses and life cycle assessment studies. Venteris *et al*. [60] combined various resources required for microalgae production to evaluate feasible locations by minimizing resource costs and showed that by utilizing 20% of carbon dioxide produced in the United States annually, it is possible to produce 21 billion gallons of fuel. A study by Quinn *et al*. [59] showed that it is possible to produce 1.9 billion gallons of fuel annually by limiting carbon dioxide transportation distances to 4.8 km.

An important aspect of microalgae production and commercialization is to understand the implications of carbon dioxide, nutrients, and water transport and delivery to microalgae production sites, since these are not explicitly quantified in the available literature. Studies often underestimate the cost of capture and delivery of carbon dioxide as they generally assume co-location of microalgae cultivation with industrial carbon dioxide point sources. However, co-location is a vital factor in the assessment of scale-up since suitable lands next to industrial facilities may not always be available. Similarly, there is a lack of literature regarding transport of water to microalgae biorefinery sites. These factors underpin the importance of building system models to quantify microalgae

production systems operated under ambient conditions. These models may then help make critical decisions regarding feasibility of commercial scale microalgae cultivation, harvest and conversion to bioproducts.

1.2 Microalgae conversion to bioproducts

Traditionally, microalgae have been utilized for production of bioenergy such as biofuels, heat and electricity. The scientific community has been pursuing the algae conversion to bioenergy for decades [22,35,74]. Despite some critical breakthroughs, most studies suggest that microalgae utilization solely for the purpose of bioenergy production is not economically viable [11,14,75,76]. Consequently, the production of other suitable products from microalgae is of utmost importance thereby also making them suitable for the generation of fossil fuel-based products in the market. It has been reported that algae when cultivated under specific conditions can accumulate significant amounts of secondary metabolites [77,78]. The secondary metabolites are extremely highly valued compounds having a broad spectrum of industrial applications, thereby providing the opportunity to develop a sustainable bio-products based economy [78,79].

Pigments are one of the most important components of algal secondary metabolites and are often considered to have the biggest potential for industrial and commercial applications [80–82]. There are mainly three different types of pigments obtained from microalgae – a) carotenoids, b) phycobilins and c) chlorophyll [81,83]. Among carotenoids, astaxanthin, the pigment responsible for the pink coloration of fish like salmon, trout, shrimp, and lobsters [84], is perhaps the most important. Astaxanthin, commonly found in saltwater, is only produced by some plants, microalgae, fungal and bacterial consortia. Animals are unable to synthesize astaxanthin naturally, and, it is often introduced into animals via microalgae through diet [85]. Thus, astaxanthin plays a huge role in the animal feed industry. It is also often considered a powerful natural antioxidant.

Antioxidants are critical for human metabolism and astaxanthin is credited with a crucial role in preventing free radical accumulation in the human body [86]. Additionally, astaxanthin helps to protect skin from harmful UV radiation and is important for applications such as anti-tumor treatment and age-related disorders [87].

The commercial potential of astaxanthin is significant. Depending on the purity of the product, on an average, the market price for astaxanthin ranges from 2500 – 7000 $ kg^{-1} [28,84]. Under special circumstances, the market price may be as high as 100,000 $ kg^{-1} [86]. The global demand and corresponding market size for astaxanthin was estimated at 280 metric tons and $ 447 million, respectively [84,86,88–90]. 95% of the astaxanthin demand is met by synthetic astaxanthin derived from fossil fuel-based products having a production cost of 1000 $ kg^{-1} [86,91]. Due to the inherent risk of toxicity, sustainability and safety posed by fossil fuel-derived synthetic astaxanthin, there is a growing demand for natural astaxanthin [91–93]. Although market potential for natural astaxanthin is significantly lower and only about 1% of the total astaxanthin demand due to the higher production costs, it is expected that with further research and optimization of natural astaxanthin production pathways, natural astaxanthin will become economically more competitive than their synthetic counterparts [28,79]. To date, there is very little information regarding commercial scale production of microalgae-based natural astaxanthin and studies are mostly based on laboratory or pilot scale facilities [91]. This existing knowledge gap in literature with regards to feasibility of commercial microalgae-based natural astaxanthin production is addressed in the present study.

Besides carotenoids, microalgae are a rich source for other value-added products in the food and feed industry [79,94,95]. Specifically, there has been significant interest in microalgae-based natural synthesis of fish oil having a high content of eicosapentanoic acid (EPA) and docosahexanoic acid (DHA). The supply of synthetic fish oils has

plateaued due to the limited availability of pelagic fisheries, thereby leading to an increased demand within the aquaculture industry. This is further compounded by an increased popularity of omega-3 fatty acids, leading to a surge in demand for natural fish oils [96]. Currently, the global fish oil market is estimated to be at 1 million tons annually of which about 70% is used as aquaculture feed [97]. The anchoveta fisheries in Chile and Peru produce more than 80% of the global fish oil demand [97]. However, due to extreme variability in weather and the environment, supply of fish oil from South America has become unstable thereby leading to significant price volatilities. This uncertainly in the supply of fish oil, coupled with its increasing popularity, has led to a significant increase in price to around 2400 $ ton^{-1} in recent times, an increase of about 3 – 8 times the price in 2005 [98]. These factors have triggered a need to find suitable alternative sources to fish oil. Microalgae is one such viable alternative that can be used to produce EPA- and DHA-rich fish oil. While previous studies have illustrated the usefulness of microalgae for production of valuable products such as feed [99–101], there is deficit of information on commercial scale microalgae-based EPA and DHA production, and its economic implications. Hence, the present work is essential to bridge this gap in current knowledge.

1.3 Economics of microalgae-based biorefinery

In order to develop sustainable, microalgae-based products, they must be economically competitive with their fossil fuel counterparts. It is unlikely that these bioproducts will be able to penetrate the market if the prices are substantially higher than other alternatives [31,102]. Hence, detailed techno-economic analysis (TEA) is an important assessment tool to evaluate the economic feasibility of microalgae based biorefineries. It not only helps identify the bottlenecks involved, but also reveals areas of research still requiring attention to realize the full potential of microalgae-based technologies. Generally, TEA studies combine process modeling with financial

assessments and estimates to evaluate the selling prices of products. Thus, a sound understanding of the technical and engineering details of the processes is essential in order to develop capital and operation cost estimates and seamlessly integrate them into microalgal technology assessment pathways.

Prior literature has primarily focused on microalgae-based biofuels with very few studies concentrating on development of high-value products from microalgae [79,95]. Correspondingly, there are a number of scientific publications that address TEA analyses of microalgae-based biofuels based on various assumptions regarding microalgae production, harvest and conversion pathways [10,11,64,103–111,12,112,113,13–19]. The results show a large variability in the cost of products, ranging between 1.65 \$ gal^{-1} and 33.16 \$ gal^{-1} as the lowest and highest production cost of biofuels respectively [105,107]. Such large variabilities in fuel costs may be attributed to number of sources like differences in production and conversion pathways, differences in boundaries, variances in financial assumptions as well as modeling of current or future systems, with little technical knowledge and experience. Cost variability is significantly influenced by the type and geometry of the reactors used for microalgae production as well [76]. Additionally, financial assumptions in the process economics, including parameters like lifetime of facility, discount rate, depreciation method and other metrics, can influence TEA results. From a process engineering standpoint, microalgae productivity is a factor of critical importance as it represents a primary input in the economic analysis. It is expected that economic analysis of microalgae-based systems will be positively affected by increased productivity. With ongoing research and technological breakthroughs, costs will likely decrease, and at the present, it may be premature to draw definite conclusions about the economic sustainability of microalgal bioproducts. Thus, TEA remains an efficient systems-engineering tool to assess economic feasibility of microalgae biorefineries.

In general, TEA studies have focused mainly on the production of bioenergy from microalgae (biodiesel, biogas, bioethanol and others), and not on specialty chemicals like food supplements, aquaculture, animal feed and others. Furthermore, researchers have mainly focused on determining breakeven biofuel costs based on the fixed costs for the other parameters and not considered the dynamic changes in energy and material prices and their impacts on microalgae product costs. Also, the effects of geographical variability and different reactor systems on the economics of the process are uncertain. Thus, the economic analysis of microalgae-based high value products on commercial scales and their feasibility in comparison to fossil-fuel based products is a major research gap yet to be fully understood. The development of TEA models to determine economic feasibility of microalgae-based high value products biorefinery is an important part of the thesis.

1.4 Knowledge gaps

Several knowledge gaps in the evaluation of microalgae as a bio-feedstock for production of value-added products and chemicals are currently extant. Here are some of the focus areas that are investigated in the thesis to assess the feasibility of microalgae as a potential biorefinery feedstock:

a) The design, development and analysis of an integrated biological principles and engineering process principles-based modeling to assess microalgae productivity incorporating geospatial variabilities
b) The effects of different reactor systems on algae growth and productivity
c) Process systems model of microalgae biorefineries with emphasis on portfolio of products which includes bioenergy and specialty chemicals, rather than a single product.
d) Detailed economic analysis encompassing the entire supply chain of microalgae cultivation, harvest and conversion to bioproducts taking into

account different growth systems, geospatial variabilities in climate factors, as well as logistics of land, water, CO_2 and nutrients.

e) Sensitivities associated with geographic variabilities as well as microalgae-based technologies. The changes in different parameters need to be incorporated to assess their influence on the product costs. This is important to assess the effect of different parameters in the commercialization of microalgae based biorefinery.

These research gaps call for more robust analyses to provide scientific community, industries, and policy makers a holistic assessment to help make informed decisions regarding the implementation of microalgae based biorefineries.

1.5 Research Objectives

The primary overarching objective of the present study was to create a comprehensive platform to evaluate feasibility of utilizing microalgae as a renewable biorefinery feedstock. Additionally, the effects of geospatial location on the success of such a biorefinery from a systems analysis perspective have been elucidated. These have been described below:

Objective #1: Evaluate microalgae productivity potential

Hypothesis: Microalgae productivity potential varies among different geospatial locations due to variability in local climate conditions.

Rationale: Biomass growth is heavily influenced by local weather conditions like solar irradiance, air temperature, relative humidity and other factors. So, it is anticipated that microalgae growth and productivity will vary across latitudes based on the local climate factors. Biological growth parameters are integrated with engineering process models to determine microalgae productivity potential. Furthermore, sensitivity analysis is also

conducted, based on known variabilities in geospatial and microalgae growth kinetic parameters, for making quantitative decisions about microalgae productivity potential.

Approach: To test this hypothesis, a comprehensive microalgae productivity model for an open raceway pond bioreactor system from a first principle approach was developed. Local climate factors, like solar irradiance, temperature, relative humidity and wind velocity, were integrated with a biological growth model to evaluate the variability of microalgae productivity based on geospatial locations. Such a fundamental integration of process engineering and biological process modeling principles helped determine potential microalgae productivity for a location more accurately. Further, a TEA model was developed to assess microalgae production costs for the commercial scale system. Also, sensitivity analysis was performed to assess influence of key parameters on microalgae production costs. The primary research questions that were addressed are:

a) What is algal productivity potential for different locations?

b) What is the production cost of microalgae for different locations?

c) Which parameters influence the production costs the most and the least?

While performing process systems-based analysis of microalgae conversion to bioproducts, traditionally researchers have mostly assumed microalgae productivity potential and the corresponding algae cost as the starting point of their analyses [11,103,107,114], thereby generating significant uncertainties. Thus, the development of the proposed growth model and corresponding economic analysis, under varying climatic and environmental conditions, can help to determine microalgae productivity and cost more accurately. Also, the geographical variations in productivity and production costs will help inform scientists, engineers, policy makers about suitable location for microalgae cultivation.

Objective #2: Assess implications of different bioreactor on microalgae growth and productivity

Hypothesis: Microalgae productivity potential is heavily impacted by choice of reactor system for cultivation.

Rationale: Biomass growth is heavily influenced by reactor type and geometry besides local weather conditions like solar irradiance, air temperature, relative humidity and other factors. Based on the difference in bioreactor design, amount of incident sunlight intercepted by biomass, aeration, corresponding temperature profile of the culture medium are expected to be different. Hence, it is anticipated that microalgae growth and productivity will be different based on the choice of cultivation system as well as across different locations. Similar to Aim #1, a microalgae productivity model is developed to determine productivity potential. This mathematical approach of determining algae growth in outdoor ambient conditions, helped to determine and compare algae productivity across different bioreactor systems and locations and throughout the year.

Approach: To test this hypothesis, a comprehensive microalgae productivity model for a flat panel photobioreactor system from a first principle approach was constructed following the framework outlined in Aim #1. Geospatial variabilities across locations were incorporated in the model to determine potential algal productivity. This fundamental approach not only helped to determine productivity potential in a different reactor system but also helped to compare the performances when the same algal species is cultivated at the same locations. The technical analysis was augmented by an economic analysis model to determine algae production costs. Furthermore, a sensitivity analysis was conducted to portray the implications of different parameters on microalgae cultivation costs. The research questions that were answered are:

a) What is microalgae productivity potential based on geospatial locations for a different reactor system?
b) What is microalgae production cost for the new system?
c) How does microalgae productivity and costs compare for the two different reactor system and locations?

Objective #3: Evaluate feasibility of microalgae-based biorefinery

Hypothesis: Geospatial effects have an impact on the technical and economic feasibility of microalgae-based product portfolio.

Rationale: Microalgae productivity potential is variable across locations and reactor systems resulting in a wide variability in production costs. As microalgae production cost (feedstock costs) heavily influences the product costs after downstream processing [11], it is anticipated that the economics of product portfolio will be different for different reactor systems and geographic locations.

Approach: To achieve this objective, a comprehensive engineering process model of microalgae based biorefinery was developed. Results from Objectives #1 and #2 served as inputs to the microalgae conversion process model for the synthesis of high-value products from microalgae. This detailed approach encompassing entire supply chain of algae growth, harvest and conversion assisted in evaluating the feasibility of the hypothetical microalgae biorefinery for a location. The models were further extended to different locations to understand implications of spatial variabilities on the economic feasibility of microalgae based biorefineries. Sensitivity analysis was also used to assess the impacts of different parameters on the type, amount and product costs from the hypothetical biorefinery for the different locations. The main research questions that are answered are:

a) What is the economic performance of microalgae based biorefinery for a location?

b) How does the economic performance vary across different geospatial locations?

c) How does microalgae-based bioproducts compete economically with fossil fuel-based counterparts?

On the process modeling of microalgae conversion front, researchers have mainly focused on the production of biofuels from microalgae [11,31,112,114,115]. Currently, the data suggest that microalgae-based fuel price is substantially higher than that of conventional fossil fuels, making them economically infeasible. Instead, specialty products like animal feed, aquaculture feed, nutraceuticals, food supplements and others may be produced from microalgae in a more competitive manner [33,36,116]. The present work investigates this crucial gap in literature and can help determine whether a product portfolio, consisting of a combination of specialty chemicals and bioenergy, has the potential of making microalgae biorefineries economically feasible.

1.6 Thesis Outline

The thesis consists of six chapters. It starts with the Introduction (Chapter 1) which outlines the literature review and research gaps that are tackled in the thesis. In Chapter 2, a detailed microalgae growth model is developed from a first principle approach to quantify algae productivity potential in commercial scale open raceway ponds. This work also incorporates geospatial variabilities to assess productivity variations across the different locations. Furthermore, to understand the economic implications of commercial scale algae cultivation in ambient conditions, a detailed economic analysis model is developed to determine algae production costs for the locations. Chapter 3 essentially deals with algae production in commercial scale flat panel photobioreactors and quantifies the differences in productivity across different reactor system and reactor geometry. In this work, the same mathematical framework is adopted as developed in Chapter 2 and corresponding growth models are developed for algae cultivation in commercial scale flat

panel photobioreactor systems. Also, an economic analysis model is developed in conjunction with the mathematical model to determine algae production costs in photobioreactors. The main focus of Chapter 4 and Chapter 5 is on the downstream conversion of algae to value-added products. In Chapter 4, process models are developed to quantify astaxanthin production from commercial scale algae production, harvesting and conversion. This is integrated with a detailed techno-economic analysis to quantify astaxanthin production costs. Different scenario analysis regarding utilization of the residual biomass is performed to understand the implications and economic competitiveness of natural astaxanthin in comparison to synthetic astaxanthin. Similar to Chapter 4, Chapter 5 highlights the implications of another algae derived high-value product (EPA and DHA) in the market. Technical process models of EPA and DHA production from microalgae are developed taking into account geospatial variabilities as well as on the basis of algae cultivation reactor. This is followed by the development of an economic analysis to determine natural EPA and DHA production costs and assess their competitiveness with fossil fuel derived synthetic products. A set of strategies are also developed and implemented to understand economic implications of commercial scale EPA and DHA production from microalgae. The different chapters finally culminate to Chapter 6 which focuses on the achievements and insights from the present study. Additionally, new directions in which the current work may be extended and moved forward are also discussed.

Chapter 2. Dynamic Process Model and Economic Analysis of Microalgae Cultivation in Open Raceway Ponds

2.1 Introduction

A rapidly growing population and rising demand for energy, food and feed throughout the world has led to an immediate need for suitable sustainable resources. Energy derived from biomass is poised to make a substantial contribution to global energy supply given its potential to generate significant amounts of renewable fuels, food, fiber and feed in addition to helping reduce greenhouse gas emission into the atmosphere [3]. While the United States has set a goal of reducing CO_2 emissions by 17% by 2020, current trends show a decrease closer to 5% relative to 2005, signifying the need for an intensified expansion of renewable energy production and use [4].

Microalgae are promising source of bioenergy due to several reasons. They are capable of growing on non-arable lands, absorbing CO_2, utilizing low quality wastewater, as well as accumulating large amounts of lipids for biofuel production [30]. Additionally, microalgae may be utilized as source of food, feed, pharmaceuticals, and nutraceuticals [33–35].

An important aspect of the analysis of the current and future potential of microalgae as a bioenergy feedstock is the assessment of productivity potential based on geographical location. Productivity is heavily dependent on geospatial location and local climatic factors such as solar insolation, ambient air temperature, local wind velocity and relative humidity. Of the various systems that can be used for the cultivation of microalgae, open raceway ponds are the most basic and cost effective for microalgae production [76,105]. In comparison with other systems such as photobioreactors, the lower

productivity in open raceway ponds is often compensated for by reduced capital and operating costs, and higher economic value of the products [18,30,76]. Open raceways ponds as a system for microalgae growth and subsequent conversion to biofuels has been quite well studied [57,72,75,117–123]. Although in some cases, an algae biomass production of greater than 11000 t km^{-2} $year^{-1}$ was assumed [119,124–126], the upper production limit seems closer to 9100 t km^{-2} $year^{-1}$ [127]. A review of existing literature suggests a wide variability in microalgae productivity depending on choice of production system, location, algae species and local climatic factors. For example, open raceway pond productivity of *P. tricornitum* was found to be 6370 t km^{-2} $year^{-1}$ in Algeria and 4150 t km^{-2} $year^{-1}$ in Netherlands, respectively [38]. Such differences in productivity may be attributed to differences in solar irradiance and local climate. Similarly, changes in productivity for the same location and cultivation system have been observed with the use of different species of microalgae [41,42]. Researchers have obtained annual productivities as dissimilar as 6.1 kg $panel^{-1}$ $year^{-1}$ and 10.6 kg $panel^{-1}$ $year^{-1}$ for the species *T.pseudonana* and *P.tricornutum* respectively in flat panel photobioreactors in France, arising primarily from differences in their biological characteristics [42]. Such diversity in microalgae productivity can potentially impact systems analysis of commercial algae-based systems significantly. Thus, there is a need for a comprehensive understanding of the fundamentals of the reaction kinetics and biological process of algal growth, and the various factors that influence growth and productivity on a year-round basis.

The current analysis was aimed at assessing the productivity potential of microalgae for various locations and conducting economic analysis to evaluate microalgae production costs for the locations considered. To achieve these goals, first, a heat and mass transfer model for open raceway pond bioreactor system was developed to assess

overall yearly temperature of growth ponds based on several climatic parameters. Next, a bioreaction kinetics-based growth model was constructed to determine microalgae productivities in open raceway ponds while considering geospatial variability. The mass and energy balances of the entire process was then used to determine the capital and operating expenditure for algae cultivation. The sites considered for the hypothetical microalgae plants were Minnesota (Minneapolis), California (San Diego), New Mexico (Albuquerque) and Arizona (Phoenix). Previous studies have mostly carried out their analyses based on assumed values for microalgae productivity potential and the corresponding price of microalgae [11,103,107,114] leading to wide variabilities and considerable uncertainties in technoeconomic evaluation. Not only does the present study allows for the determination of microalgae costs more accurately, the results can help influence the choice of locations for construction of commercial scale microalgae production plants in the United States. The mathematical model developed here is intended to serve entrepreneurs, scientists, engineers and policy makers as a guideline for the effective assessment of the feasibility of microalgae as feedstock for bioproducts.

2.2 Methods

In the present study, open raceway ponds, an extensively used microalgae cultivation system along with photobioreactors, were considered for modeling microalgae production. In such a system, microalgae growth occurs under diurnal light and temperature conditions. The growth phase involves the utilization of large amounts of carbon dioxide (CO_2) and nitrogen and phosphorus-based nutrients accompanied by the release of oxygen. While atmospheric CO_2 may be sufficient for growth, additional supplied CO_2 greatly boosts productivity and promotes suitability for biofuel/bioproducts production. Therefore, raceway ponds are usually equipped with submerged aerators to supply additional CO_2 and paddlewheels to facilitate proper mixing of the microalgal cultures

[128]. Paddlewheels are mechanical rotating devices operated continually to ensure appropriate stirring and prevention of sedimentation as well as alternating microalgae cells in dark and light regimes to optimize growth. Although open raceway ponds offer low operating costs and capital investments, there are a few drawbacks to the system. The volumetric productivity is a few folds lower that of a closed system (0.1 kg m^{-3} in comparison to 1.5 kg m^{-3}) [129], possibly due to the huge loss of water due to evaporation from the open surface. Moreover, the risk of contamination limits the productivity potential as well as species sustainability [41,130].

In this study, the algal species, *Nannochloropsis sp.* was selected for the purposes of developing a model-based framework relying on variables such as geographical location and system design. *Nannochloropsis sp.* is considered a promising feedstock for biofuel production due to their high productivity potential and lipids content, high temperature tolerance and ability to utilize saline and brackish water for growth [48,131]. Each raceway pond was assumed to have a surface area of be 0.81 hectare or 8100 m^2 with a depth of 0.3 m [128]. The proposed theoretical framework of the model is shown in Figure 2.1.

Microalgae productivity for a specific geographic location was determined by first developing a combined heat and mass model for microalgal growth in open raceway ponds by integrating several factors such as local climate, reactor geometry and species-specific characteristics and then followed by integrating biological growth kinetics. Next, economic analysis was conducted for determining the production cost of microalgal paste. This revealed the differences in microalgal cultivation cost for the different geospatial locations. An assumption was made that the open raceway ponds were provided with algae harvesting and dewatering units that led to the production of microalgal pastes with

a solids concentration of 20% (ash free dry weight [AFDW] bases). The entire supply chain is depicted in Figure 2.2.

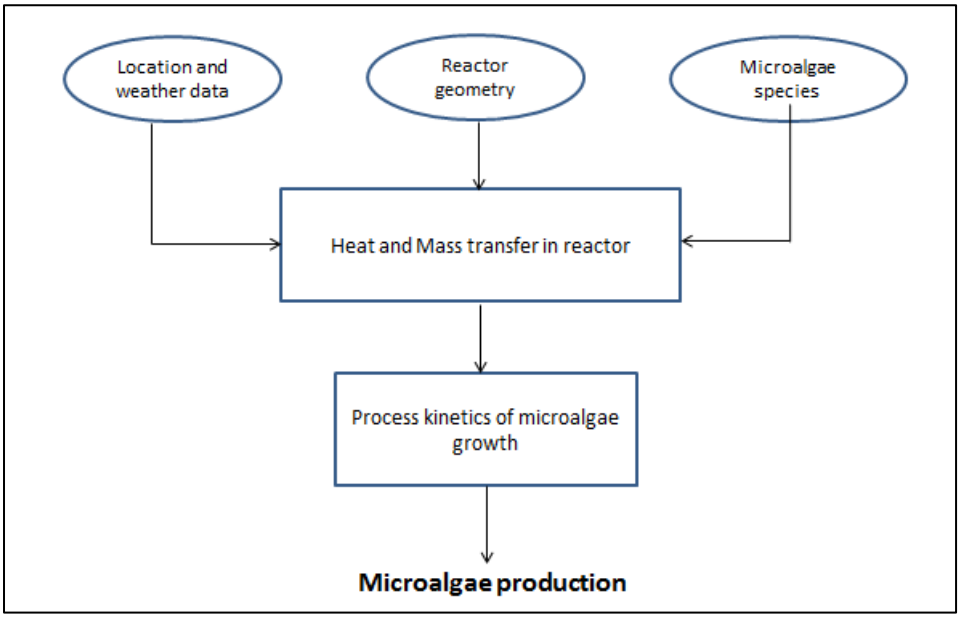

Figure 2. 1. Model framework to assess microalgal productivity in open raceway ponds

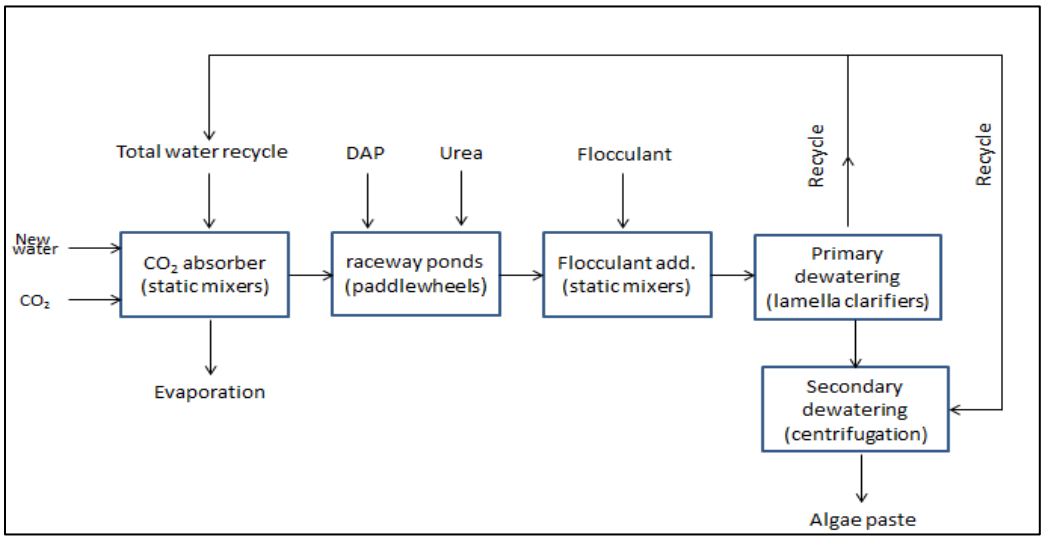

Figure 2. 2. Model framework for economic analysis of microalgae production supply chain [128]

2.3 Model

The following factors were considered for the development of the model:

Model input

- Local weather data- Weather information for a particular geographical location including solar irradiation, air temperature, wind velocity, relative humidity was obtained from the United States National Climatic Data Center [132]. This data was used to the quantify the water temperature of open raceway ponds.
- Model specific parameters- A list of model parameters is presented in Table 2.1. This includes CO_2 and nutrients like phosphorous and nitrogen in the form of diammonium phosphate (DAP) and urea, which were assumed to be provided in surplus to ensure that growth was not limited under any circumstances.

Model Output

The mass production of microalgae was considered as the output of the microalgal growth model. A precise estimate of microalgal productivity and raw material consumption is deemed essential to be able to assess the lifecycle costs of the microalgal growth system.

Table 2. 1 Parameters used in the microalgal growth model [41,48,133–136]

Symbol	Definition	Unit	Value
ρ_{water}	density of water	kg m^{-3}	998
$C_{p_{water}}$	heat capacity of water	J kg^{-1} K^{-1}	$4.2x10^3$
L_{water}	latent heat of water	J kg^{-1}	$2.26x10^6$
ε_{water}	emissivity of water	--	0.97
M_{water}	molecular weight of water	Kg mol^{-1}	0.018

k_{soil}	thermal conductivity of soil	W m^{-1} K^{-1}	1.7
$C_{p_{soil}}$	specific heat capacity of soil	J kg^{-1} K^{-1}	1.25 x10^3
ρ_{soil}	soil density	kg m^{-3}	1.9 x10^3
$T_{s_{z=z_{ref}}}$	soil temperature at reference height	K	281.15
ε_{air}	air emissivity	--	0.8
ν_{air}	air kinematic viscosity	m^2 s^{-1}	1.5 x10^{-5}
k_{air}	air thermal conductivity	W m^{-1} K^{-1}	2.6 x10^{-2}
Pr_{air}	air Prandtl number	--	0.7
ρ_{air}	density of air	kg m^{-3}	1.2
α_{air}	thermal diffusivity of air	m^2 s^{-1}	2.2 x10^{-5}
$D_{water,air}$	mass diffusion coefficient of water vapor in air	m^2 s^{-1}	2.4 x10^{-5}
V	volume of pond	m^3	2430
S	surface area of pond	m^2	8100
$\varepsilon_{photosynthesis}$	absorption fraction by algae	%	2.5
L	characteristic length of pond	m	10
σ	Stephen-Boltzmann constant	W m^{-2} K^{-4}	5.67 x10^{-8}
$R_{universkal}$	Universal Gas Constant	J K^{-1} mol^{-1}	8.314
$\varepsilon_{gas\ holdup}$	gas holdup	---	0.2
$G_{molar\ flow}$	gas molar flow	mol day^{-1}	48.3
p	partial pressure	atm	0.00032
T	temperature of CO_2	K	293.15
H	Henry's constant	--	0.0316
K_{O2}	O_2 mass transfer coefficient	m s^{-1}	6.67x10^{-5}
D_{CO2}	CO_2 diffusivity in water	m^2 s^{-1}	1.97x10^{-9}
D_{O2}	O_2 diffusivity in water	m^2 s^{-1}	2.10x10^{-9}
z	pond depth	m	0.3

Y_{algae}	algae yield	kg-algae (mol carbon consumed)$^{-1}$	0.02016
$MW_{bicarbonate\ ion}$	molecular weight	kg-bicarbonate (mol)$^{-1}$	0.061
$N_{max\ specific\ uptake\ rate}$	N_2 max. specific uptake rate	kg kg^{-1} day^{-1}	0.06
$N_{biomass,minimum}$	minimum N_2 in cell	kg kg^{-1}	0.010
$N_{medium,initial}$	initial N_2 in medium	kg m^{-3}	0.015
$HSC_{nitrogen\ uptake}$	half saturation constant for N2 uptake	kg m^{-3}	0.005
RR_N	N_2 respiration rate	per day	0
$P_{max\ specific\ uptake\ rate}$	P max. specific uptake rate	kg kg^{-1} day^{-1}	0.05
$P_{biomass,minimum}$	minimum P in cell	kg kg^{-1}	0.004
$P_{medium,initial}$	initial P in medium	kg m^{-3}	0.015
$HSC_{phosphorus\ uptake}$	half saturation constant for P uptake	kg m^{-3}	.025
RR_P	P respiration rate	day^{-1}	0
$HSC_{carbon\ uptake}$	half saturation constant for CO_2 uptake	mol m^{-3}	9x10^{-4}
K_S	inhibition constant of CO_2 uptake	mol m^{-3}	180
HSC_{light}	half saturation constant for light	W m^2	43.5
K_I	inhibition intensity of light	W m^2	608.7
μ_{max}	maximum specific growth rate	day^{-1}	1.15
k_{decay}	biomass decay rate	day^{-1}	0.06
$K_{absorption}$	absorption coefficient	m^2 kg^{-1}	75
$C_{biomass}$	constant biomass concentration	kg m^{-3}	0.3
μ_{max}	maximum specific growth rate	per day	1.15
φ	land fraction used for water	--	0.8
A_{ha}	hectare	m^2	10000

2.3.1 Heat Transfer Model

An accurate estimation of pond water temperature is of utmost importance in order to calculate the productivity of *Nannochloropsis sp.* correctly. This is due to the influence of temperature on photosynthesis as the efficiency of the Rubisco enzyme responsible for CO_2 capture tends to decrease outside an optimal temperature range [137]. An appropriate temperature model also ensures the correct addition and removal of energy from open raceway ponds to maintain the optimal temperature range during the day for maximizing productivity. Moreover, pond temperature influences evaporation thereby directly affecting the water footprint of the process [138]. These factors together dictate the need for a robust thermal balance model for microalgae growth ponds.

While developing the energy balance model, it was assumed that the thermodynamic properties were measured at the appropriate pond water temperature and pressure. Assuming thorough mixing and a relatively low pond depth (0.3m), a lumped parameter model was employed to predict uniform water temperature. Since light can penetrate only two-thirds of the microalgal culture depths [139], air and solar insolation were assumed to be fully absorbed before reaching the base of the raceways. On average, microalgae are known to utilize 2-5% of solar energy through photosynthesis [140]. Accordingly, microalgae conversion efficiency was taken to be 2.5% [133]. The input parameters for the heat transfer model considered were solar irradiation, air temperature, relative humidity, wind velocity and the temperature of the inflowing make-up water. Rainfall associated temperature variations and heat flux accompanying incoming CO_2 required for microalgae growth were assumed to be negligible. A schematic representation of the heat transfer model is depicted in Figure 2.3.

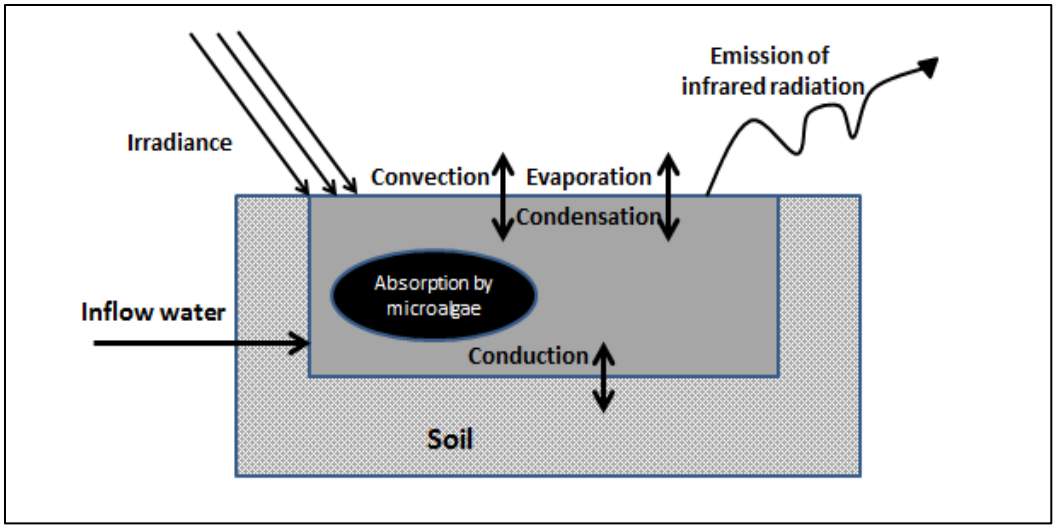

Figure 2. 3. Thermal energy balance in open raceway ponds [41]

Model description

The dynamic water temperature was calculated by the energy balance of raceway ponds as illustrated previously [133] by using dimensionless values for heat transfer and evaporation. The governing equation of the heat transfer model for microalgal ponds is:

$$\boldsymbol{\rho_{water}} \forall \boldsymbol{C_{p_{water}}} \frac{\boldsymbol{dT_{water}}}{\boldsymbol{dt}} = \boldsymbol{Q_{radiation,water}} + \boldsymbol{Q_{radiation,sun}} + \boldsymbol{Q_{radiation,air}} + \boldsymbol{Q_{evaporation}} + \boldsymbol{Q_{convection}} + \boldsymbol{Q_{conduction}} + \boldsymbol{Q_{incoming\ water}} \quad (1)$$

where T_{water} is open raceway temperature (in K), ρ_{water} is density of water (in kg m^{-3}), $C_{p_{water}}$ is specific heat capacity of water (in J kg^{-1} K^{-1}), V is volume of the pond (in m^3), $Q_{radiation,water}$ is radiation from the surface of water (in W), $Q_{radiation,sun}$ is total solar radiation (in W), $Q_{radiation,air}$ is radiation from air to open raceways (in W), $Q_{evaporation}$ is evaporation (in W), $Q_{convection}$ is convective heat transfer from pond water surface (in W), $Q_{conduction}$ is conductive heat transfer at the pond bottom with ground (in W), and $Q_{incoming\ water}$ is energy associated with the water inflow (in W). Details of the heat transfer model are given in Appendix section of the thesis.

2.3.2 Mass Transfer Model

The primary objective of the mass transfer model was to predict microalgae growth patterns in open raceway ponds by utilizing engineering principles and biological growth characteristics. In order to predict microalgal productivity, data available from literature was used to develop a bulk growth model [41,48,130,134–136,141,142]. The factors that influence microalgal growth rate include light intensity, photosynthetic rates, respiration rate, temperature of the culture medium, and availability and uptake of nutrients and CO_2 [52,143,144]. Light intensity and temperature of water obtained from the thermal energy model were used as input and microalgal productivity was the output from the model.

Modeling of microalgae growth

The following equation was used to denote specific microalgal growth rate (μ), a function of temperature, light intensity, nitrogen and phosphorous uptake, and bio-uptake of carbon, as a Michaelis-Menten type kinetic relationship.

$$\mu = \mu_{max} * \left(\frac{C_{CO2,dissolved}}{HSC_{carbon\ uptake} + C_{CO2,dissolved} + \frac{C_{CO2,dissolved}^2}{K_S}} \right) * \left(\frac{N_{medium}}{N_{medium} + HSC_{nitrogen\ uptake}} \right) * \left(\frac{P_{medium}}{P_{medium} + HSC_{phosphorus\ uptake}} \right) * \left(\frac{I_{average}}{HSC_{light} + I_{average} + \frac{I_{average}^2}{K_I}} \right) * 1.066^{(T_{water} - 293.15)}$$

Biomass Growth Model

Areal microalgal productivity (t ha^{-1} $year^{-1}$, 1 ha= 0.01 km^2) was expressed by the following equation:

$$Productivity\ (P_{areal}) = \varphi * A_{ha} * \int_0^{0.3} (\mu - k_{decay}) * C_{biomass} dz$$

To calculate total microalgal productivity (t ha^{-1} $year^{-1}$), areal productivity was integrated over the entire year, and was determined by the equation shown below:

$$P_{total} = \int_0^{365} P_{areal} dt$$

The areal productivity can also be expressed as t km^{-2} $year^{-1}$ instead of t ha^{-1} $year^{-1}$ given that 1 ha=0.01 km^2. The system of differential and algebraic equations described above represent the microalgal growth model. The set of differential equations were solved by the mathematical software, MATLAB [145]. After assigning approximate initial conditions, a finite difference approach was used to solve the set of differential equations. The heat and mass transfer model as well as microalgae growth kinetics models are presented in further detail in the Appendix section.

2.3.3 Microalgae Harvesting

The next step in the process is to harvest the microalgae. This is an energy intensive process owing to the small size and low concentration of microalgae in the growth medium which needs to be separated out, a process known as dewatering [18,78,107]. Different methods of microalgae harvesting and dewatering have been described previously [78,146]. In the present study, it is assumed that microalgae harvesting involves the addition of polyacrylamide flocculants, lamella clarifier mediated dewatering and a secondary dewatering step by centrifugation which resulted in a microalgal with a concentration of 200 kg m^{-3} (20% solids) AFDW [128]. Furthermore, it is assumed in this study, that microalgal paste with a solids concentration of 20% would be used for hydrothermal liquefaction and biofuel production after further upgrading and no additional drying steps were deemed necessary [103].

2.3.4 Economic Analysis

For the economic analysis of the microalgae productivity system, the full value chain including microalgal growth, dewatering and harvest was taken into consideration. Such a comprehensive approach was vital for determining the production cost of microalgal paste which could then be channeled through different conversion routes to produce value-added products. Economic analysis performed previously [10,11,13,18,108,121,122,128,147] was used as a guideline for the evaluation of capital and operating expenditures in the current study. Large scale microalgae productivity of 1000 t day^{-1} was estimated from industry and literature for the development of the baseline model. A harvesting rate of 10% and an extraction rate of 80% were also assumed [128]. A pond size of 8100 m^{-2} was chosen to ensure optimum paddlewheel capacities [128], wages and salaries were estimated to be 12% of the total operating expenditure [10], and maintenance cost was assumed to be 3% of the equipment and reactor costs [128]. Land prices and electricity charges for the different locations studied were obtained from the United States database [148,149].

The capital and operating costs of the microalgae production were approximated assuming a 1000 t day^{-1} microalgae cultivation facility. To calculate mixing energy requirements, energy requirements for microalgae harvesting, and on-site water recirculation, available literature sources were utilized [108,128]. It was assumed that pond liners such as High-Density Polyethylene (HDPE) liners would be used to prevent soil erosion and contamination. A transparent cover was assumed to be used to minimize evaporation and reduce bacterial contamination. For the subsequent steps of microalgae harvesting and dewatering, it was assumed that three static mixers would be required for flocculant addition and three lamella clarifiers would facilitate the primary dewatering. The concentration of slurry derived from the primary dewatering process was assumed to be

30 kg m^{-3} [10]. A centrifugation step requiring 18 centrifuges was included to further reduce the water content, increasing the microalgal paste concentration to 200 kg m^{-3} [128]. Additional infrastructure costs associated with the microalgae cultivation plant included the necessary roads, railways, pipes, building and construction. For pumping and piping estimation, a volumetric flow rate of 0.3 m s^{-1} was assumed to be maintained [128]. This was chosen because lower rates lead to decreased productivity owing to increased residence times of microalgae in dark zones, and a rate higher than 0.3 m s^{-1} translates into a significant rise in microalgae costs arising from cubically increasing power requirements to attain the flow rate [150].

A few assumptions were made to simplify the present analysis. The cost of nutrients, water, CO_2, operation and maintenance were assumed to be consistent between the different locations. Water was assumed to be easily accessible, and pumping being the only cost allotted for it. Industrial pumps served as the basis of computing the capital expenditure associated with pumps through the production plant.

2.4 Results

2.4.1 Results from Heat and Mass Transfer model

The water temperature of open raceway ponds was calculated with the help of hourly solar irradiance, air temperature, relative humidity and wind velocity for each location over an entire year. The entire year of operation is represented by 8760 data points. The results for New Mexico are discussed in greater detail. The water temperature profile of a theoretical microalgae open raceway open is presented below in Figure 2.4.

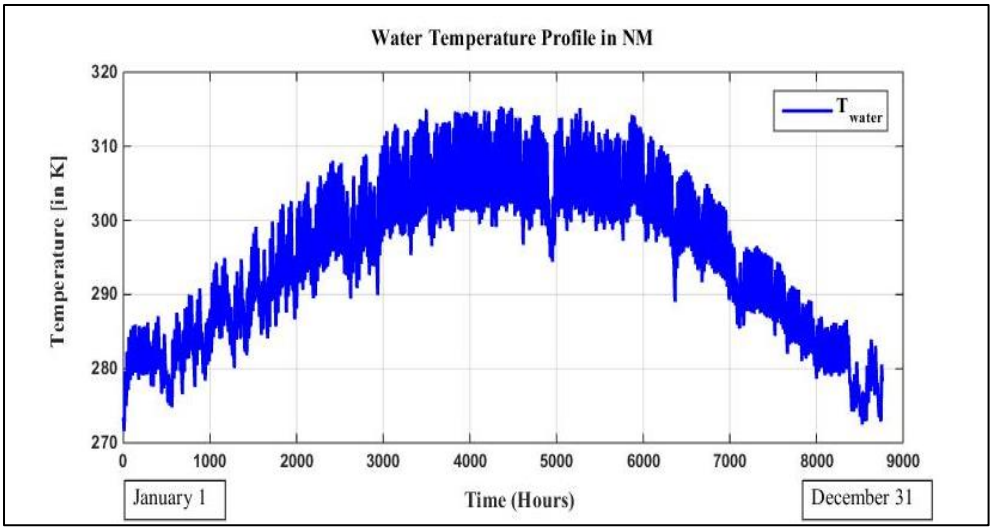

Figure 2. 4. Temperature profile of a hypothetical open raceway pond in New Mexico

From this figure, we observe that water temperature corresponds well with daily and seasonal variations in temperature. Our analysis suggests that as pond water temperature and air temperature differed by 5-10 ºC, the radiation fluxes from pond water and air, which are functions of pond water and air temperatures raised to the power of 4, roughly cancel each other. Thus, it can be inferred that solar irradiance is the driving factor behind the rise in temperature during the day, and evaporation and convection are the primary factors contributing to cooling during the dark periods. In the energy balance model, the effects of conduction heat flux to the soil and the flux due to incoming water are considered negligible.

As discussed previously, it is imperative to develop a thermal energy balance model to determine the temperature of the raceway ponds because microalgal productivity and the resulting economic and environmental success of microalgae cultivation depends on the accurate prediction of water temperature. It has been reported that there is an increase in productivity of *Spirulina* by 20% when the culture is heated in the morning

[151]. Moreover, a 50% increase in productivity of *Chlorella sorokiniana* was achieved when the temperature of the culture medium was maintained within an optimal range without allowing it to be affected by ambient conditions [152]. Given that the growth rate of microalgae has been shown to double with a temperature increase of 10˚C [153], an error in temperature prediction by even 5˚C could translate into large inaccuracies in microalgae productivity of ~40% [133].

2.4.2 Results from Algae Growth Bioreactor Kinetics and Mass Transfer Model

To determine areal productivity of a hypothetical microalgal pond in New Mexico, several parameters such as pond water temperature, climatic conditions, and rate of nutrients and CO_2 uptake were considered. Like the previously described energy balance model, the microalgal growth model also encompasses 8760 data points representing an entire year of operations. The hourly areal microalgae productivity for a 0.3 m deep pond is shown in Figure 2.5.

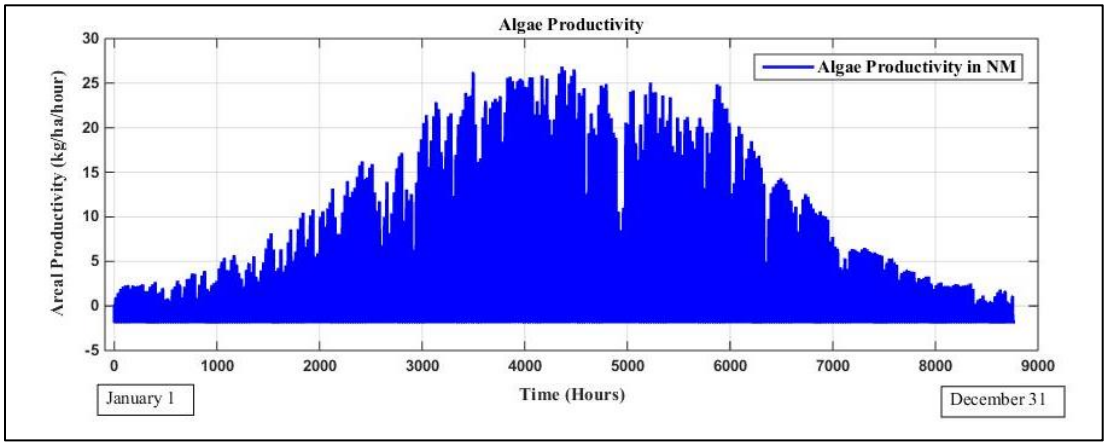

Figure 2. 5. Yearly microalgae productivity profile in open raceway ponds in New Mexico

From the figure, it is evident that areal productivity correlates well with daily and seasonal changes in temperature. A bell-shaped curve is observed for New Mexico signifying growth in the summer months and an almost complete lack of growth in winter. While the present results reflect raceway temperature and microalgae productivity in a

plant operated for the whole year, in practical or commercial use, microalgae cultivation systems would only be operated when net productivity is positive.

As stated before, annual productivity patterns rely on various local meteorological conditions such as solar irradiance, latitude, relative humidity, wind velocity, and varying raceway water temperatures. These variations lead to differences in productivity for different regions considered in the study as depicted in Figure 2.6.

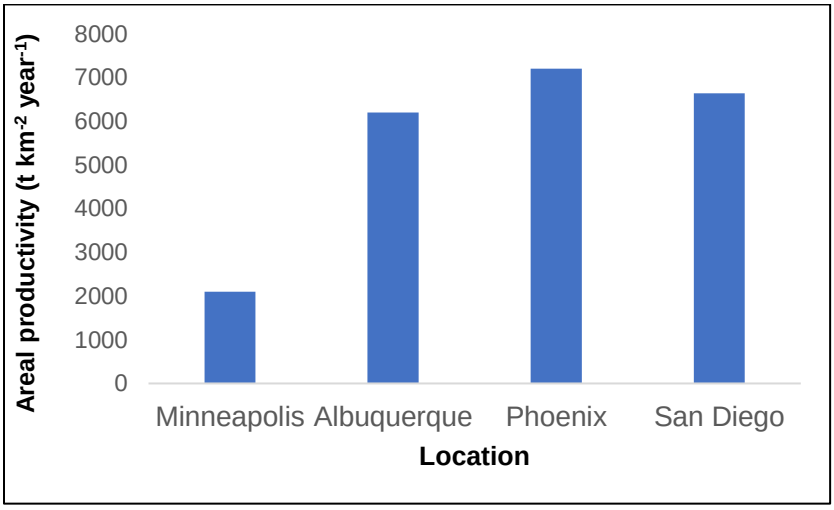

Figure 2. 6. Geospatial variation of microalgal productivity

2.4.3 Economic Analysis Results

To proceed with the study, a hypothetical microalgae cultivation plant with a capacity of 1000 t day $^{-1}$ was assumed as the baseline case. For the mass and energy balance of the system, demand for nutrients like nitrogen and phosphorous, CO_2 as well as consumption of electricity were taken into consideration. The minimum CO_2 uptake required for microalgae growth is 1.83 kg CO_2 per kg of algal biomass produced [129]. In reality, this number is often higher due to the use of a technique known as degassing [13,154,155]. A degassing unit [18], along with thorough mixing, is often included within open raceway ponds to ensure the removal of oxygen which is a byproduct of microalgae

cultivation and is often detrimental to microalgae growth at higher concentrations [129]. To meet the demand for nutrients like nitrogen and phosphorous, fertilizers are proposed as demonstrated previously [13,107,108,128]. Other micronutrients required for microalgae growth were left out in the present study. As per previous studies, CO_2, nitrogen and phosphorous recovery were assumed to be 50%, 76% and 50% [128].

The production cost of microalgal paste was now determined based on the mathematical growth model, and assumptions for growth, dewatering and harvesting outlined previously. Results were obtained for the hypothetical production plant in New Mexico and are discussed in detail here. The annual productivity was taken as 365,000 t corresponding to 365 days of operation. The production cost was founded on yearly operation costs and a 20-year return of the net capital investment. The net capital investment was 959 M$ and the net cost of yearly operation and maintenance was 149 M$. The breakdown of the capital and operation costs estimates are provided in detail in Table 2.2 and Table 2.3. The capital costs estimates were dominated by the price of paddlewheels, pond liners and pond covers (88%) and the cost of nutrients, maintenance and harvesting dictated most of the operation costs.

Table 2. 2. Capital cost estimates for 1000 t day^{-1} microalgae production plant in New Mexico

Equipment	**Cost**	**Cost ($ ha^{-1})**	**Cost ($ $year^{-1}$)**	**Cost ($ t^{-1})**	**Percentage Contribution**
CO2 Absorber (static mixer)	257,634	43	12,882	0	0.03%
Paddlewheels (1 per pond)	148,718,576	24,691	7,435,929	20	15.51%
Flocculant addition (static mixer)	171,756	29	8,588	0	0.02%
Lamella separators	3,743,590	622	187,179	1	0.39%

Centrifuges	9,972,923	1,656	498,646	1	1.04%
Pumps	977,499	162	48,875	0	0.10%
Land	21,683,168	3,600	1,084,158	3	2.26%
Liners	304,710,733	50,590	15,235,537	42	31.78%
Landscaping	64,832,071	10,764	3,241,604	9	6.76%
Cover	388,992,426	64,583	19,449,621	53	40.57%
Railways	1,250,000	208	62,500	0	0.13%
Roads	600,000	100	30,000	0	0.06%
Operating buildings	450,000	75	22,500	0	0.05%
Construction costs	2,500,000	415	125,000	0	0.26%
Pipes	9,929,700	1,649	496,485	1	1.04%
Total	**958,790,076**	**159,185**	**47,939,504**	**131**	100%

Table 2. 3. Operation cost estimates for 1000 t day^{-1} microalgae production plant in New Mexico

Equipment	**Operating cost ($ year^{-1})**	**Operating cost ($ t^{-1})**	**Percentage contribution**
Paddlewheels	6,970,496.15	19.10	4.60%
Lamella separator	9,616.21	0.03	0.01%
Centrifuge	533,352.60	1.46	0.36%
On-site pumping circulation	3,965,207.26	10.86	2.62%
Material input			
DAP	8,916,246.83	24.43	6.02%
Urea	33,401,355.06	91.51	22.55%
Pumping replacement water	1,423,731.13	3.90	0.94%

Absorber CO2	15,331,960.23	42.01	10.35%
Flocculent	36,499,487.25	100.00	24.65%
Operations			
Maintenance	26,024,245.11	71.30	17.19%
Wages	15,969,083.75	43.75	10.71%
Total	**149,044,781.70**	**408.34**	100.00%

2.4.3.1 Economic Sensitivity Analysis

The various parameters and assumptions used in this study have an inherent degree of uncertainty and are subject to change. To assess the impact of these parameters on the production cost of microalgae, a sensitivity analysis was conducted. The objective of the sensitivity analysis was to quantify the effect of these variations in the production costs and determine the most important parameters for microalgae cultivation. The results are shown in Figure 2.7 and it is evident that microalgae cultivation costs are affected most profoundly by annual productivity, nutrient and harvest costs, and design of the open raceway ponds.

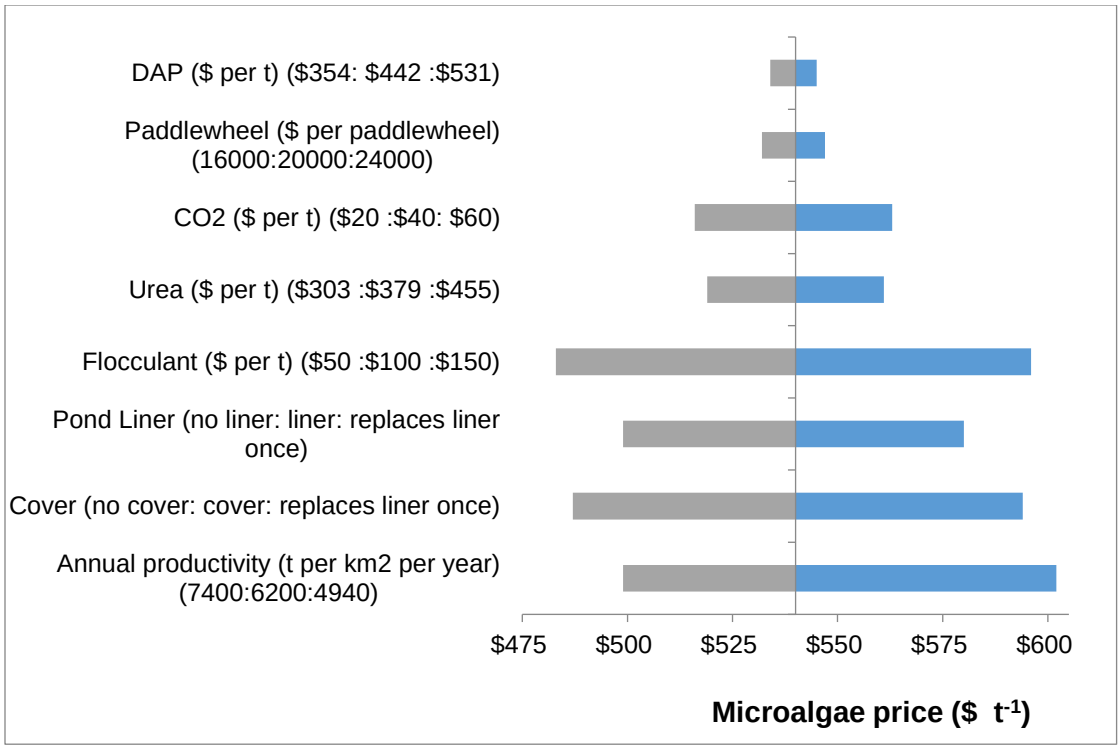

Figure 2. 7. Economic sensitivity analysis for New Mexico based on price variation of several parameters. The baseline microalgae production cost in New Mexico was considered to be 540 $ t^{-1}. Microalgae production costs are provided based on AFDWs.

The sensitivity analysis demonstrates that an increase in annual areal productivity leads to a decrease in microalgae production price. When microalgal productivity in New Mexico increases to 7400 t km^{-2} $year^{-1}$ (20% higher than the baseline scenario of 6200 t km^{-2} $year^{-1}$), the price falls to 500 $ t^{-1}. Correspondingly, when the productivity drops to 4950 t km^{-2} $year^{-1}$ (20% reduction from baseline), the production cost jumps to 600 $ t^{-1}. As discussed before, pond liners and covers have a significant impact on the capital expenditure and this is evident from the sensitivity study as well. It is seen that prices for microalgae produced in raceway ponds with and without liners can fluctuate by ± 40 t^{-1} in the present scenario. Similarly, the presence or absence of covers can impact microalgae price by ± 50 $ t^{-1} in the 20-year scenario considered. The most dominating factor affecting harvesting costs of microalgal biomass is the price of flocculants, which was found to have a substantial influence on the cost of production. Changing the price of flocculants by ±

50% amounts to a microalgae production price variation of about ± 55 $ t^{-1}. The price of nutrients and CO_2 are also major contributors to microalgae price as seen in Figure 2.7.

2.4.4 Comparative Analysis of the Effect of Geographic Locations on Microalgae Productivity and Cost

It was observed that microalgae productivity was variable based on geospatial locations due to changes in climatic conditions as presented in Figure 2.6. Other than the productivity differences, land and electricity prices are also dependent on location as shown in Table 2.4.

Table 2. 4. Variations between different geospatial locations

	Areal Productivity (t km^{-2} $year^{-1}$)	Electricity Price ($ kWh^{-1})	Land Price ($ ha^{-1})	Microalgae Price ($ t^{-1})
Minneapolis	2100	0.072	11875	$1,074
Albuquerque	6200	0.0615	3600	$540
Phoenix	7200	0.0611	4350	$502
San Diego	6640	0.1377	26750	$581

Microalgae production costs based on the variations outlined above were ascertained and presented in Figure 2.8. For simplicity, it was assumed that operating costs like cost of nutrients, CO_2, maintenance and labor were constant among the different locations studied.

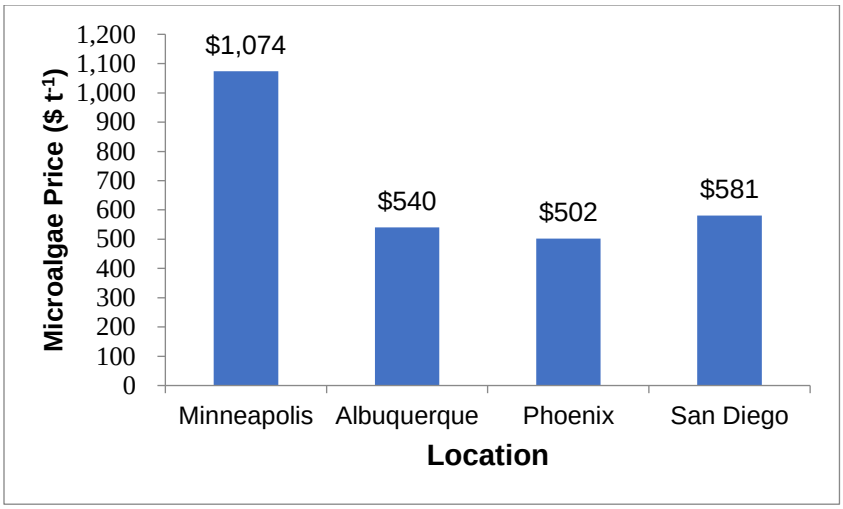

Figure 2. 8. Microalgae production price for various geospatial locations

The capital and operating costs for the four different locations are given in Table 2.5. Production costs ranged between 1074 $ t^{-1} for Minnesota (Minneapolis) to 502 $ t^{-1} for the Phoenix in Arizona (Table 2.4) on an AFDW basis. This is explained by the three times higher productivity potential in Arizona (Phoenix) compared to Minnesota (Minneapolis). The comparable microalgae prices ranging between 500 $ t^{-1} to 580 $ t^{-1} for Arizona (Phoenix), New Mexico (Albuquerque) and California (San Diego) may be ascribed to the similar weather patterns for the three locations which are more favorable for microalgae growth. These results highlight the importance of choice of location in determining microalgae production price, a factor that may have far-reaching consequences on the economics of microalgae conversion [156].

Table 2. 5. Capital costs, operating costs and land requirement for 1000 t day^{-1} microalgae production plant

	Capital Costs (M$)	Operating Costs (M$)	Land area (ha)
Minneapolis	3001	242	17381
Albuquerque	959	149	6023
Phoenix	815	142	5069
San Diego	1005	162	5497

2.5 Discussion

The primary goal of this study was to assess the feasibility of large-scale microalgae cultivation while considering geospatial variability. The results obtained here are comparable to that of other research groups. Microalgae productivity was found to be approximately 6000 t km^{-2} $year^{-1}$ in California [157]. Areal productivity in open pond systems in Netherlands and Algeria were reported to be 4150 and 6370 t km^{-2} $year^{-1}$ respectively [41]. Similarly, productivity of microalgae plants located in Bissau (Guinea Bissau), Huelva (Spain) and Uppsala (Sweden) were found to be 5400, 4700 and 1700 t km^{-2} $year^{-1}$ [13]. Therefore, results from the present study ranging between 2000 – 7200 t km^{-2} $year^{-1}$ are in accordance with reported literature. The microalgae productivity model described here was based on a mathematical growth model and augmented by assessing the effect of climate-related variability and rates of nutrient and CO_2 uptake. This model was then used for economic analysis to determine the cost and economic practicality of microalgae cultivation on an industrial scale.

While several studies have been published on the economics of microalgae biofuel production in open raceway ponds and photobioreactors [105,121,122,156,158,159], there does not exist much information on microalgae feedstock production cost based on different geospatial locations and considering yearly production. Often, researchers who conduct techno-economic and lifecycle assessment studies simply assume microalgae productivity costs and feedstock selling price thereby creating and propagating significant uncertainties [11,103,107,114]. The present analysis will be useful for addressing the existing gaps and contributing to the accuracy of future studies on this subject.

Recently, an economic analysis of microalgae production in open raceway ponds after assuming microalgae productivity by Davis *et al*. [160] evaluated microalgae production cost to be \$491 t^{-1} for a hypothetical plant based in California. Correspondingly,

after using actual geospatial climatic data and other growth data for determining microalgae productivity, the present study found that algae production costs ranges between \$502 - \$1074 t^{-1} (\$581 t^{-1} for San Diego, California) for the various locations considered. While the subtle difference in projected price between the two studies may be attributed to the locations considered and dissimilarities in design specifications, the similarities in results underscores the robustness of the present study.

2.6 Conclusion

The purpose of the study was to evaluate the technical and economic feasibility of large-scale microalgae production at different geographical locations within the United States. For the practical implementation of microalgae based biorefineries, it is imperative that the associated risks and uncertainties be minimized. In order to achieve that, a thorough and clear understanding of the variabilities and their effect on the process for each location is needed. Consequently, rather than annual averages, actual hourly climate data was utilized to obtain more robust values for annual microalgae productivity potential. This ensured a more realistic assessment of production capability across the lifespan of the facility. Technical feasibility was determined by developing mathematical growth models for microalgae and factoring in geospatial variability. Economic feasibility was then elucidated by establishing the capital and operation costs of such a facility and determining the corresponding microalgae production cost. A sensitivity analysis provided further insight into the economic implications of the various design factors such as pond liners, pond covers and paddlewheels. These factors were found to contribute significantly to the cost of algae production but were deemed necessary to facilitate proper mixing and protect the ponds from predators. The results obtained here also point to certain challenges to the execution of large-scale open pond microalgae cultivation systems, such as nutrient demands, CO_2, water and energy requirements; however, these may be addressed by

technical breakthroughs in the near-future. Overall, this work provides a more precise prognosis of microalgae productivity potential and serves to underline the importance of design specifications and choice of location for the determination of microalgae cultivation costs. Further research into the different systems and parameters of microalgae production will be useful to inform policy makers and navigate the commercialization of such systems.

Chapter 3. Dynamic Process Model and Economic Analysis of Microalgae Cultivation in Flat Panel Photobioreactors

3.1 Introduction

Microalgae are widely considered to be a valuable bio-renewable resource for food, feed and energy production. High photosynthetic efficiency, superior productivity, and flexible land and water requirements are a few of the factors that makes this diverse group of ubiquitous microorganisms an attractive candidate for commercial biofuel and bioproduct applications in the near future [64,161]. Two types of reactor systems are generally utilized for microalgae cultivation, namely open raceway ponds and photobioreactors [162]. As discussed in Chapter 2, the open raceway configuration is cheaper and relatively simple compared to the more sophisticated and complex photobioreactor systems. This complexity is often reflected both in the quality and quantity of the resultant microalgae output from the photobioreactor systems [18,76].

Accurate assessment of microalgae productivity is a key factor behind ensuring the success of microalgae based biorefineries. Apart from the cultivation system, microalgae productivity is dependent on various environmental factors such as solar irradiance, temperature, rainfall, local wind velocity and relative humidity [41,163]. A lack of available data for industrial systems means that researchers often have to extrapolate productivity potential from laboratory settings [64]. Moreover, the feasibility of such biorefineries is heavily dependent on upstream microalgae cultivation costs [11]. Therefore, developing comprehensive computational models to quantify microalgae productivity potential based on local climatic factors, and performing downstream techno-economic analyses to assess cultivation costs is of the utmost importance. These results may then be utilized in further processing to value-added products or specialty chemicals.

The goal of this analysis was to assess microalgae productivity potential cultivated in flat panel photobioreactors, as an alternate to open raceway ponds, for several locations within the United States. An economic analysis was also conducted to determine microalgae costs for the various locations. Finally, a sensitivity analysis demonstrated the economic implications of various parameters on microalgae costs. Only a few previous studies have modeled microalgae cultivation in flat panel photobioreactors on a commercial scale [42,164]These were limited in scope because either the influence of reactor temperature was neglected or the only factors considered were reactor temperature and light intensity. To the best of our knowledge, this study is novel in its approach to determine commercial scale microalgae cultivation costs by integrating a combined heat and mass transfer model, algae growth model with detailed techno-economic analysis. Such an integrated, quantitative and comprehensive approach will help minimize the assumptions and uncertainties associated with microalgae production in flat panel photobioreactors and is a significant step forward towards realizing the full potential of microalgae-based biorefineries. The results obtained here are intended to act as a guide to help the scientific community and policy makers pave the way for the commercialization and widespread utilization of microalgae in future production scenarios.

3.2 Methods

Photobioreactors are regarded as more effective systems for microalgae cultivation than open pond systems due to the higher productivity and low risk of contamination and culture crashes [39,165]. We have previously shown the feasibility and the effect of geospatial locations on open raceway ponds microalgae cultivation systems [5]. In this section, we examine the utility of flat panel photobioreactors for microalgae cultivation.

Microalgal growth is enabled by several factors such as sunlight, temperature of the growth culture medium, carbon dioxide (CO_2) and essential nitrogen and phosphorus -based nutrients. To facilitate growth, bioreactors are generally supplied with an external supply of CO_2 as atmospheric CO_2 levels are often not sufficient for robust microalgae growth. To determine reactor water temperature, a combined heat and mass transfer model was developed as described in Chapter 2. A bioreaction kinetics-based model was employed for determining annual productivity potential. The capital and operating costs of the projected commercial scale microalgae plant was established by quantifying the mass and energy balances of the entire supply chain. The microalgae production costs thus determined revealed the geospatial variation associated with microalgae cultivation [64,156]. Four locations within the United States were chosen: Minneapolis (Minnesota), San Diego (California), Albuquerque (New Mexico) and Phoenix (Arizona). *Nannochloropsis sp.* was chosen as the suitable algal species for reasons explained in Chapter 2 [48,131]. The results obtained from the heat and mass transfer model were combined with the microalgal growth kinetics model to determine microalgal productivity for a given location. Additionally, an economic analysis was undertaken to compute microalgae production costs for a hypothetical 1 hectare (ha) plant (1ha= 0.01 km^2). The theoretical framework of the microalgal productivity model and the supply chain of microalgae cultivation are demonstrated in Figures 3.1 and 3.2 respectively. The comprehensive computational model developed here will help minimize the need for assumptions and thereby reduce risks and uncertainties associated with techno-economic and environmental assessment of microalgae growth, harvest and conversion [103,114,156].

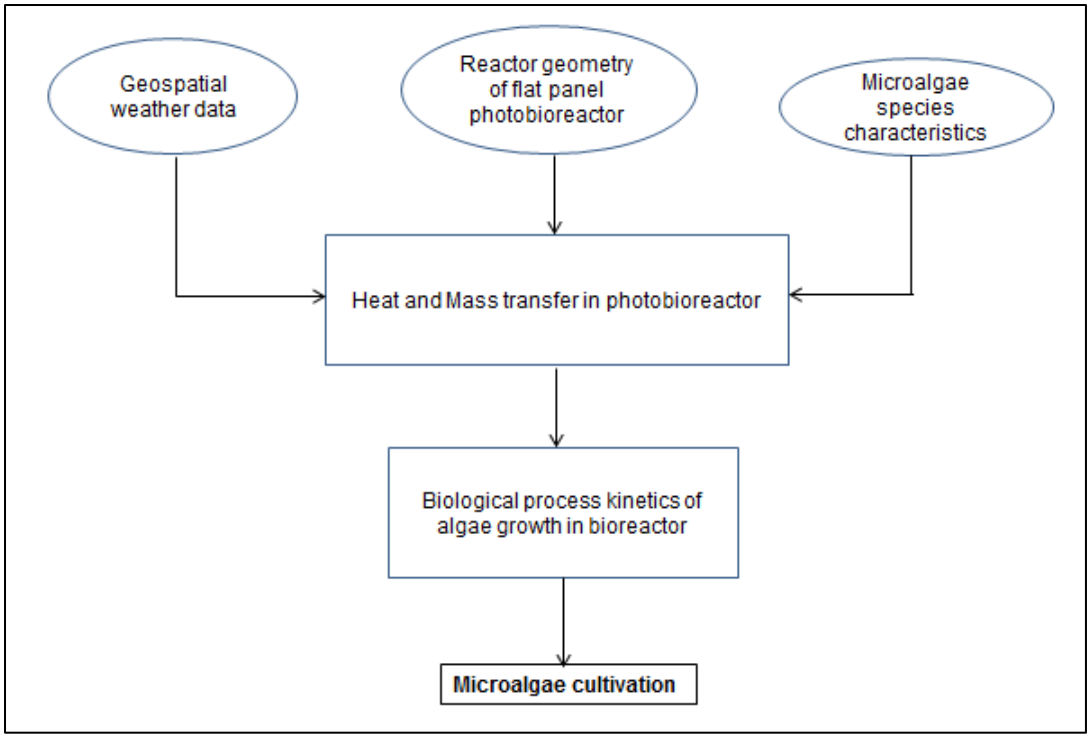

Figure 3. 1. Theoretical framework for assessing algae productivity in flat panel photobioreactors

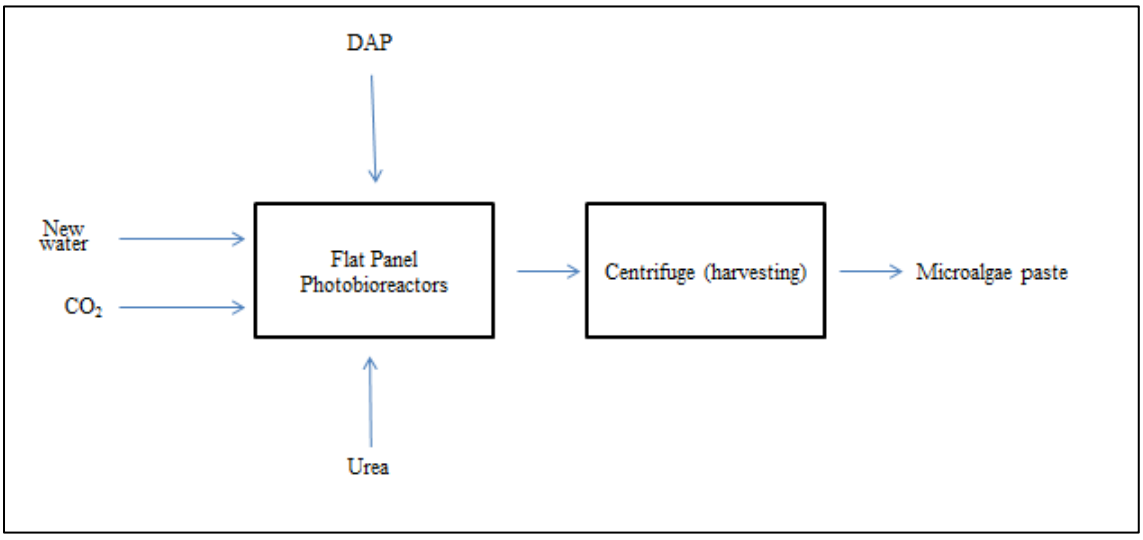

Figure 3. 2. Supply chain model of microalgae cultivation in an array of flat panel photobioreactors

3.3 Model

The model was developed following the approach described in Chapter 2 and in our previous work [163,166]

Model input

Local weather and climatic data were collected from the National Renewable Energy Laboratory's National Solar Radiation Database (NSRDB) including solar insolation, ambient air temperature, wind velocity and relative humidity [167]. Factors required for microalgae growth such as CO_2, nitrogen in the form of urea and phosphorus as Diammonium phosphate (DAP) were assumed to be available in excess to not prevent hindrance to growth.

Model output

The primary output of this model were microalgae productivity and cultivation costs for a particular geographic location. Assuming that the plant would be operated throughout the year, microalgae productivity for each panel was determined and total areal productivity was determined on the basis of total number of flat panel bioreactors in a hypothetical 1 hectare plant.

3.3.1 Combined heat and mass transfer model

The reactor temperature is a key factor governing microalgal productivity for reasons described in Chapter 2 and in literature [137]. The input to the thermal balance model included direct and diffuse solar irradiance, air temperature, relative humidity and wind velocity. Variations in temperature as a result of rainfall and associated heat flux for CO_2 were omitted from the process model.

Model Description

The combined heat and mass transfer model relevant for microalgae growth was developed based on previous work [42,168,169]. The various heat fluxes considered in the model included direct and diffuse solar irradiance, radiation from air, ground and reactor surface, reflections between adjacent panel and from ground, convective heat transfer between reactor surface and adjacent air, as well as heat transfer due to aeration of the panels. The governing equation describing the energy balance for microalgae growth in photobioreactors is:

$$\rho_{water} V C_{p_{water}} \frac{dT_{water}}{dt} = \sum Q \quad (1)$$

where, ρ_{water} is the density of the growth medium or water (in kg m^{-3}), V is the volume of the reactor (in m^3), $C_{p_{water}}$ is the specific heat capacity of water (in J kg^{-1} K^{-1}), T_{water} (in K) is the dynamic reactor temperature and *Q* (in W) signifies respective heat flux. Detailed model equations, description of the assumptions and more information about the various components of heat flux may be found in Appendix section.

3.3.2 Microalgae growth kinetics model

Microalgal growth in photobioreactors are determined by different factors such as light distribution within the culture medium, rates of photosynthesis and respiration, temperature profile of the growth medium and utilization of nutrients and CO_2 by microalgae [39,143,165]. In addition to temperature, light is one of the main requirements for photosynthesis. To address this, parameters such as local hourly solar irradiance, the incidence and transmission of light through the reaction, and the influence of reactor geometry were considered, as described in greater detail in the Appendix section. The reactor temperature obtained from the heat and mass transfer model, and the light

intensity were integrated into a biological growth kinetics model following previous studies [42,134,136,163].

Microalgae growth modeling

As shown in Chapter 2, a Michaelis-Menten type reaction kinetics equation was formulated to reveal specific growth of microalgae (μ) (day^{-1}) for the microalgal species, *Nannochloropsis sp.* [48,131].

$$\mu = \mu_{max} * \left(\frac{C_{CO2,dissolved}}{HSC_{carbon\ uptake} + C_{CO2,dissolved} + \frac{C_{CO2,dissolved}^2}{K_S}} \right) * \left(\frac{N_{medium}}{N_{medium} + HSC_{nitrogen\ uptake}} \right) * \left(\frac{P_{medium}}{P_{medium} + HSC_{phosphorus\ uptake}} \right) * \left(\frac{I_{mean,culture\ medium}}{HSC_{light} + I_{mean,culture\ medium} + \frac{I_{mean,culture\ medium}^2}{K_I}} \right) * f(T)$$

where, $C_{CO2,dissolved}$ was the concentration of the dissolved CO_2 in the culture media (kg m^{-3}), $HSC_{carbon\ uptake}$ was the concentration of carbon in the medium (kg m^{-3}), N_{medium} was the concentration of nitrogen in the medium (kg m^{-3}), $HSC_{nitrogen\ uptake}$ was the half-saturation constant of uptake of nitrogen (kg m^{-3}),), P_{medium} was the concentration of phosphorus in the medium (kg m^{-3}), $HSC_{phosphorus\ uptake}$ was the half-saturation constant of uptake of phosphorus (kg m^{-3}), $I_{average}$ was the average light intensity within the culture medium, HSC_{light} is half saturation constant for light and f(T) is a function of culture media temperature. This model with the appropriate kinetic parameters may be adapted for predicting the growth and productivity potential for other algal species as well.

Biomass growth model

The specific growth rate, and concentration ($C_{biomass}$) of microalgae (kg m^{-3}), was used to determine instantaneous microalgae areal productivity per panel as denoted by the following equation:

$$Productivity\left(P_{areal,panel}\right) = \int_0^z \int_0^d (\mu - k_{decay}) * C_{biomass} dz\, dy \qquad (2)$$

where, *d* (m) and *z* (m) are the depth and height of each flat panel, respectively.

The above equation was then applied to the number of panels (N) that may be installed on a 1 km^2 land area to give the total annual productivity in flat panel photobioreactors as follows:

$$P_{total} = N * \int_0^{365} P_{areal} dt \qquad (3)$$

The mathematical software MATLAB was used to solve the set of algebraic and differential equations outlined above. Further details regarding the biomass growth model may be found in Appendix.

3.3.3 Microalgae harvesting

The following step in the process is to harvest the microalgae, a highly energy intensive process owing to the minute size of algal cells and their low in the growth medium [18,147]. The harvesting process was modeled as done previously [170]. Centrifuges with an efficiency of >95% were assumed to be used, yielding a microalgal paste of concentration of 200 kg m^{-3} (or a 20% solids concentration). This algal paste could then be utilized in numerous downstream applications [39]. The paste may also be directly utilized for hydrothermal liquefaction and transformation of bio-oils to biofuels without the need for additional drying steps [103].

3.3.4 Techno-Economic analysis

Techno-economic analysis was performed as described in Chapter 2. A comprehensive approach was taken to quantify production price when subjected to geospatial variation, a step important for the downstream processing of microalgae to value-added chemicals and bioproducts. Available literature was consulted to execute the economic analysis [18,121,122,128,147,156,163,170]. Microalgae cultivation in flat panel photobioreactors in a 1 ha facility was used as baseline for this model. Land and electricity prices relevant for construction and operation of the biorefineries were acquired from appropriate databases [171,172].

The capital costs for microalgae cultivation were intended to include purchase and installation of equipment, piping and sensors and controls. For capital costs estimation, initial cost of equipment was divided by the total lifespan assuming linear depreciation [173]. The lifespan of the plant was estimated to be 20 years [128,163]. Infrastructure needs such as electricity, water, and transportation were assumed to be readily available. Capital costs were split into direct and indirect capital costs. Direct capital costs consisted of machinery and equipment costs, and indirect costs entailed involved installation fees, taxes, and engineering and supervision fees. The fees associated with taxes and insurance were assumed to be 1% of direct capital costs as demonstrated previously [170,173]. Equipment installation costs were set at 10% and engineering and supervision fees at 5% of total direct costs [173]. The lifespan of equipment and machinery beyond which they would need to be replaced were also derived from literature [170].

Operating costs for microalgae cultivation included labor and accompanying salaries, fertilizer, CO_2, electricity and consumables costs. For optimal plant performance, maintenance and overhead fees were expected to be 5% of direct capital costs and 10% of direct operating costs, respectively [170]. The cost of raw materials and water for the

different locations were assumed to be identical. Industrial sized centrifugal pumps were assumed to be used with pumping taken as the only cost for water transport and delivery.

3.4. Results

3.4.1 Results from combined heat and mass transfer model

It has been demonstrated previously that the microalgae strain, Spirulina responded to the application of additional energy to the culture medium by showing a 20% jump in productivity [151]. Similarly, a temperature control strategy where the culture was maintained at an optimum range increased the productivity of the species Chlorella by 50% [152]. These examples emphasize the importance of accurate determination of yearly temperature to accurately model microalgae productivity. The temperature profile model for flat panel photobioreactors was built on local climatic parameters such as direct and indirect solar insolation, ambient temperature, wind velocity and relative humidity. Illustrative results from Albuquerque, New Mexico (USA) are presented in more details here. The annual reactor temperature profile for the flat panel photobioreactors is given in Figure 3.3. Of the various heat fluxes incident on the photobioreactor surface, the most influential were found to be radiation from the atmosphere, radiation from the ground surface, and radiation from surface of the reactor. Reflection from the ground and the reactor surface were found to be negligible in their contribution to the temperature profile.

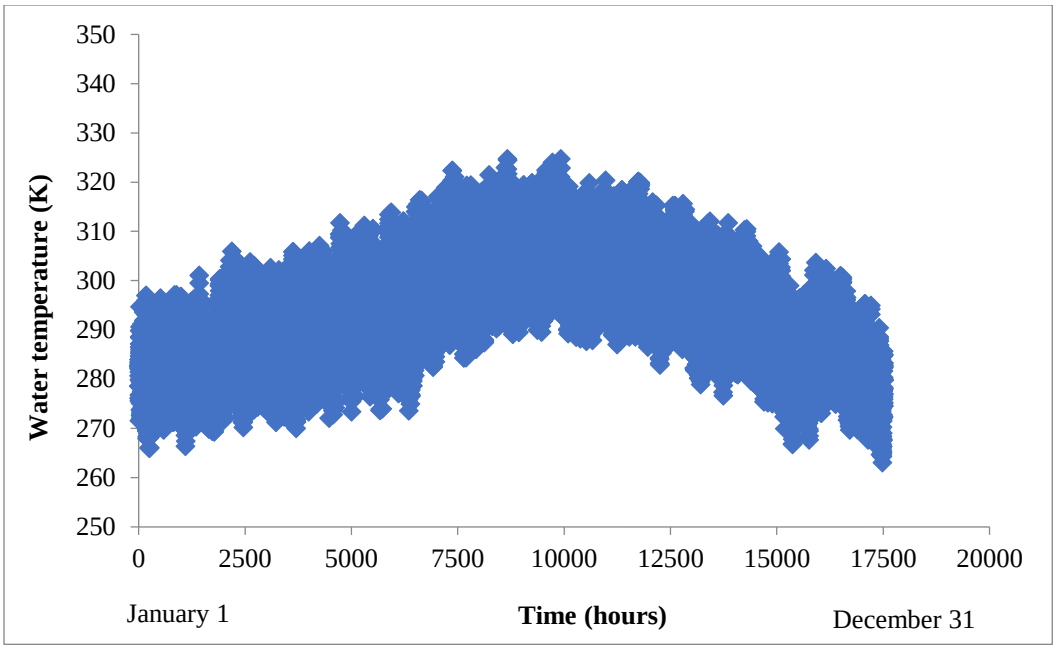

Figure 3. 3. Predicted yearly temperature profile in flat panel photobioreactors in the model algae cultivation plant in Albuquerque, New Mexico (U.S.A.)

3.4.2 Microalgae bioreactor growth kinetics model

Next, the productivity potential for a given location was determined by applying the photobioreactor temperature profile obtained above to the microalgae growth kinetics model. Each photobioreactor was assumed to be 1m x 1m x 0.05m (length x height x width (thickness)) [166,174]. An important contributor to the success of the photobioreactors is the spacing between adjacent rows of reactor panels to ensure that the optimal amount of sunlight is intercepted by the panels [42]. In this case, the reactor panels were assumed to be positioned 1 m away from its neighboring panel configuration [170]. Figure 3.4 shows the effect of geospatial location and related climatic factors on microalgae productivity. It is observed that microalgae productivity in Minneapolis at 3800 t km^{-2} $year^{-1}$, a relatively colder region in the northern part of the United States is significantly lower compared to the relatively warmer southern regions. The highest performance for microalgae was found to be in Phoenix was at approximately 13000 t km^{-2} $year^{-1}$ which is about 3.42 times than the productivity in Minneapolis. Microalgae productivity in Albuquerque and San

Diego are 10800 and 11500 t km^{-2} $year^{-1}$, respectively. Thus, it appears that climatic factors play an important role in determining microalgae productivity potential alongside characteristic factors such as uptake of CO_2 and nutrients.

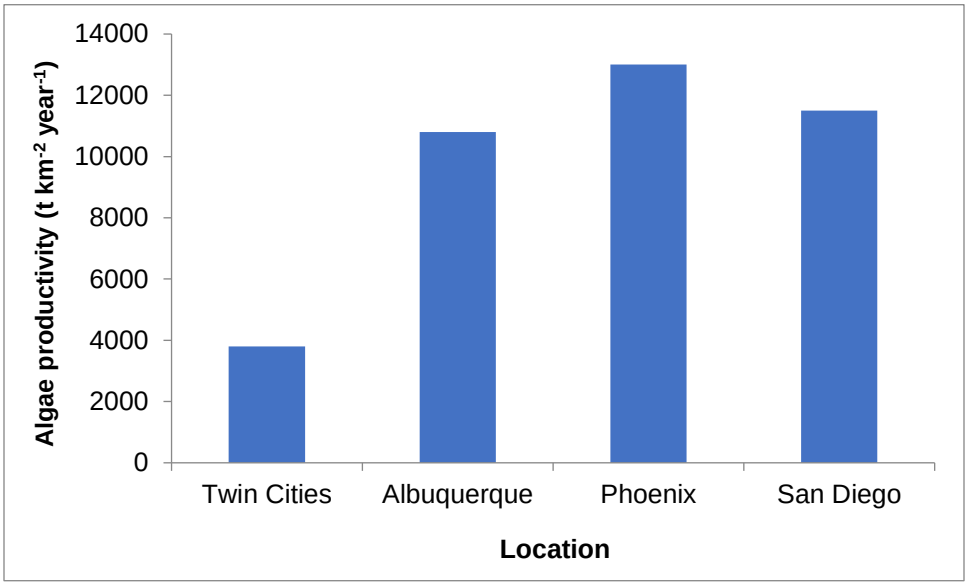

Figure 3. 4. Microalgae productivity potential for the different locations

3.4.3 Economic Analysis

For this section, the mass and energy balance of the entire microalgal supply chain was taken into consideration as described in Chapter 2. For the microalgal species *Nannochloropsis sp.*, the consumption of raw materials such as CO_2, and nitrogen and phosphorus-based fertilizers used for agriculture [128,163] were quantitated.

The results for a hypothetical microalgae cultivation plant located in Albuquerque, New Mexico are analyzed here. The yearly microalgae production for this model manufacturing facility was found to be 10800 t km^{-2} $year^{-1}$, assuming 365 days of operation. For a 20 year projection, the annual capital and operating costs were determined to be $94,350 and $278,000, respectively. The corresponding total cost of microalgal production was seen to be 3450 $ t^{-1}. The complete list of capital and operating

costs is provided in Tables 3.1 and 3.2 respectively. Direct costs included the cost of the photobioreactors, piping, fittings, pumps and other equipment and amounted ~76% of the total capital expenditure. Operating costs were dominated by annual wages and salaries of personnel constituting 69% of the total amount.

Table 3. 1. Capital cost estimates for a 1 ha microalgae production plant in Albuquerque, New Mexico

Direct Capital Costs	**Cost ($)**	**Cost per annum ($ year^{-1})**
PBR cost	540,698	32,557
Piping and fitting	148,969	7,448
Pumps and other equipment	49,7023	24,851
Electrical equipment	29,1819	14,591
Field laboratory	50,000	2,500
Total Direct Cap. Costs (TDC)	**1,528,508**	**81,948**
Indirect Capital Costs		
Engineering & Supervision (5% of TDC)	76,425	3,821
Installation (10% of TDC)	152,851	7,643
Tax & insurance (1% TDC + Land)	18,885	944
Total indirect capital costs	248,161	12408
Fixed capital investment (FCI)	**1,776,670**	**94,356**
Land	3600	
Total Fixed Capital (TFC)	**1,780,270**	**94,356**

Table 3. 2. Operating cost estimates for a 1 ha microalgae production plant in Albuquerque, New Mexico

Direct Operating Costs	**Costs per annum ($ year^{-1})**
Employee expenditure	191,958
Raw materials	15,711
Electricity	13,188
Consumables	7,000
Total Direct Operating Costs (TDO)	**227,856**
Indirect Operating Costs ($/y)	
Maintenance (5% of TFC)	4,718
Overhead (10% of TDO)	22,786
Administration (10% of TDO)	22,786
Total Indirect Operating Costs	**50,289**
Total Operating Costs	**278,146**

3.4.3.1 Economic sensitivity analysis

An important facet of the economic analysis is to gauge the effect of diverse parameters on microalgae costs. Economic sensitivity analysis helps provide insights into this process by estimating the influence of changeable parameters such as prices of raw material and equipment that are susceptible to market uncertainties on commercial microalgae prices. The effect of several parameters for the hypothetical plant located in Albuquerque, New Mexico on total microalgae costs is shown in Figure 3.5. As expected, microalgae cost is highly sensitive to productivity potential for that location. For Albuquerque, New Mexico, a variation of 20% in microalgae productivity led to a change in the corresponding price from 2903 $ t^{-1} and 4267 $ t^{-1} compared to the baseline cost of 3450 $ t^{-1}. Labor costs were also seen to heavily influence microalgae costs. Changing the number of workers and thereby labor costs by ± 50% caused the microalgae cost to vary by more than ± 16% from the baseline scenario. It is also evident that capital cost of equipment, piping, fitting and reactor costs, as well as nutrients and raw materials costs

are major determinants of microalgae price. In general, it was shown that an increase of microalgae productivity and decrease in the costs of the various associated elements can potentially reduce microalgae price by 35% to 2230 $ t^{-1} from the baseline of 3450 $ t^{-1}.

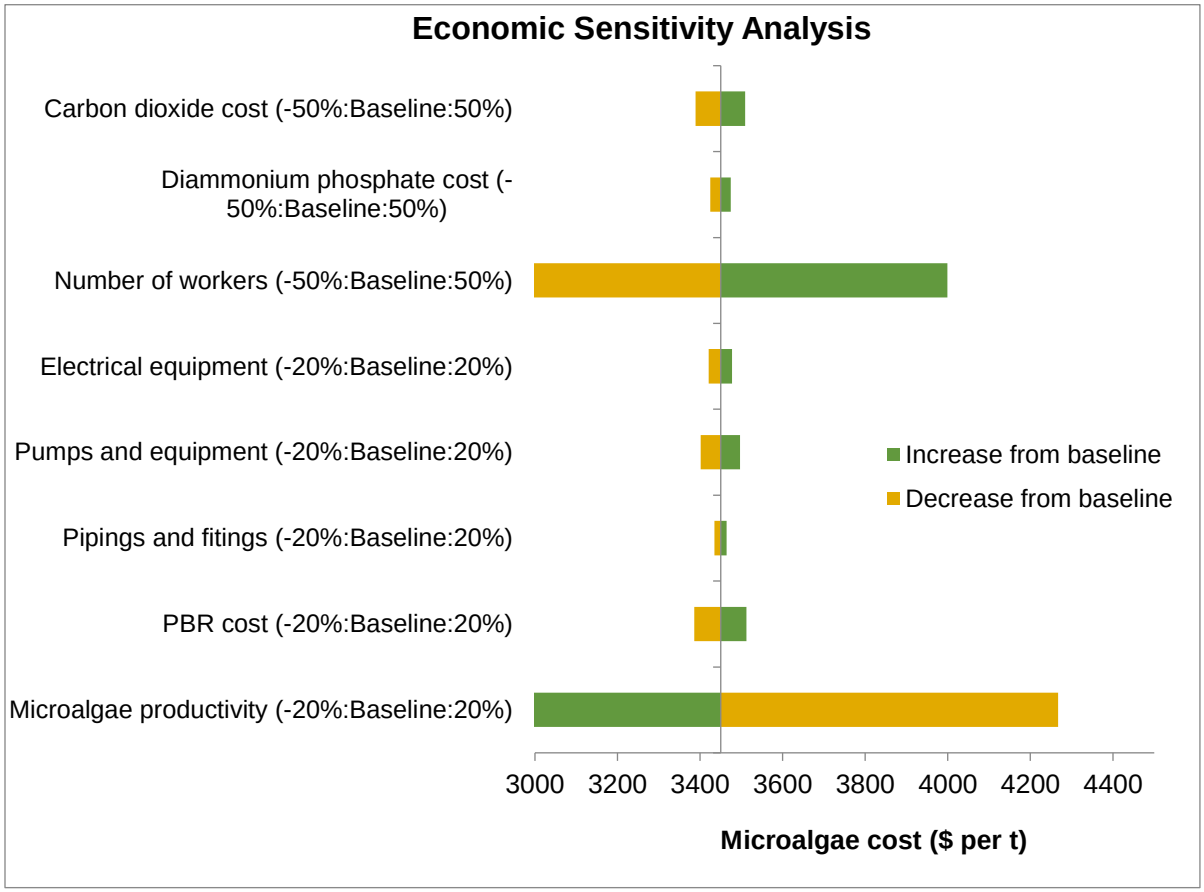

Figure 3. 5. Economic sensitivity analysis of commercial microalgae cultivation in flat panel photobioreactors. Baseline microalgae cost in a hypothetical plant in Albuquerque, New Mexico is 3450 $ t^{-1}

3.4.4 Geospatial effects on microalgae productivity and production costs

Based on the changes in microalgae productivity arising from geospatial variation described in Figure 3.4, and differences in land and electricity costs, the variability in microalgae costs based on location was investigated next. This is an essential step in the commercialization of microalgae as upstream feedstock production may have complex consequences on the downstream processing of microalgae and ensuing prices of value-added chemicals and bioproducts [115]. For this analysis, land and electricity prices for

the locations studied were adopted from Chapter 2 [163]. For purposes of simplification, costs of raw material, nutrient and employee wages were assumed to be constant between different locations. The results of the analysis are outlined in Figure 3.6. A broad range was observed in the cost of microalgae production in flat panel bioreactors for the separate locations, from about 9564 \$ t^{-1} (~9.5 \$ kg^{-1}) in the Twin Cities (Minnesota) area to approximately 2895 \$ t^{-1} (~3 \$ kg^{-1}) in the Phoenix (Arizona) region. The higher cost in Twin Cities compared to Phoenix may be attributed to the three times lower productivity in this region. Predictably, microalgae prices were comparable between Phoenix (Arizona), San Diego (California) and Albuquerque (New Mexico), ranging between about 2895 \$ t^{-1} (~3 \$ kg^{-1}) to about 3450 \$ t^{-1} (~3.5 \$ kg^{-1}), presumably owing to the similar climatic conditions among the locations. Thus, geographical location was found to play a crucial role and must be carefully considered when designing such outdoor photobioreactors to ensure the commercial and economic fruitfulness of such facilities.

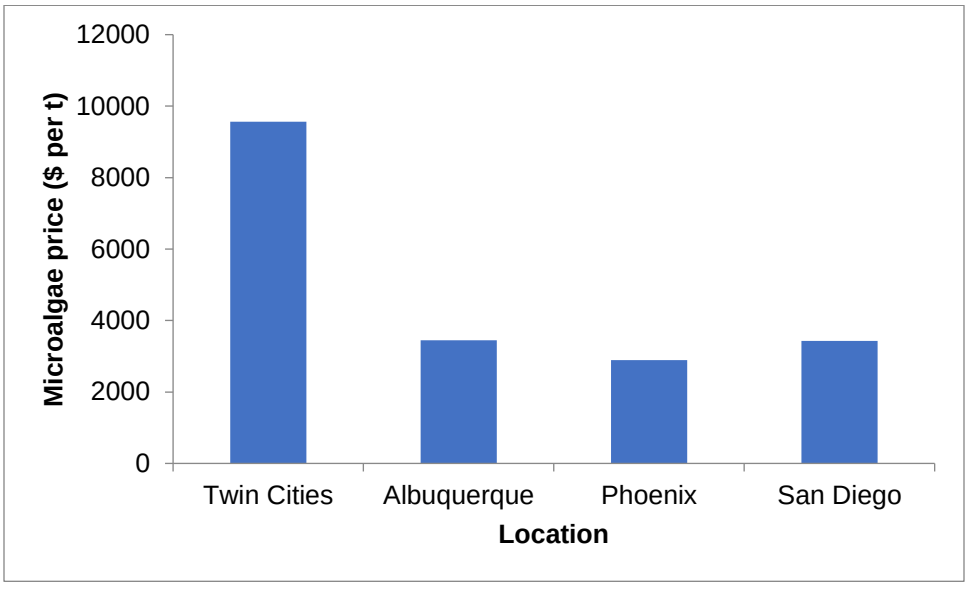

Figure 3. 6. Cost of microalgae cultivation for the different locations

3.5 Discussion

The aims of the present study were to model microalgae productivity in outdoor commercial scale flat panel photobioreactors and carry out the corresponding economic analysis to determine microalgae costs from commercial scale production systems. The mathematical microalgae growth model constructed here was based on a solid foundation of detailed heat and mass transfer integrated with biological growth kinetics. The model was enhanced by the incorporation of geographical factors to elucidate impacts of geospatial variabilities on microalgae productivity and cultivation costs. While direct validation through experimental data from commercial year-round microalgae cultivation systems is not practical due to a lack of availability of information, comparison with existing experimental data in the literature supports the validity of the model proposed here. For example, reports suggest that the productivity of flat panel bioreactors based in Netherlands, France and Algeria are 12000 t km^{-2} $year^{-1}$, 12900 t km^{-2} $year^{-1}$ and 15900 t km^{-2} $year^{-1}$, respectively [42]. For the Tuscan coast in Italy, productivity of *T. suecica* was found to be 3600 t km^{-2} $year^{-1}$ for 8 months of operation [174]. The results from the present study ranging from 3800 – 13000 t km^{-2} $year^{-1}$ are well within the reported range, although it is worth mentioning that a different algal strain was considered here.

Techno-economic analyses for microalgae cultivation utilization are generally focused on the downstream processing of microalgae to bioproducts and tend to assume values for microalgae productivity or feedstock costs [103,114,121,122,156], thereby generating considerable uncertainties. In the present study, mathematically determined microalgae productivities were utilized for in-depth economic and sensitivity analyses to ultimately determine the economic feasibility of large-scale microalgae cultivation in flat panel bioreactors. This methodology together with the incorporation of geospatial factors

is well-suited for the determination of microalgae production costs. The results obtained here ranged between approximately 3 – 10 \$ kg^{-1} for the different locations. In comparison, a recent study carried out by Tredici *et al*. where detailed economic analysis of *T. suecica* cultivated in flat panel photobioreactors in a 1 ha plant located in Italy and Tunisia were performed, the corresponding prices were found to be 14.5 \$ kg^{-1} and 7.3 \$ kg^{-1} respectively [170]. Other researchers have reported production costs in large scale photobioreactors in the range of approximately 0.50 – 29 \$ kg^{-1} [18,112,158,175]. These results from published articles are reasonably comparable to those obtained from the current analysis and reinforce the suitability of the novel methodology employed here.

3.6 Conclusion

Microalgae-based biorefineries, currently in the nascent stages of commercial development, are often viewed as financially precarious due to the many economic and technical uncertainties they are associated with. To circumvent these difficulties and ensure their commercial success, there is need for a clear understanding of microalgae growth, harvest, and the influence of process parameters on these processes. The first principles-based microalgae growth model for a given microalgal species developed in this study is a significant step forward in predicting algae productivity for a particular geographical location. The economic analysis in the study demonstrated the total capital and operating costs of microalgae cultivation in flat panel photobioreactors operated on an industrial scale. Correspondingly, the microalgae production cost was determined based on the capital and operating expenditures for four different locations. A sensitivity analysis helped to quantify the influence of biological and process engineering parameters on total production costs. The multifaceted approach presented here may be applied to other geographic locations in the world and other microalgal species provided that the relevant climatic variables and biological growth kinetic parameters are available. The

present techno-economic analysis confirms that microalgae-based technologies have substantial potential for generation of food, feed, pharmaceuticals and nutraceuticals. However, the challenges that commercial biorefineries continue to face include the availability of raw materials, nutrients, and competition over land and water resources. Further research is thus essential to provide the technological knowhow to overcome such challenges and implement economically robust and environmentally sustainable approaches to microalgae cultivation and utilization.

Chapter 4. Process model and techno-economic analysis of natural astaxanthin production from microalgae incorporating geospatial variabilities

4.1 Introduction

An increase in global population, the corresponding rise in demand for energy, food, feed and fiber, and the need to curtail atmospheric greenhouse gas emissions to limit climate change, has sparked much interest in the pursuit of renewable resources. Microalgae is one such option with enormous potential to meet some of these growing demands in a sustainable manner [35,88]. Microalgae are a versatile bio-based feedstock capable of producing multiple compounds including lipids, proteins, carbohydrates, and carotenoids [35,36,84]. Although microalgae have often been touted as an attractive feedstock for biofuels and bioenergy production, its economic feasibility is yet to be established [11,158,175]. Hence, investigation of the synthesis of high-value bioproducts and chemicals from microalgae is critical to understand the economic implications of commercial scale microalgae-based biorefineries. Microalgae, when cultivated under specific conditions can accumulate secondary metabolites such as carotenoids besides lipids, carbohydrates and proteins. These secondary metabolites are valuable compounds with a variety of industrial applications and the potential to significantly impact the transition towards a bioproduct-based economy [77,88].

Among the different metabolites synthesized by microalgae, astaxanthin is often considered as one of the most valuable with applications ranging from feed to the cosmetic and pharmaceutical industry, due to its anti-aging, anti-inflammatory properties [28,86,88,90,176,177]. The market potential for the carotenoid industry has been estimated at about $1.21 billion in 2015 and has been on the rise due to the growing interest in the use of these compounds in the food and feed sector [88]. Among the

different carotenoids, commercial market price of astaxanthin is about $2000 - $7000 kg^{-1}, with a global market potential estimated at $447M in 2014 [84,86,88–90]. The production cost of synthetic astaxanthin, which dominates more than 95% of the commercial astaxanthin market [86], is significantly lower in comparison and is estimated at about $1000 kg^{-1} [91]. Since synthetic astaxanthin is primarily produced from fossil fuel-based resources, and poses risks of toxicity, food safety, as well as sustainability, it is unfit for direct human consumption and is only used in aquaculture [91]. Because of this shortcoming pertaining to food safety coupled with a growing interest in natural products, algae-based astaxanthin has emerged as a viable alternative to synthetic astaxanthin [91,92].

Among the different algal strains, the freshwater algae, *Haematococcus pluvialis* has the highest concentration of astaxanthin and is considered a viable source of natural astaxanthin [88,178]. Information regarding astaxanthin production on a commercial scale is limited as most studies have been executed at laboratory and pilot scales. Moreover, information about the economic implications of commercial scale cultivation of natural astaxanthin and its cost competitiveness with synthetic astaxanthin is scarce in literature [79,86,91]. One of the primary aims of this part of the study is to address this gap in current knowledge. To do so, process models to quantify productivity potential of natural astaxanthin from *Haematococcus pluvialis* considering geospatial variabilities were constructed. Detailed economic analyses were also performed to evaluate the production cost of natural astaxanthin and to assess the economic feasibility in comparison to synthetic astaxanthin for the different locations. The current work is intended to provide researchers, entrepreneurs and policymakers information about the economic competitiveness of natural astaxanthin production from microalgae.

4.2 Methods

In order to quantify the productivity potential of natural astaxanthin from microalgae, detailed process models for algal growth, harvesting and extraction, were developed. *Haematococcus pluvialis* is a unique species that may be cultivated in two stages, the 'green stage' and 'red stage' respectively, to optimize production efficiency and maximize astaxanthin productivity [79,179–181]. In the 'green stage', microalgae cells replicate by cell division and proliferation, thereby synthesizing chlorophyll, whereas in the 'red stage' due to the absence of growth nutrients, cell division is impeded and chlorophyll levels remain constant leading to accumulation of astaxanthin [182,183]. Consequently, in order to maximize astaxanthin production, a hybrid set of reactor systems combing the 'green stage' and 'red stage' have been proposed [179,181]. Although a single stage strategy for astaxanthin production from *Haematococcus pluvialis* has been reported in literature resulting in decreased complexity of the cultivation system and making it more economical, astaxanthin productivity is significantly less efficient in a one-step cultivation process compared to the two-step strategy [181]. Thus, to achieve maximal astaxanthin productivity, a two-stage hybrid cultivation system was utilized in the current study [91]. To facilitate microalgae cell proliferation and growth under ambient conditions ('green stage'), a flat panel photobioreactor system is used, followed by open raceway ponds where microalgae are cultivated in stressful conditions to impede growth and elicit the accumulation of astaxanthin ('red stage'). Open raceway ponds are used for the 'red stage' to offset the higher costs of algae cultivation in photobioreactors. Also, existing literature suggests that it is comparatively easier to induce stress conditions in open raceways for greater astaxanthin accumulation during the 'red stage' [91]. The hybrid reactor system is considered to have equally sized reactors, each comprising an area of 1 hectare as suggested previously [86]. Microalgae cultivation stage is followed by the harvesting

phase and extraction of astaxanthin. In the harvesting phase, microalgae slurry is subjected to dewatering to obtain a paste with a desired moisture content which is followed by suitable extraction steps for recovery of astaxanthin. The details of algae cultivation, harvesting and extraction phases are discussed in greater details in the Models (Section 4.3) part of the study.

To understand the implications of geospatial variabilities on astaxanthin productivity, hypothetical commercial scale astaxanthin models developed here were extended to four locations in the United States – Minnesota (Minneapolis), California (San Diego), New Mexico (Albuquerque) and Arizona (Phoenix). As microalgae growth and productivity are heavily influenced by local climatic parameters, the extension of the models to the different locations assisted in the quantification of commercial scale astaxanthin production by incorporating geospatial effects [163,166].

Based on annual astaxanthin productivity, detailed mass and energy balances were quantified for the entire supply chain of algae cultivation, harvesting and astaxanthin extraction. The capital and operating costs were further estimated to determine the commercial cost of astaxanthin production ($\$ kg^{-1}$) for the different locations. Furthermore, a Profit and Loss (P&L) analysis was executed to interpret the economic implications of astaxanthin cultivation for the chosen locations. The P&L analysis is a financial model that incorporates profits as determined by commercial price of astaxanthin and astaxanthin extracted biomass to determine the return on investment (ROI) for the hypothetical locations [86]. The system boundary considered for the value-chain of astaxanthin production which includes algae cultivation, harvesting, pigment extraction, and subsequent economic analysis is provided in Figure 4.1. Since, combined process modeling and economic analysis of microalgae-based high-value products are scarce in literature, the detailed process modeling and corresponding economic analysis presented

in this study are significant steps forward and are designed to inform policy makers and researchers of location suitability and economic implications of microalgae-based natural astaxanthin production.

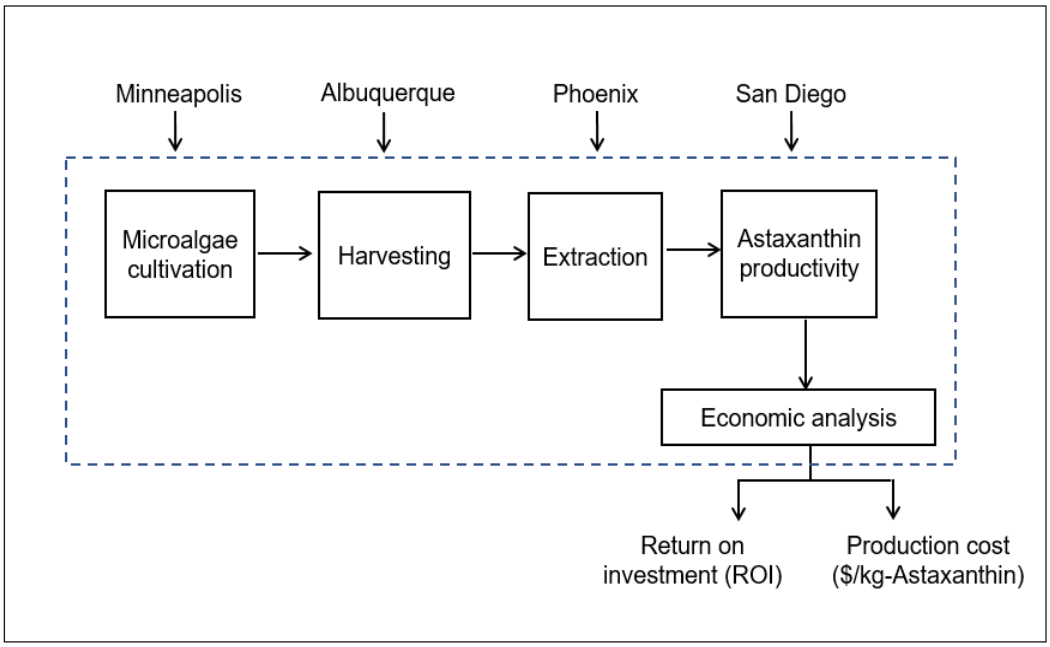

Figure 4. 1. Process flow diagram of natural astaxanthin production and corresponding economic analysis

4.3 Models

4.3.1 Algae cultivation

To model *Haematococcus pluvialis* growth and productivity, a hybrid system of flat panel photobioreactor and open raceway pond system was considered in the study. The 'green stage' for microalgae growth and cell proliferation was modeled based on algae growth in flat panel photobioreactors whereas the 'red stage' for astaxanthin accumulation under stress growth conditions was modeled considering open raceway ponds cultivation. To quantify algae productivity in flat panel photobioreactors, the methodology described in Chapter 3 and applied in our previous work was adopted here [166] . The first step in

determining algae productivity for a location constitutes the development of a quantitative model to delineate culture temperature profile of algae growth in flat panel photobioreactors. The main inputs to the quantitative model were hourly values of direct and diffuse solar radiation, ambient air temperature, wind velocity and relative humidity for the location as obtained from national database [167]. The results from the heat and mass transfer model were further coupled with a detailed microalgae growth kinetics model to determine algae productivity in the reactor. Microalgae require copious amounts of carbon dioxide (CO_2) and nitrogen and phosphorus based nutrients for growth [11]. In the present study it was assumed that the growth reactors are supplied with the necessary CO_2, and urea and Diammonium phosphate (DAP) as sources of nitrogen and phosphorus respectively as described in Chapter 3. To determine algae productivity potential, a detailed biological growth kinetics model was developed which took into account light intensity and temperature profile in the growth reactor, rates of photosynthesis and respiration of *Haematococcus pluvialis*, and uptake rates of CO_2, nitrogen and phosphorus-based nutrients. Oxygen is a by-product of microalgae photosynthesis and its presence in the culture medium often impedes algal growth [162]. Oxygen level in the solution beyond a concentration of 25 – 40 mg $litre^{-1}$ of solution is detrimental to algal heath [13]. To circumvent this issue, flat panel photobioreactors are provided with degassers to vent off the oxygen to facilitate algae growth. In the present study, it was assumed that the microalgae growth reactors were facilitated with flue gases as the source of CO_2 with a concentration of 10% (v/v) [32,184]. Previously, researchers have determined algae productivity based on empirical correlations [86] or on pilot scale which was further scaled up to determine astaxanthin production in Kunming, China [91]. Although this is an excellent starting point for the analysis of commercial scale natural astaxanthin production, scaling up pilot scale data inherently leads to uncertainties since pilot studies are performed in highly regulated environments. Hence, development of the

microalgae productivity model is highly beneficial to the assessment of the implications of industrial scale natural astaxanthin production.

Following growth in flat panel photobioreactors, microalgae are transferred to open raceway ponds via conveyer belts where they are cultivated in stress conditions to induce astaxanthin accumulation [185]. This is known as the 'red stage' in *Haematococcus pluvialis* in hybrid reactor system. In this study, microalgae are considered to be cultivated in 1-hectare ponds 0.3 m deep, facilitated by paddlewheels for efficient mixing. Details of raceway pond construction and operation are described in greater detail in literature [163], and have also been addressed in Chapter 2. The same approach was adopted in the current study for *Haematococcus pluvialis* cultivation in open raceway ponds. In the 'red stage', microalgae are cultivated under stress conditions in the absence of nutrients to inhibit cell proliferation and promote astaxanthin accumulation. Thus, in the absence of nitrogen and phosphorus-based nutrients supply, the required CO_2 is supplied in the open raceway ponds by submerged aerators.

4.3.2 Microalgae harvesting

Microalgae harvesting is an important step following microalgae growth and often constitutes a significant fraction of microalgae production costs [35,94,121,128]. The high harvesting costs of microalgal biomass are mainly attributed to the low cellular concentration of microalgae in the growth medium, ranging from 0.3-5 kg m^{-3} as well as the very small cell size of microalgae which ranges from 2 – 40 µm [86]. Also, faster growth rates and higher productivity of microalgae in comparison to terrestrial biomass necessitates frequent and robust harvesting methods [35,186,187]. For microalgae harvesting, generally a two-step methodology is prevalent in literature [187,188]. First in the two-step method, microalgae solution is harvested by organic or bioflocculants followed by a primary dewatering step that transforms the solution into a slurry with 2-7%

solids concentration. In the second step, a secondary dewatering step is often applied to produce a microalgal paste with about 15-25% solids concentration after drying. Currently in algae cultivation, mechanical, chemical and biological harvesting techniques are widely implemented for harvesting [186,187].

In the present study, a two-step dewatering technique involving the addition of an organic flocculants to facilitate primary dewatering followed by centrifugation as the secondary dewatering step was applied, as described in chapters 2 and 3. It has been established in literature that a two-step algae harvesting method by bio-flocculation or mechanical harvesting followed by centrifugation is ideal for astaxanthin extraction from *Haematococcus pluvialis* [91,92,176,189]. Microalgae dewatering by centrifugation is an extremely energy intensive process and well suited for extraction of high-value products from microalgae like polyunsaturated fatty acids, as well as nutraceuticals and pharmaceuticals [186]. Additionally, due to its short operational time and applicability towards different algal strains without the risk of contamination, it is often considered as a very reliable process and applied for commercial scale cultivation [190–192]. For microalgae harvesting in the present study, it was assumed that first a polyacrylamide flocculent was added in order to partially separate and harvest the algal cells in the solution, followed by primary dewatering facilitated by lamella clarifiers which results in algal slurry of 30 kg m^{-3} concentration [10,128]. In the secondary dewatering step, centrifugation was applied to produce an algal paste with 20% suspended solids concentration. Thus, the resulting final microalgae concentration in the solution was 200 kg m^{-3}.

4.3.3 Astaxanthin extraction

Following algae harvesting, extraction of astaxanthin is the most critical step in the value-chain of natural astaxanthin production. Commercial production, economic

feasibility and successful marketing of natural astaxanthin in comparison to synthetic fossil fuel-derived astaxanthin depends heavily on a successful and efficient extraction phase. *Haematococcus pluvialis* are often characterized by having a tough exterior wall composed of spores and pollen grains. Due to the presence of this tough exterior wall or sporopollenin, astaxanthin extraction from the intracellular part may be inefficient [189,193]. Consequently, astaxanthin extraction occurs in three primary steps – 1) cell disruption, 2) cell dehydration and 3) recovery of the desired carotenoid [92,194]. For algal cell disruption, bead milling, an efficient process to disrupt algal cells in a solution with a concentration of 100 – 200 kg m^{-3} was considered [195]. This is followed by dehydration of the disrupted cells rapidly to minimize the risk of cell degradation. For the dehydration step, spray drying, a process that has been successfully implemented previously to extend shelf-life of high-value products from microalgal biomass was considered in the current study [35,79,193]. It was also assumed that the efficiency of this method for the recovery of dry biomass is 95% [196,197]. After cell disruption by bead milling and cell dehydration by spray drying, recovery of the desired carotenoid becomes easier since intracellular materials are now only encapsulated by the thin walls of the cell [86]. An efficient and widely accepted way of extracting desired metabolites from microalgae is by supercritical fluid extraction [198,199]. Supercritical CO_2 extraction is an attractive option for carotenoid production from microalgae due to its critical temperature and pressure (31.1 ^oC and 7.4 Mpa, respectively). Furthermore, since it remains in the gaseous state at ambient conditions, it can be recovered easily [200–202]. In the present study, it was assumed that astaxanthin extraction from microalgae was performed by super critical CO_2 extraction. Supercritical CO_2 at a temperature and pressure of 60 ^oC and 30 Mpa, respectively, mixed with 9.4% ethanol as a co-solvent was utilized for astaxanthin extraction as described in literature [86,203]. The resulting spent algal biomass after supercritical CO_2 extraction is often rich in protein and other chemical compounds and may be marketed as bio-fertilizer

[93]. In this case, it was assumed that the hypothetical biorefinery produces two main products – 1) astaxanthin, which has been fully extracted from *Haematococcus pluvialis* and 2) spent algal biomass after the carotenoid extraction. It was further assumed that both these products have a commercial demand and are sold in the market as substitutes for fossil fuels-based products. The value chain of natural astaxanthin production comprising the different stages of algae cultivation, harvesting and astaxanthin extraction is provided in Figure 4.2.

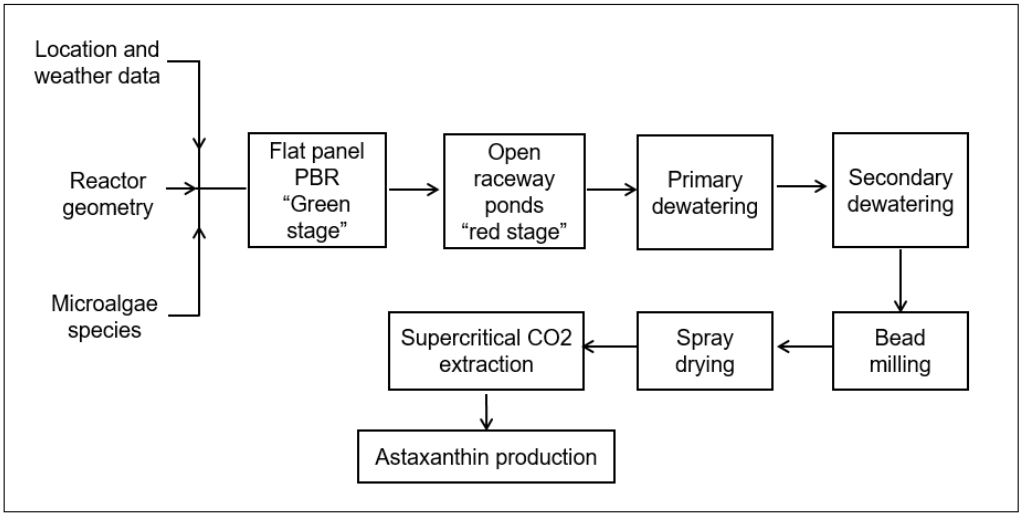

Figure 4. 2. Supply chain of natural astaxanthin production model

4.4 Results

4.4.1 Microalgae productivity and astaxanthin yield

Based on the combined heat and mass transfer model coupled with a biological growth kinetics model, microalgae productivity and corresponding astaxanthin yields were determined for the different locations. The model was first run separately to simulate microalgal growth and cell proliferation in the 'green stage' where cultivation takes place in the flat panel photobioreactors. Following the 'green stage', the model was used to simulate algae growth in the 'red stage' where the cells are subjected to nutrient starvation, thereby limiting cell division and growth, eventually resulting in astaxanthin production in the cells. The annual biomass productivities for the 'green' and 'red stages' for the four locations are provided in Table 4.1. Here, it is seen that under ambient conditions, when optimal amount of nutrients are supplied, the 'green stage' algal productivity ranges between 29 – 98 t ha^{-1} $year^{-1}$ for the different locations. The significant difference in productivity among the locations can mainly be attributed to local geographical variabilities. The results are similar to those obtained in our previous study that dealt with the productivity of *Nannochloropsis* in open raceways and flat panel photobioreactors [163,166] (described in chapters 2 and 3). Algal productivity in 'red stage' in considerably lower for all the locations due to growth inhibition leading to cell death and astaxanthin accumulation [91,181]. In this case, 'red stage' algal biomass productivity ranges from 15 – 54 t ha^{-1} $year^{-1}$ for the different locations which corresponds to about 45-48% decrease from the 'green stage'. Finally, based on the various harvesting and extracting strategies applied in the study, annual astaxanthin productivity was determined for the different locations.

Table 4. 1. Productivity of *Haematococcus pluvialis* cultivated in a hypothetical hybrid reactor system for different locations

Locations	'Green stage' productivity (t ha^{-1} $year^{-1}$)	'Red stage' productivity (t ha^{-1} $year^{-1}$)
Minneapolis	29	15
Albuquerque	85	46
Phoenix	98	54
San Diego	89	49

For the different locations studied, astaxanthin productivity from the hypothetical commercial scale cultivation model is depicted in Figure 4.3. Astaxanthin production in Phoenix is the highest at 1258 kg $year^{-1}$, and lowest in Minneapolis at 349 kg $year^{-1}$ which is only about 28% of the productivity potential in Phoenix, assuming the concentration of astaxanthin in the algae was identical among all the locations. This is primarily due to the corresponding lower microalgae productivity potential in Minneapolis that is about 73% less than that in Phoenix. This difference may be attributed to the different geospatial conditions and climate factors. Astaxanthin productivity potential for Albuquerque, Phoenix and San Diego are similar at 1071 kg $year^{-1}$, 1258 kg $year^{-1}$, 1141 kg $year^{-1}$, respectively primarily due to the similar microalgae productivity potential for the locations characterized by similar geospatial variable and climate patterns. Thus, for Phoenix, San Diego and Albuquerque, astaxanthin production are 3.6 times, 3.27 times and 3 times than astaxanthin productivity potential in Minneapolis. Thus, it is evident that the choice of location plays a critical role in establishing commercial scale microalgae-based refineries to achieve optimal performance.

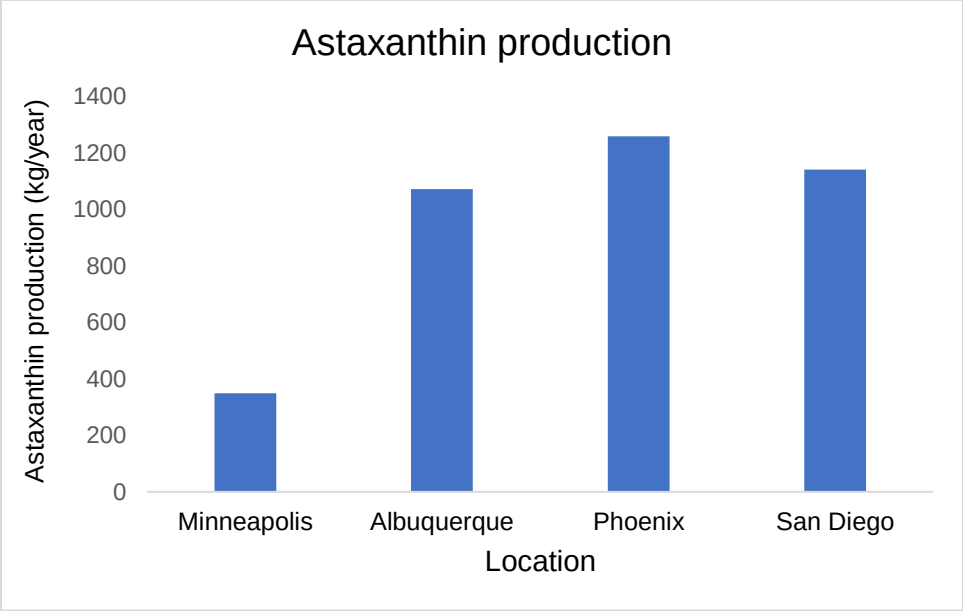

Figure 4. 3. Astaxanthin productivities incorporating geospatial variabilities

4.4.2 Economic analysis

To elucidate the financial implications and feasibility of commercial scale natural astaxanthin production, a detailed economic assessment was conducted to determine astaxanthin production costs, and extended to the different locations to highlight the effects of geospatial variabilities on production costs. Such a combined engineering and economic analysis is a significant step forward to understanding commercial implications of natural astaxanthin production from microalgae.

Natural astaxanthin cultivation in a hybrid system of photobioreactor and open raceways for the location of Albuquerque, New Mexico was considered as the baseline scenario. For algal cultivation and corresponding astaxanthin production, detailed capital costs estimate for the photobioreactor and open raceways, pumps, airlift systems, CO_2 storage tanks, sedimentation tanks and centrifuges were either obtained from literature or scaled accordingly [86,91,163,166]. Based on the total capital expenditure for the biorefinery, Lang factors were used to determine the direct, indirect and other costs for the

biorefinery. Lang factors are often used to determine the installed costs of a plant based on purchased equipment costs and have been well studied in literature [204,205]. The different Lang factors adopted in the study were obtained from previous literature [94] and presented in Table 4.2. Based on the Lang factors, total capital and operating expenditures for the natural astaxanthin plant were computed. The installation costs for the biorefinery is significant and was determined to be 47% of the major equipment costs. Instrumentation, control and piping infrastructure in a biorefinery are substantial investments and assumed to be 47% and 35% respectively, of the major equipment costs in this study [94]. Construction and engineering and supervision expenses were accounted for at 15% and 10% of the direct costs. Also, contingency and contractors' fees were considered as well in order to determine the other costs for the biorefinery. Major equipment cost is assumed to depreciate over 10 years with a 8% interest rate [94]. Purchase tax of the equipment are disregarded in the present study on the assumption that this may be recovered. The land and electricity prices for the hypothetical biorefinery for the different locations were obtained from our previous work (as provided in chapters 2 and 3). The total fixed capital investment of the biorefinery considering the different Lang factors in the study was estimated to be about 462% of the major equipment cost.

In determining the operating expenditure of the natural astaxanthin biorefinery, the amount of nitrogen and phosphorus-based nutrients and CO_2 required to facilitate algal growth in the hybrid system were computed through the mass and energy balances of each step of the supply chain. Utility requirements were determined similarly and adjusted from power requirement calculation in microalgae productivity in flat panel photobioreactors and open raceways. In order to ensure proper mixing of the culture medium to facilitate growth, flat panel photobioreactors and open raceway ponds were assumed to be facilitated by an airlift system and paddlewheels respectively. Power

consumption for mixing and circulation for airlifts and paddlewheels were quantified based on our previous work (explained in Chapters 2 and 3). Power requirements utilized for capture and compression of CO_2 from flue gas for the hybrid reactor system was taken as 0.2 kWh/$\mathrm{kg}_{\mathrm{CO}_2}$ [206]. Oxygen, a major byproduct of microalgae photosynthesis, is toxic to algal growth and needs to be removed. Flat panel photobioreactors were facilitated by degassers to remove oxygen from the culture medium. For open raceways, oxygen removal takes place by evaporation from the reactor through exposure to the atmosphere. Annual energy consumption for degassing used in the study is 47 MWh/hectare [13]. Power consumption for cooling the system is obtained and calculated based on available data [86,91]. For microalgae harvesting, the secondary step comprising algae dewatering and harvesting by centrifugation is an extremely energy intensive step. Power consumption by centrifuges is calculated to be 55kW on the basis of 10 hours of operation daily in the course of a year. Astaxanthin extraction by bead milling, spray drying, and supercritical CO_2 extraction consumes a significant amount of energy. The respective values used for the three extraction steps are 6.4 kWh/$\mathrm{kg}_{\mathrm{algae}}$, 103.4 kWh/$\mathrm{kg}_{\mathrm{astaxanthin}}$, and 158 kWh/$\mathrm{kg}_{\mathrm{astaxanthin}}$, respectively after being adjusted to the current scale of the system [86,93]. Based on these different factors and assumptions, capital and operating expenditures of natural astaxanthin production plant were quantified.

Using the natural astaxanthin production model, detailed economic analysis was conducted to determine astaxanthin production costs for the different locations. First, the results of the economic analysis for the hypothetical plant in Albuquerque, New Mexico is discussed. Based on annual productivity of 1071 kg $year^{-1}$, astaxanthin production cost at a hypothetical plant in New Mexico is 1595 \$ kg^{-1}. Contribution of capital and operating estimates are almost equal at 50% each. For the commercial scale production, the capital expenditure and operating expenditure are \$ 862,650 $year^{-1}$ and \$ 846,384 $year^{-1}$,

respectively. The breakdown of the capital and operating expenditure of the plant is provided in Tables 4.3 and 4.4 respectively. Also, contributions of the different capital and operating costs are provided in Figures 4.4 and 4.5 respectively. From these figures, it is seen that the cost of the dual photobioreactor and open raceway system as well as the cost of pumps and other equipment incur the major expenditure. Together, they contribute about 70% of the total capital expenditure. For operating costs, overheads and wages of workers, supervisors, and biologists have the greatest impact on the expenditure. Together, they are responsible for 75% of the total capital expenditure for the hypothetical plant in Albuquerque, New Mexico.

Table 4. 2. Capital costs estimates for biorefinery [94]

Direct Costs (DC)	Major Equipment Costs (MEC)	
	Installation costs	47% MEC
	Instrumentation and control	35% MEC
	Piping	40% MEC
	Insulation	8% MEC
	Electrical	10% MEC
	Buildings	18% MEC
	Land improvements	10% MEC
	Service facilities	40% MEC
Indirect costs (IC)	Construction expenses	15% DC
	Engineering and Supervision	10% DC
Other costs (OC)	Contractor's fee	5% (DC+IC)
	Contingency (Major equipment)	15% (DC+IC)
Fixed Capital Investment		DC+IC+OC

	Depreciation	(DC+IC+OC)/10
	Interest	8% Depreciation
	Property tax	1% (Depreciation + interest)
	Insurance	0.6% (Depreciation + interest)
Total Capital Expenditure		Depreciation + Interest + Property tax + Insurance

Table 4. 3. Capital costs estimate of astaxanthin production in hypothetical plant in Albuquerque, New Mexico

			Capital expenditure ($)	**Capital expenditure ($ kg astaxanthin^{-1})**
		Photobioreactor cost	540,697	505
		Open raceway ponds	139,908	131
		Airlift system	41140	38
		Pumps and other equipment	497,022	464
		CO_2 storage tank	38720	36
		Sedimentation tank	22000	21
		Centrifuge	63800	60
		Centrifuge feed pump	12529	12
		Biomass conveyer belt	13750	13
		Biomass storage tank	19360	18

		Bead miller	66000	62
		Spray dryer	29040	27
		Supercritical CO_2 extractor	93500	87
		Packaging line	22000	21
		Laboratory equipment	88000	82
	Major Equipment Cost (MEC)		**1,687,466**	**1575**
	Installation costs	47% MEC	793109	740
	Instrumentation and control	35% MEC	590613	551
	Piping	40% MEC	674989	630
	Insulation	8% MEC	134997	126
	Electrical	10% MEC	168747	158
	Buildings	18% MEC	303744	284
	Land improvements	10% MEC	168747	158
	Service facilities	40% MEC	674989	630
Total Direct Costs (DC)			**5,197,395**	**4851**
	Construction expenses	15% DC	779609	728
	Engineering and Supervision	10% DC	519739	485
Indirect costs (IC)			**1,299,349**	**1213**
	Contractor's fee	5% (DC+IC)	324837	303
	Contingency (Major equipment)	15% (DC+IC)	974512	910

Other Costs (OC)			**1,299,349**	**1213**
Fixed capital investment (FCI)		**DC+IC+OC**	**7,796,092**	**7277**
	Depreciation	(DC+IC+OC)/10	779609	728
	Interest	8% Depreciation	62369	58
	Property tax	1% (Depreciation + interest)	8420	8
	Insurance	0.6% (Depreciation + interest)	5052	5
	Land	2 hectares	7200	7
Total capital expenditure ($ year^{-1})			**862650**	**805**

Table 4. 4. Operating costs estimate of astaxanthin production in hypothetical plant in Albuquerque, New Mexico

	Operating expenditure ($)	**Operating expenditure ($ kg astaxanthin $^{-1}$)**
Raw materials	25282	24
CO_2 distribution	5500	5
Water (including recycling)	14168	13
Power – mixing/circulation	15094	14
Power – flue gas supply	32223	3
Power – oxygen removal	2890	3
Power – water pumping	4102	4

Power - cooling	19680	18
Power - centrifuge	12346	12
Power – bead milling	18106	17
Power – spray drying	6946	6
Power – supercritical CO_2 extraction	13291	12
Worker salary (8 workers)	197736	185
Supervisor salary (2 supervisors)	111280	104
Biologist salary (2 biologists)	74900	70
Maintenance	67499	63
Operating supply	541	1
Contingency	5918	6
Overhead	248278	232
Total operating expenditure ($ year^{-1})	846777	790

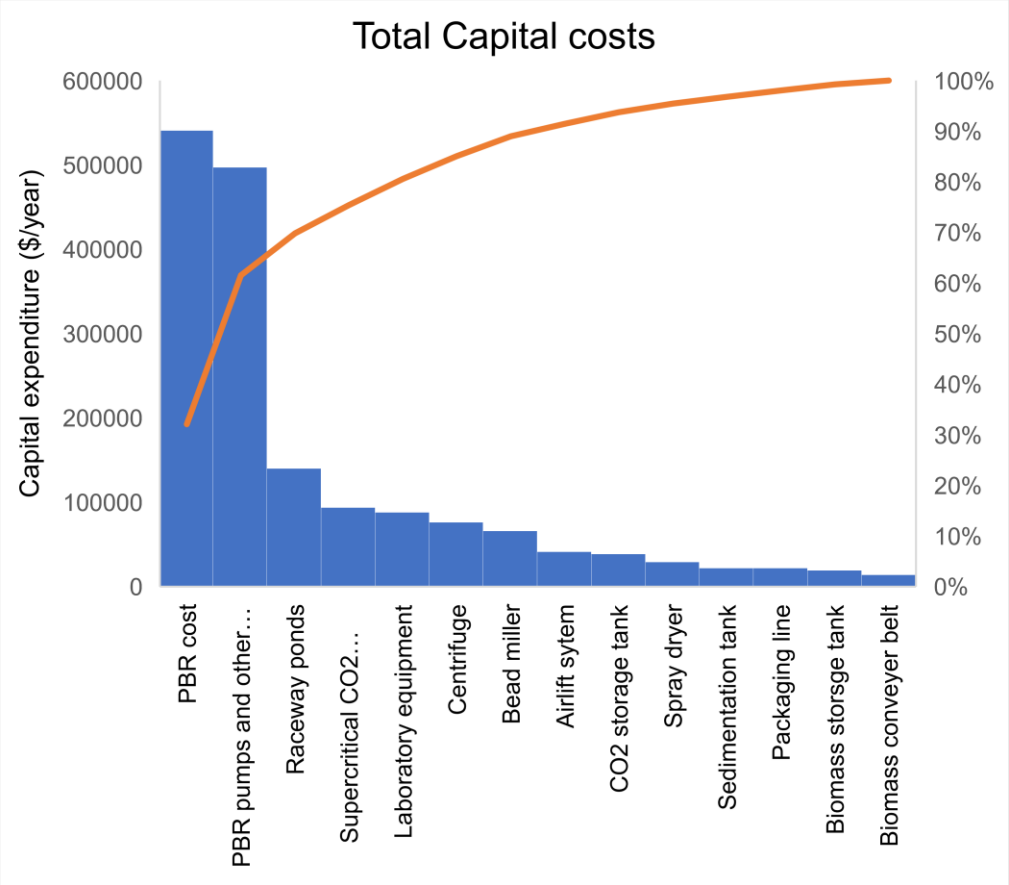

Figure 4. 4. Capital cost contribution for natural astaxanthin production plant in Albuquerque, New Mexico

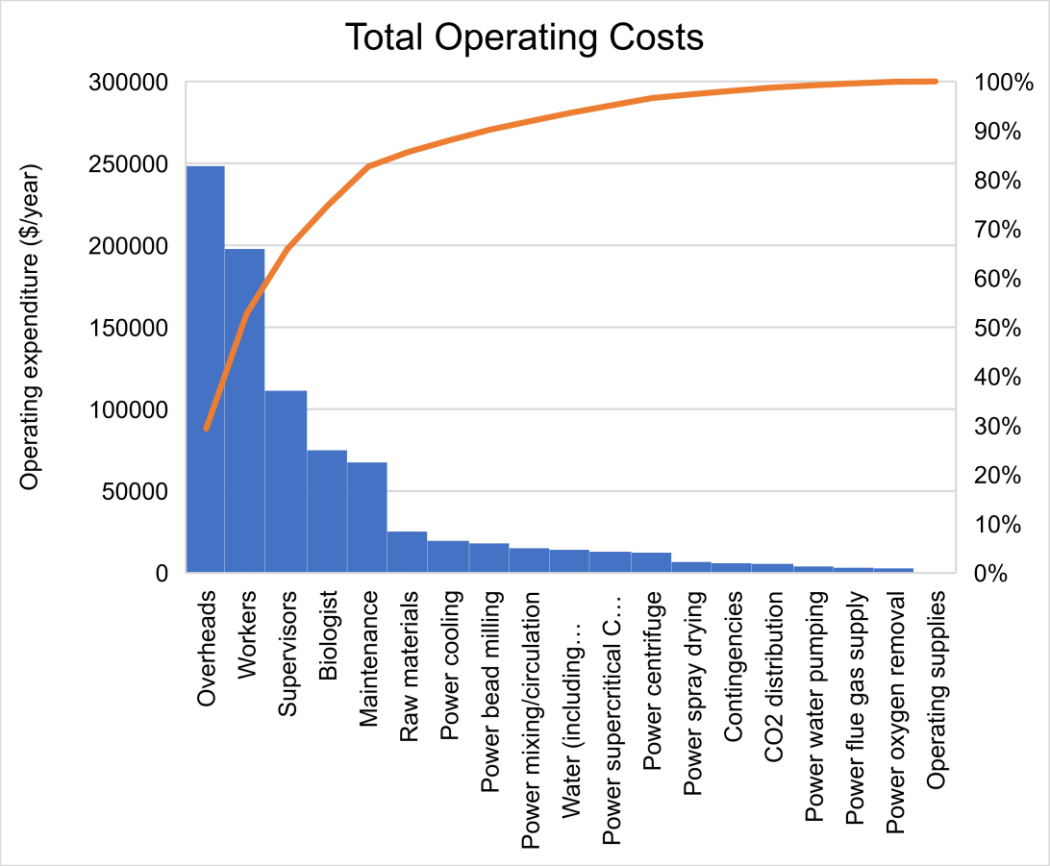

Figure 4. 5. Operating cost contribution for natural astaxanthin production plant in Albuquerque, New Mexico

4.4.3 Comparative analysis of the effect of geospatial variabilities on natural astaxanthin production cost

To understand the influence of geospatial variabilities on the economic implications of commercial scale natural astaxanthin cultivation, the economic analysis model was extended to the different locations. Such an approach helped to determine natural astaxanthin production costs for the locations considering spatial variabilities. In order to simplify the economic analysis model, it was assumed that the only differences among the locations are land prices and electricity prices besides astaxanthin productivity potential. Capital costs of the cultivation systems, harvesting and extraction systems as well as other

operating costs like costs of nutrients and CO_2, flocculants, wages of supervisors, biologists and workers were assumed to be same for the studied locations. Such an assumption has been used in our previous work [163,166] and is explained in Chapter 2 and 3. This is indeed a simplification and the incorporation of these factors may help determine natural astaxanthin production costs even more accurately.

Natural astaxanthin production costs for the different locations are shown in Figure 4.6. Production costs vary greatly among the different locations and range from 1365 – 4884 \$ kg^{-1}. Natural astaxanthin production cost is lowest in Phoenix at 1365 \$ kg^{-1} and highest in Minneapolis at 4884 \$ kg^{-1}. For Albuquerque and San Diego, Astaxanthin production costs are 1595 and 1626 \$ kg^{-1}, respectively. Such significant differences may be attributed to the differences in astaxanthin productivity among the locations. Since astaxanthin productivity in Minneapolis is only about 28% than that in Phoenix, which is a location characterized by highest astaxanthin productivity, corresponding production cost in Minneapolis is 3.6 times than production cost in Phoenix. Similarly, astaxanthin production costs in Albuquerque and San Diego are about 33% of natural astaxanthin production costs in Minneapolis. It is interesting to note that although yearly productivity in Albuquerque is less than that in San Diego by about 6%, astaxanthin cost in San Diego is about 2% higher than in Albuquerque. This higher production cost despite higher astaxanthin productivity in San Diego is mainly due to the differences in the land and electricity prices of the two locations. The yearly capital and operating expenditure of hypothetical astaxanthin production plants for the different locations are provided in Table 4.5. From the detailed economic analysis, it can be inferred that location choice for natural astaxanthin production is extremely important for its economic feasibility. Hence, the commercial success of natural astaxanthin is very much location dependent as geospatial

variability plays a crucial role in determining productivity thereby impacting production costs significantly.

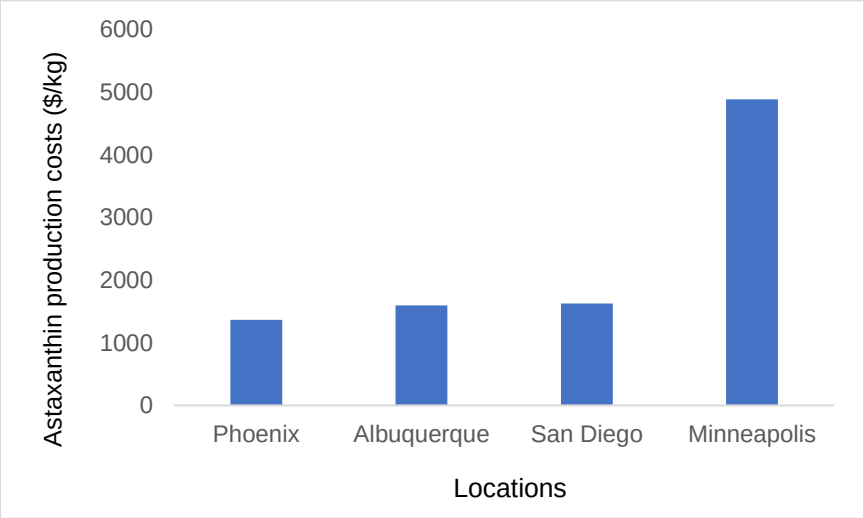

Figure 4. 6. Astaxanthin production costs incorporating geospatial variabilities

Table 4. 5. Capital and operating expenditures of hypothetical natural astaxanthin production plants

	Capital expenditure ($ year^{-1})	Operating expenditure ($ year^{-1})
Minneapolis	879200	827000
Albuquerque	862650	846384
Phoenix	864150	853444
San Diego	908950	947927

4.4.4 Profit and loss (P&L) analysis

In order to understand the economic implications of commercial scale natural astaxanthin production plant, a P&L analysis was conducted. This is a financial statement that helps determine the total revenues and total expenditure of the plant and on the basis of which the Return on Investment (ROI) for the plants are determined. ROI is a valuable economic metric which is often used in business to determine the financial attractiveness

of the company and industry [207–209]. ROI for the commercial scale natural astaxanthin plant is calculated by the following equation:

$$ROI = \frac{CAD}{CAPEX} * 100\%$$

where, CAPEX is the total capital expenditure for the plant, CAD is the available cash that it distributed to the different stakeholders. CAD is computed by subtracting corporate taxes from Earnings before interest, tax, depreciation and amortization (EBITDA). EBITDA is an important metric often used in industry to compare and analyze profitability between organizations and industries [208,209]. In the present study, amortization and interests are not considered under the assumption that no financing has been obtained for the construction and operations of the plant. Apart from ROI, the payback period for the hypothetical facilities are also computed to understand the time required for the initial capital investment to be recovered.

To conduct the P&L analysis and assess economic feasibility for natural astaxanthin production plants for the different locations, several scenarios were considered by varying astaxanthin market prices to 1500, 2000, 2500, 3000, 4000, 5000, and 6000 \$ kg^{-1}. Since the residual biomass after astaxanthin extraction can be utilized as a bio-fertilizer, it is assumed to be sold in the market to gain financial returns. In this study, market price of bio-fertilizer was assumed to be 33.5 \$ kg^{-1} [86]. Based on the analysis, ROI for New Mexico (Albuquerque), Minnesota (Minneapolis), Arizona (Phoenix) and California (San Diego) are calculated at 16.92 – 50.25%, -0.58 – 14.94%, 20.6 – 59.73%, and 17.42 – 52.92%, respectively. Correspondingly, the payback period for the hypothetical plants at the locations are calculated at 14.5 – 2.5 years, -9.4 – 20.2 years, 9.4 – 2 years, and 13.5 – 2.3 years, respectively, with the different astaxanthin market prices. P&L analysis for Arizona and Minnesota are provided in Table 4.6 and 4.7,

respectively. Results of the P&L analysis indicate that economic feasibility of natural astaxanthin production is highly dependent on location. For New Mexico (Phoenix), Arizona (Phoenix) and California (San Diego), the high ROI indicates microalgae-based commercial scale astaxanthin production is indeed feasible in these locations with proper exploitation of the astaxanthin derived residual biomass. It may also be inferred that commercial natural astaxanthin production is not favorable in Minnesota primarily due to the very low astaxanthin productivity which resulted in significant higher astaxanthin production costs in comparison to other locations.

Table 4. 6. P&L analysis for natural astaxanthin production plant in Arizona (Phoenix)

Market Price ($/kg)	Astaxanthin	1500	2000	2500	3000	3500	4000	5000	6000
Market Price ($/kg)	Astaxanthin extracted algae	33.5	33.5	33.5	33.5	33.5	33.5	33.5	33.5
Quantity (kg)	Axtaxanthin	1258	1257.6438	1257.6438	1257.6438	1257.6438	1257.6438	1257.6438	1257.6438
Quantity (kg)	Astaxanthin extracted algae	52742	52742.356	52742.356	52742.356	52742.356	52742.356	52742.356	52742.356
Gross revenue ($)		3,653,335	4,282,157	4,910,978	5,539,800	6,168,622	6,797,444	8,055,088	9,312,732
VAT (23%) ($)		840,267	984,896	1,129,525	1,274,154	1,418,783	1,563,412	1,852,670	2,141,928
Total revenue ($)	Gross revenue - VAT	2,813,068	3,297,261	3,781,453	4,265,646	4,749,839	5,234,032	6,202,418	7,170,803
OPEX ($)		852,985	852,985	852,985	852,985	852,985	852,985	852,985	852,985
EBITDA ($)	Total revenue - OPEX	1,960,082	2,444,275	2,928,468	3,412,661	3,896,854	4,381,047	5,349,432	6,317,818
Depreciation ($)	10%	779,609	779,609	779,609	779,609	779,609	779,609	779,609	779,609
EBIT or EBT ($)		1,180,473	1,664,666	2,148,859	2,633,052	3,117,245	3,601,438	4,569,823	5,538,209
Tax ($)	30%	354,142	499,400	644,658	789,916	935,173	1,080,431	1,370,947	1,661,463
EAT ($)		826,331	1,165,266	1,504,201	1,843,136	2,182,071	2,521,006	3,198,876	3,876,746
CAD ($)		1,605,940	1,944,875	2,283,810	2,622,745	2,961,680	3,300,615	3,978,485	4,656,356
FCI/CAPEX ($)		7,796,092	7,796,092	7,796,092	7,796,092	7,796,092	7,796,092	7,796,092	7,796,092
ROI		20.60%	24.95%	29.29%	33.64%	37.99%	42.34%	51.03%	59.73%
Payback period (years)		9.4	6.7	5.2	4.2	3.6	3.1	2.4	2.0

Table 4. 7. P&L analysis for natural astaxanthin production plant in Minnesota (Minneapolis)

Market Price ($/kg)	Astaxanthin	1500	2000	2500	3000	3500	4000	5000	6000
Market Price ($/kg)	Astaxanthin extracted algae	33.5	33.5	33.5	33.5	33.5	33.5	33.5	33.5
Quantity (kg)	Axtaxanthin	349	349.3455	349.3455	349.3455	349.3455	349.3455	349.3455	349.3455
Quantity (kg)	Astaxanthin extracted algae	14651	14650.6545	14650.6545	14650.6545	14650.6545	14650.6545	14650.6545	14650.6545
Gross revenue ($)		1,014,815	1,189,488	1,364,161	1,538,833	1,713,506	1,888,179	2,237,524	2,586,870
VAT (23%) ($)		233,407	273,582	313,757	353,932	394,106	434,281	514,631	594,980
Total revenue ($)	Gross revenue - VAT	781,408	915,906	1,050,404	1,184,902	1,319,400	1,453,898	1,722,894	1,991,890
OPEX ($)		826,850	826,850	826,850	826,850	826,850	826,850	826,850	826,850
EBITDA ($)	Total revenue - OPEX	(45,442)	89,056	223,554	358,052	492,550	627,048	896,044	1,165,040
Depreciation ($)	10%	779,609	779,609	779,609	779,609	779,609	779,609	779,609	779,609
EBIT or EBT ($)		(825,051)	(690,553)	(556,055)	(421,557)	(287,059)	(152,561)	116,435	385,431
Tax ($)	0%	-	-	-	-	-	-	-	-
EAT ($)		(825,051)	(690,553)	(556,055)	(421,557)	(287,059)	(152,561)	116,435	385,431
CAD ($)		(45,442)	89,056	223,554	358,052	492,550	627,048	896,044	1,165,040
FCI/CAPEX ($)		7,796,092	7,796,092	7,796,092	7,796,092	7,796,092	7,796,092	7,796,092	7,796,092
ROI		-0.58%	1.14%	2.87%	4.59%	6.32%	8.04%	11.49%	14.94%
Payback period(yrs)		-9.4	-11.3	-14.0	-18.5	-27.2	-51.1	67.0	20.2

4.5 Discussion

The primary objective of this study was to assess commercial-scale natural astaxanthin production from the algal species, *Haematococcus pluvialis*, while considering geospatial variabilities. A detailed economic analysis model was developed to determine astaxanthin production costs and to assess economic feasibility of microalgae-based natural astaxanthin biorefinery. Commercial-scale natural astaxanthin production is not very prevalent, as reflected by a lack of information in the literature about this process.

Furthermore, this data is often proprietary and thus not easily accessible. The current analysis attempts to address this research gap to provide a more comprehensive overview of commercial scale astaxanthin production from microalgae.

Annual astaxanthin productivities in Livadeia, Greece and Amsterdam, Netherlands have been reported to be 426 and 143 kg $year^{-1}$ respectively [86]. In a pilot facility involving a hybrid cultivation system in Shenzhen, China, Li *et al*. reported astaxanthin productivity from *Haematococcus pluvialis* to be 900 kg $year^{-1}$ [91]. While the work of Li *et al*. [91] was conducted in a pilot scale facility, Panis *et al*. [86] determined astaxanthin productivity through computational modeling efforts comparable to the current study. Upon comparison, it may be claimed that astaxanthin productivities for the various locations obtained from the present model, ranging between 350 – 1250 kg $year^{-1}$, are in reasonable agreement with previous studies [86,91]. At the same time, it is essential to note that there are significant divergences in methodology between the present study and existing literature, primarily with regard to the choice of reactor system and determination of theoretical astaxanthin productivity for a location. The model developed by Panis *et al*. [86] was based on theoretical algae yield and astaxanthin productivity on the basis of annual incident sunlight interception, and different process efficiencies and loss mechanisms. The approach of the current study was more focused on the development of a mathematical model based on first principles modeling to determine algae growth and corresponding astaxanthin productivity. The present effort accounts for multiple factors such as determination of the temperature profile of the algal growth medium, and uptake rates of different nutrients and CO_2, making the resulting dynamic model more robust.

Based on astaxanthin productivity for the different locations, a detailed techno-economic analysis was also conducted to determine astaxanthin production costs. Due to limited information regarding commercial scale astaxanthin production costs in the

literature along with wide variabilities, direct comparison or validation of the results was not practical. However, similar studies conducted for Livadeia, Amsterdam [86] and in Shenzhen [91] provide a baseline for comparison.

For Livadeia and Amsterdam, astaxanthin costs were reported to be 1925 \$ kg^{-1} and 7295 \$ kg^{-1}, respectively [86]. Similarly, astaxanthin cost was found to be 718 \$ kg^{-1} for the pilot scale production in Shenzhen, China [91]. Economic analysis results in the present study, ranging from 1365 – 4885 \$ kg^{-1} of natural astaxanthin, reasonably concur with the reported values. The widespread variability in the production costs in the reported studies may mainly be attributed to differences in astaxanthin productivity among different locations. Additionally, the lower astaxanthin costs in Shenzen of 718 \$ kg^{-1} may be ascribed to the significantly lower wages of laborers and workers in Shenzhen, China than in the United States. The results obtained here suggest that natural astaxanthin production may be more viable in places characterized by favorable environmental profiles of high solar irradiation and optimal temperature profile that are more conducive to algae growth. This is evidenced by the fact that commercial plants for the two biggest producers of natural microalgae-based astaxanthin, Cyanotech Corporation and Algatech are based in Hawaii and Israel, respectively [210,211], locations characterized by weather patterns favorable for commercial scale microalgae cultivation. It has been reported that production costs of synthetic astaxanthin is 1000 \$ kg^{-1} with a market price often greater than 2000 kg^{-1} [91]. The current study suggests that although the obtained astaxanthin costs for the different locations are higher than those for synthetic astaxanthin, commercial production of microalgae-based natural astaxanthin is highly feasible and may be successfully utilized to meet the increasing demand for healthy and natural products.

4.6 Conclusion

The present study focused on the techno-economic analysis of natural astaxanthin production from *Haematococcus pluvialis* for four different locations in the United States. First an astaxanthin productivity model was developed based on first-principles approach to quantify annual astaxanthin yield incorporating geospatial variabilities. Subsequently, the process model was integrated with a detailed economic analysis to determine natural astaxanthin products costs. Resulting astaxanthin costs obtained ranged from 1365 – 4885 $ kg^{-1} for the locations studied. Although natural astaxanthin costs obtained here are higher than synthetic astaxanthin by about 35-40%, results indicate that there does exist significant opportunity for microalgae-based astaxanthin production especially in the natural and bio-based products market. With an increase in demand for natural products and continued research on microalgae utilization, commercial produced natural astaxanthin may soon act as a viable alternative to synthetic astaxanthin in the global market.

Chapter 5. Process model and techno-economic analysis of EPA and DHA production from microalgae incorporating geospatial variabilities

5.1 Introduction

Fish oil is an important component of aquafeed that adds functionality and health benefits to fish, specifically, salmon and tuna [212]. These fish are often regarded as healthy food products due to the high concentration of long chain omega three fatty acids like eicosapentanoic acid (EPA) and docosahexanoic acid (DHA) [213,214]. Synthesis of long chain fatty acids in salmon is enabled through their feed that is abundant in fish oils [215]. Traditionally, fish oils are obtained from pelagic feed fisheries with a global annual supply estimated at around 1,000,000 metric tons [216]. Of this, around 70% is utilized in fish feed and salmonids production [97,214]. In the last decade, global supply of fish oil has remained more or less constant; however, there are wide irregularities among yearly fish landings and oil yields [216]. On the other hand, the global demand for fish oils has been increasing steadily, primarily driven by the growth in the aquaculture industry, and intensified by the rapidly emerging omega-3 market. The anchoveta fishery stock in South America (Peru and Chile) has been the most important source of fish oil for decades and supplies about 70% of the global demand [97]. However, due to extreme climate and environmental conditions and occasional upwelling events, there has been significant volatility in fish oil production and supply over the last decade [217,218]. The difference between the demand and supply has made the current market very competitive in terms of fish oil prices. The price was reported to be between 300 – 800 \$ ton^{-1} in 2005 with an increase to around 2000 \$ ton^{-1} in 2012 – 2014 [219]. More recently reported prices of fish oil have escalated to about 2400 \$ ton^{-1} and is predicted to further increase by more than 25% in the next 5 years [219].

This disproportionate supply and demand of fish oil globally has necessitated the implementation of feasible alternatives. One viable option is microalgae-derived EPA and DHA that may act as substitutes for fish oil from pelagic fisheries [220–222]. Microalgae are very productive photosynthetic organisms capable of synthesizing omega-3 fatty acids and hence regarded as promising alternatives to EPA and DHA in fish oil [220]. Primarily composed of proteins, lipids, carbohydrates and pigments, microalgae may be converted to a plethora of products for the food, feed, and energy industry [28,94,112]. Industrial utilization of microalgae for feed is an active area of research in conjunction with microalgae-based biofuels production [99,100,223]. The main difference between the two applications is the type and quantity of fatty acids synthetized by the algae. While short chain fatty acids are ideal for biofuels production, long-chain polyunsaturated fatty acids play a bigger role in feed applications. Another important distinction is the level of microalgal biomass processing for the two applications. In algae-based biofuels production, there are several processing steps including lipids extraction and transesterification to biodiesel. On the other hand, microalgae reportedly may be directly utilized as feed [223]. This part of the study focuses on the detailed techno-economic analysis of commercial scale production of EPA and DHA-based fish oil. For the base case scenario, a detailed microalgae growth kinetics model was used to determine EPA and DHA productivity and then combined with a detailed economic analysis to determine production costs of the system. The model was extended to different locations to highlight the implications of geospatial variability for the production and cost of EPA and DHA. Furthermore, scenario analysis was used to find optimal plant sizes and to elucidate the effect of different parameters on the productivity and production cost. The present study is first of its kind to incorporate the entire supply chain of microalgae cultivation, harvest and conversion to feed and provides valuable insights about commercial scale natural EPA and DHA production in different regions in the United States.

5.2 Methods

To quantify EPA and DHA production from microalgae, detailed process models encompassing the entire value chain of microalgae growth, harvesting and EPA and DHA extraction were developed. Following our previous studies evaluating commercial scale microalgae cultivation in open raceways and flat panel photobioreactors (described in Chapter 2 and Chapter 3 of the thesis), *Nannochloropsis sp.* was utilized as the algal strain for EPA and DHA synthesis and production following previous studies [94,224,225]. Although the concentration of EPA and DHA in microalgae is low, often less than 5% of the total dry weight of algae, research is underway to increase the percentage of these compounds [98,216,221] and enable greater productivity.

The supply chain of natural EPA and DHA production begins with microalgae cultivation on a commercial scale. In this study, algal growth was modeled in open raceway ponds as well as flat panel photobioreactors, facilitated by incident sunlight, carbon dioxide (CO_2), and nutrients. Microalgae cultivation in bioreactors is generally followed by algal harvesting when the slurry is essentially dewatered to obtain a paste of 20% solids concentration (that is, concentration of 200 kg m^{-3}). Finally, EPA and DHA are extracted from the harvested microalgae. This arrangement was modeled here exactly as described in the previous chapters. Again, the techno-economic analysis was extended to four locations within the United States, namely Minnesota (Minneapolis), California (San Diego), New Mexico (Albuquerque) and Arizona (Phoenix), to assess the implications of locations and corresponding variabilities on algae and EPA and DHA productivity.

The detailed process model for natural EPA and DHA production from microalgae together with meticulous economic analysis was used to determine production costs. This was accomplished by performing a mass and energy balances of the entire EPA and DHA supply chain. The economic analysis was also applied to the different locations to quantify

EPA and DHA production cost ($ kg^{-1}) and to elucidate the implications on spatial variabilities. Similar to the process modeling of natural astaxanthin production described in Chapter 4, a Profit & Loss (P&L) analysis was performed to determine the financial attractiveness of commercial scale natural EPA and DHA production. The supply chain of natural microalgae-based EPA and DHA production is provided in Figure 5.1. This is one of the first studies detailing process modeling and techno-economic analysis of microalgae-based EPA and DHA production and is a significant step forward in assessing feasibility of natural EPA and DHA production and their competitiveness with the synthetic products in the market.

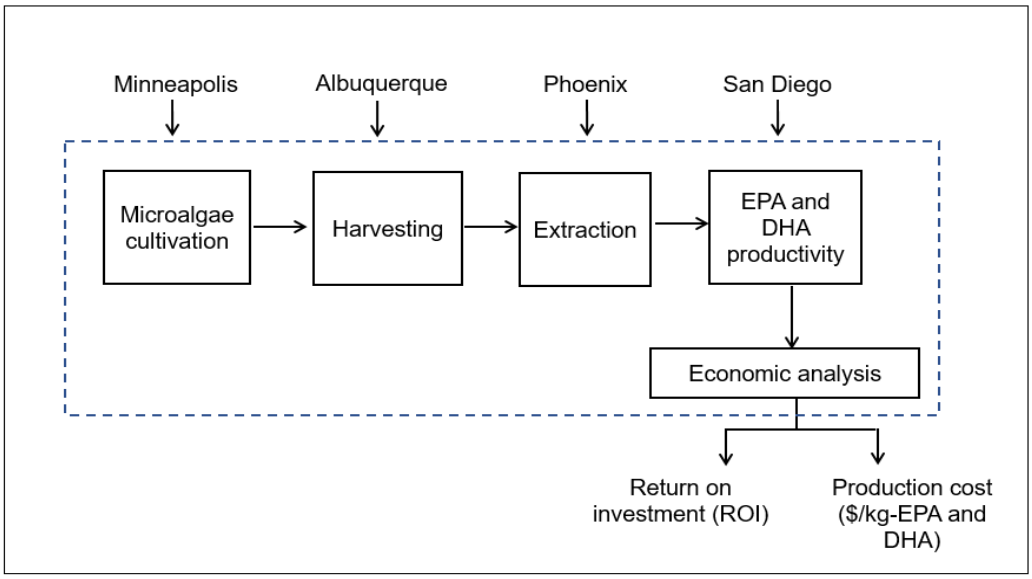

Figure 5. 1. Framework of natural EPA and DHA and economic analysis

5.3 Models

5.3.1. Algae cultivation

In order to model microalgae growth and cultivation on commercial scales, the same approach described in Chapter 2 and Chapter 3 was adopted [163,166]. As described previously, first a detailed heat and mass transfer model was developed

combining local weather data to determine temperature profile of the microalgae growth reactors. This result was further used to develop a microalgae biological growth kinetics model to compute productivity for a location. It was again assumed that phosphorus and nitrogen-based nutrients, as well as CO_2 essential for microalgae growth were provided adequately. The reactor configuration and operating procedure were the same as described in Chapters 3. In the baseline scenario, hypothetical flat panel photobioreactor was assumed to be 1 hectare in area facilitating microalgae cultivation.

5.3.2 Microalgae harvesting

One of the most important steps in biorefinery supply chain is microalgae harvesting. Microalgae being unicellular organisms and due to presence of enormous quantity of water in the suspension, harvesting algae is a challenging and energy intensive process. Correspondingly, harvesting costs are quite high and is a significant percentage of total microalgae production costs [35,94,121,128]. The microalgae harvesting technique used in astaxanthin production described in Chapter 4 was adopted in the current study. The two-step harvesting step involved bio-flocculation, which is the addition of organic polyacrylamide flocculants to separate the algae phase from the solution and to facilitate primary dewatering by lamella clarifiers. The second step or mechanical harvesting consisted of the use of centrifuges to further dewater microalgae solution. Although centrifuge usage is an extremely energy intensive step, previous researchers have demonstrated its utility in extracting high value products with omega-3 fatty acids [186,226]. Hence, the centrifugation step for secondary dewatering was considered an ideal method for mechanical harvesting. The concentration of resulting microalgae solution after primary dewatering was 30 kg m^{-3}. After centrifugation, the concentration of the microalgal paste was taken as 200 kg m^{-3} (20% solids content). The two stage

microalgae harvesting technique has often been regarded as an ideal harvesting method to derive high-value products from microalgae [186,187,227].

5.3.3 EPA and DHA extraction

The final step in the microalgae-based biorefinery process model was the extraction of EPA and DHA from the harvested microalgae. In order to facilitate extraction, two major steps were utilized in this study: 1) cell disruption and 2) lipids extraction. Microalgal cells may be disrupted by several methods including mechanical processes such as bead milling and high pressure homogenization or by chemical or enzymatic procedures [228–230]. In this study, microalgae cells were disrupted by high pressure homogenization which is considered an efficient cell lysis method when algae concentration is between 100 – 200 kg m^{-3} [195]. After cell lysis, extraction of the lipids was facilitated by organic solvents like acetone, hexane, methyl ethyl ketone, as well as by supercritical CO_2 extraction [231,232]. In this study, it was assumed that algal oils were extracted by hexane and isopropanol which are often regarded as suitable organic solvents that have been used extensively [232–234]. The resulting solution was further processed through a flash evaporator in order to recover the costly solvents which were recycled back to the oil extraction phase. To avoid contamination and degradation, the polyunsaturated fatty acids (PUFA) enriched oil was refrigerated before being sold in the market as natural EPA and DHA. Since, PUFAs are often utilized as food supplements or for direct human consumption, it is desirable for their purity to be >95%. In order to achieve this purity level, extra refining steps may be necessary that are beyond the scope of the present work [222,235,236]. The microalgae after oil extraction is essentially a protein rich compound and was assumed to be directly sold in the market as a bio-fertilizer. The supply chain of PUFA enriched microalgal oil production comprising of algae cultivation, harvesting and extraction of the desired products is provided in Figure 5.2.

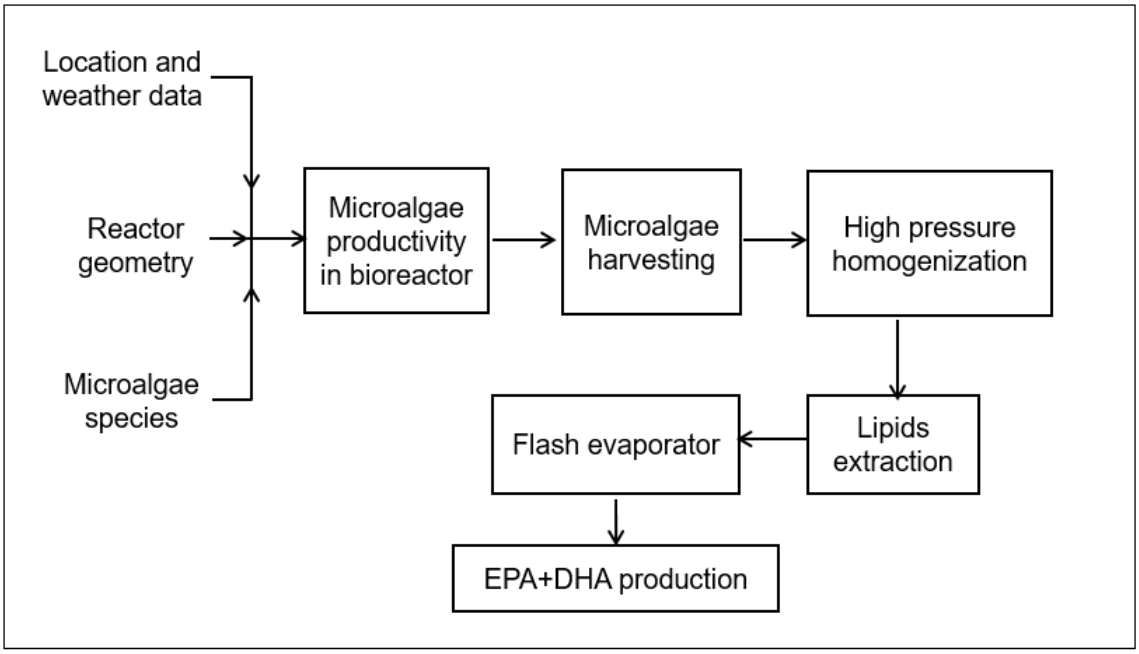

Figure 5. 2. Supply chain of microalgae-based EPA and DHA production model

5.4 Results

5.4.1 EPA and DHA productivity potential

The combined heat and mass transfer model for determining the temperature profile of microalgae cultivation reactor, and the microalgae biological growth model with its corresponding PUFA concentration, were employed to ascertain annual EPA and DHA productivity potential. Extending the framework helped to determine EPA and DHA productivity potential for the different locations, provided in Figure 5.3. Among the different locations studied, EPA and DHA productivity for the hypothetical biorefinery in Minneapolis was the lowest at 2525 kg year^{-1}, and the highest in Phoenix at 8645 kg year^{-1}. EPA and DHA concentration in the microalgae species was assumed to be identical across all the locations. This huge difference in omega-3 fatty acids productivity between the two locations may be primarily attributed to the different algae productivities arising from the geospatial variability. Microalgae productivity in Phoenix is about 70% more than in

Minneapolis, thereby explaining the significantly lower EPA and DHA productivity in Minneapolis compared to Phoenix. The productivity results for Albuquerque and San Diego were found to be 7182 kg $year^{-1}$ and 7647 kg $year^{-1}$ respectively. Thus, Albuquerque, San Diego and Phoenix were found to have similar EPA and DHA productivity potential due to similar weather patterns resulting in similar microalgae productivity ranging between 108 – 130 t ha^{-1} $year^{-1}$. These results demonstrate that the correct choice of location is imperative for microalgae biorefinery siting, given the heavy dependence of performance on local geospatial factors.

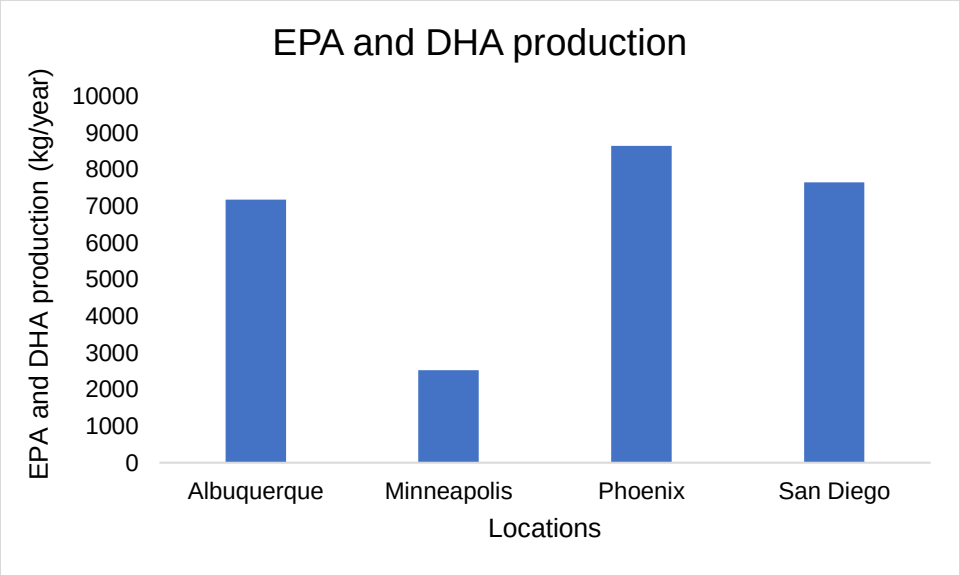

Figure 5. 3. EPA and DHA annual productivities for different locations incorporating geospatial variabilities

5.4.2 Economic analysis

The process modeling framework developed in the present study was combined with detailed economic analysis to elucidate the financial implications of microalgae-based EPA and DHA production. Following the approach used in comparing the productivity model, the economic analysis was performed for different locations to assess the influences of geospatial variability on EPA and DHA production costs. This combined

techno-economic analysis is a valuable tool for studying the production of natural PUFA from microalgae on a commercial scale.

In the baseline scenario, EPA and DHA were cultivated in a commercial scale flat panel photobioreactor biorefinery with an area of 1 hectare. The cost of the reactor systems, equipment and piping were obtained from literature and previous work on algae cultivation and natural astaxanthin production (described in Chapters 3 and 4) [86,91,163,166]. Based on capital cost estimates, various Lang factors were applied in order to quantify the direct, indirect and other costs, which were then used to derive the fixed capital investment for the biorefinery [94]. A linear depreciation of 10% was assumed in order to compute the interest, property tax and insurance, and determine the annual total capital expenditure of the biorefinery [94]. The breakdown of the total capital expenditure and the corresponding Lang factors used were similar to those described for Astaxanthin production in Chapter 4, and also mined from literature [94].

To establish the operating expenditure of the microalgae biorefinery, mass and energy balances were calculated to determine the total amount of nutrients, CO_2, and utilities required. In order to facilitate proper mixing in a microalgae growth reactor, an airlift system was used. Power consumption for airlift systems was determined based on our previous work on algae cultivation in photobioreactors (Chapter 3). Oxygen, a byproduct of photosynthesis is detrimental to algae growth. To remove it from the system, reactors were facilitated with degassers and the power consumption for the process was determined from literature [13]. Power requirements for microalgae harvesting were identical to those described in Chapters 3 and 4. The next step in the process is cell disruption, an energy intensive process. Energy requirement for high pressure homogenization was obtained from literature at 2 MJ kg^{-1} of algae which causes a 100% disruption of algal cells followed by hexane extraction [237]. To extract long chain fatty

acids from disrupted algal cells, the organic solvents hexane and isopropanol were used. Total requirement of the organic solvents necessary was obtained from literature and scaled up according to the present mass flow in the biorefinery [234]. It was also assumed that 1 biologist, 1 plant supervisor and 4 workers would be necessary for the functioning of the plant and their wages and salaries were incorporated in the economic analysis. Plant maintenance, contingencies and overheads were also considered to determine the total annual operating expenditure of the plant.

Based on the capital and operating expenditure thus obtained, production costs of microalgae-based EPA and DHA were determined. In the base case scenario, the results of the 1-hectare hypothetical biorefinery in Albuquerque, New Mexico is discussed in greater detail first. The annual production cost of EPA and DHA was 168 \$ kg^{-1} based on yearly productivity of 7182 kg. Of the total production cost, contributions of capital costs and operating costs expenditures were 94 \$ kg^{-1} and 74 \$ kg^{-1}, respectively. The resulting total annual capital and operating expenditures were calculated to be 674,713 \$ $year^{-1}$ and 531,735 \$ $year^{-1}$, respectively. Detailed capital and operating costs expenditure for the base case scenario is provided in Table 5.1 and Table 5.2, respectively. Furthermore, contributions of different capital and operating costs components and parameters are provided in Figure 5.4 and Figure 5.5, respectively. The cost of photobioreactors, pumps and equipment are the most dominant factors and constitute about 80% of the total capital expenditure. Of the operating expenditures, overheads, maintenance and total wages of personnel are the most impactful and comprise about 75% of the total costs.

Table 5. 1. Capital costs estimate of EPA and DHA production in hypothetical plant in Albuquerque, New Mexico

			Capital expenditure ($)	**Capital expenditure ($ kg EPA and DHA $^{-1}$)**
		Photobioreactor cost	540,697	75
		Airlift system	41140	6
		Pumps and other equipment	497,022	69
		CO_2 storage tank	38720	5
		Sedimentation tank	11000	1.5
		Centrifuge	63800	9
		Centrifuge feed pump	6600	1
		Biomass conveyer belt	13750	2
		Biomass storage tank	19360	2.7
		High pressure homogenizer	9000	1
		Solvent extractor	8056	1
		Packaging line	22000	3
		Laboratory equipment	88000	12
	Major Equipment Cost (MEC)		**1,359,145**	**189**
	Installation costs	47% MEC	638798	89
	Instrumentation and control	35% MEC	475701	66
	Piping	40% MEC	543658	76
	Electrical	10% MEC	135915	19
	Buildings	18% MEC	244646	34
	Land improvements	10% MEC	135915	19
	Service facilities	40% MEC	543658	76
Total Direct Costs (DC)			**4,077,435**	**568**
	Construction expenses	15% DC	611615	85
	Engineering and Supervision	10% DC	407744	57

Indirect costs (IC)			**1,019,359**	**142**
	Contractor's fee	5% (DC+IC)	254840	35
	Contingency (Major equipment)	15% (DC+IC)	764519	106
Other Costs (OC)			**1,019,359**	**142**
Fixed capital investment (FCI)		**DC+IC+OC**	**6,116154**	**852**
	Depreciation	(DC+IC+OC)/10	611615	85
	Interest	8% Depreciation	48929	7
	Property tax	1% (Depreciation + interest)	6605	1
	Insurance	0.6% (Depreciation + interest)	3963	0.6
	Land	1 hectare	3600	0.5
Total capital expenditure ($ year^{-1})			**674,713**	**94**

Table 5. 2. Operating costs estimate of EPA and DHA production in hypothetical plant in Albuquerque, New Mexico

	Operating expenditure ($)	**Operating expenditure ($ kg astaxanthin $^{-1}$)**
Raw materials	15711	2
CO_2 distribution	5500	1
Water (including recycling)	14168	2
Power – mixing/circulation	13187	2
Power – CO_2 supply	3113	-
Power – oxygen removal	6110	1
Power - centrifuge	12346	2
Power – high pressure homogenization	3690	1
Hexane	30530	4

Isopropanol	40210	6
Worker salary (4 workers)	98868	14
Supervisor salary (1 supervisor)	55640	8
Biologist salary (1 biologist)	37450	5
Maintenance	54366	8
Operating supply	276	-
Contingency	4482	1
Overhead	135478	19
Total operating expenditure ($ year^{-1})	**846777**	**74**

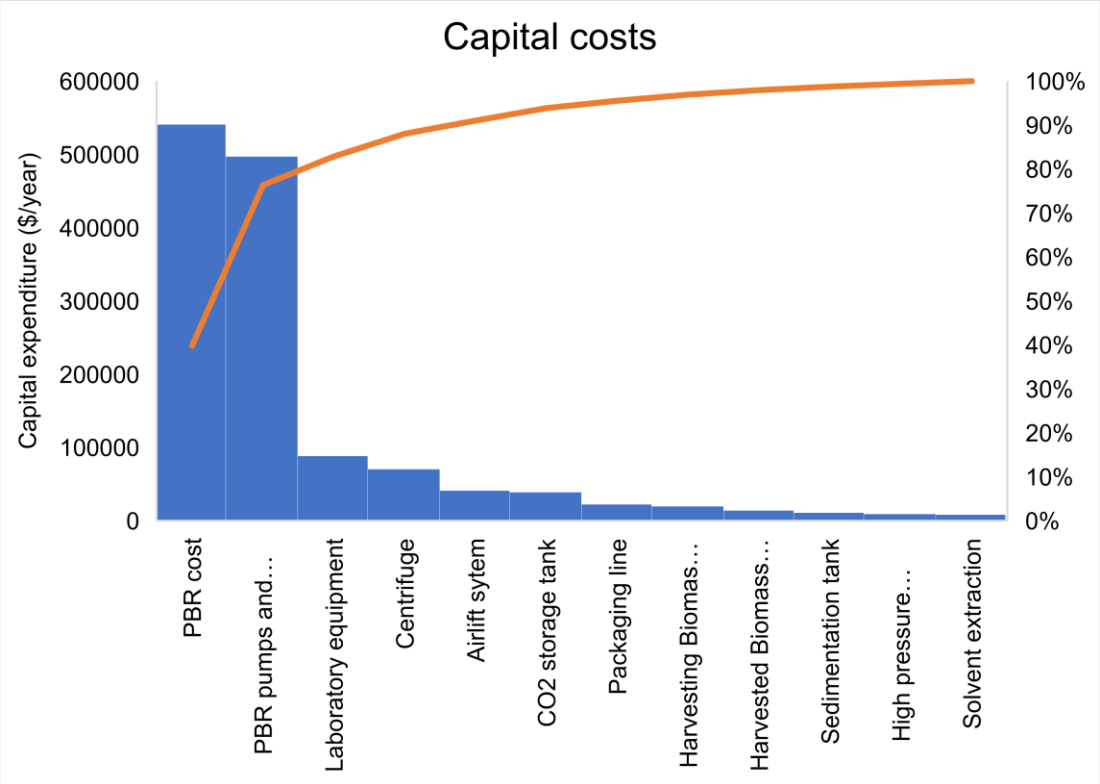

Figure 5. 4. Capital cost contribution for natural EPA and DHA production plant in Albuquerque, New Mexico

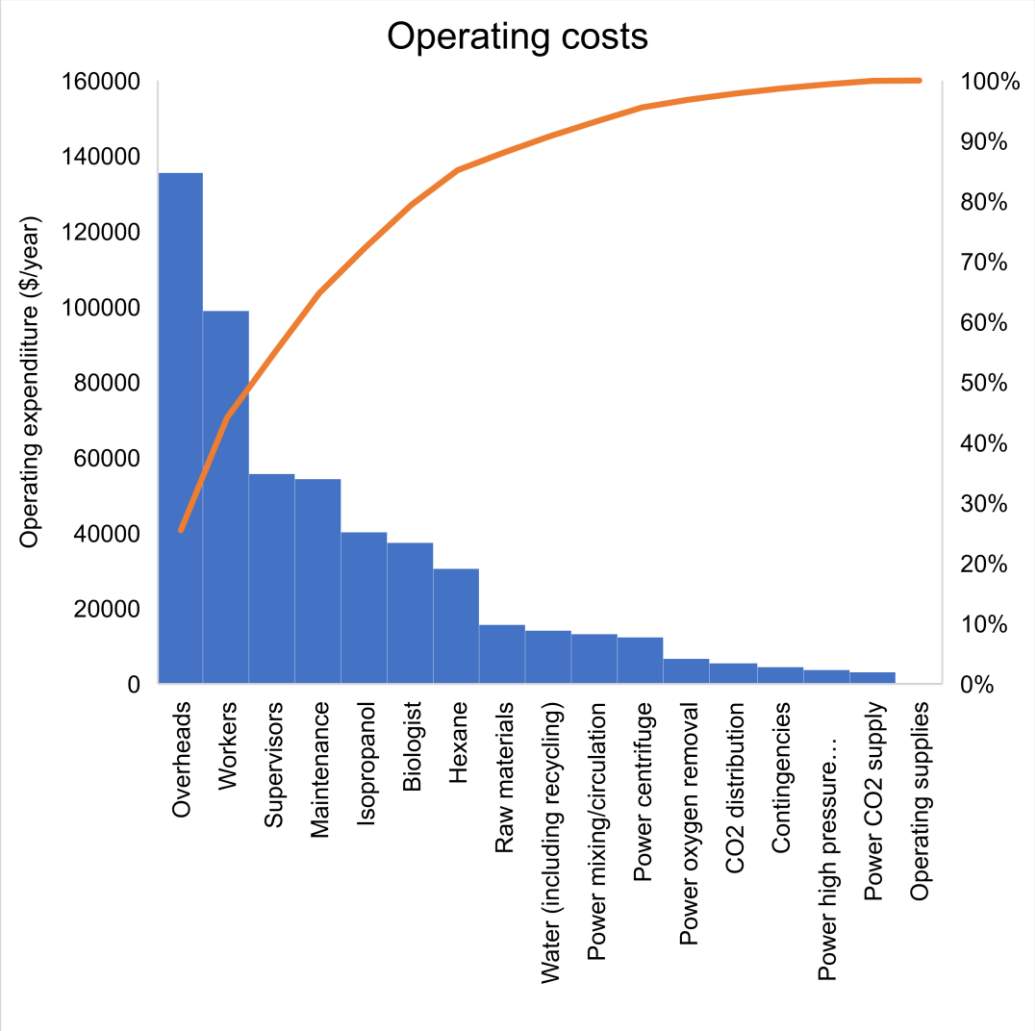

Figure 5. 5. Operating cost contribution for natural EPA and DHA production plant in Albuquerque, New Mexico

5.4.2.1 Comparative analysis of the effect of geospatial variabilities on microalgae-based EPA and DHA production cost

To elucidate the ramifications of geospatial variabilities on natural EPA and DHA production costs, the economic framework developed in the study was extended to other locations. It is essential to account for the variations of the different cost parameters across locations in order to determine natural EPA and DHA cost more accurately. For simplification, it was assumed that electricity and land prices were the only varying factors

between the locations. The cost of the cultivation systems and operating expenditures like wages of personnel and price of raw materials were assumed to be identical for the locations. The reasoning behind the assumptions may be found in the previous chapters (2, 3, and 4).

Microalgae-based EPA and DHA production costs for the studied locations in 1-hectare plant are provided in Figure 5.6. From the analysis, it can be inferred that production costs vary significantly across the locations with costs ranging from 141 – 461 \$ kg^{-1}. The cost of production of EPA and DHA is the lowest in Phoenix at 141 \$ kg^{-1} and the most expensive in Minneapolis at 461 \$ kg^{-1}. Production costs were found to be very similar for Albuquerque and San Diego at 168 \$ kg^{-1} and 162 \$ kg^{-1}, respectively. The huge difference in production costs between Minneapolis and Phoenix may be mainly attributed to the difference in EPA and DHA annual productivity. The productivity of EPA and DHA in Minneapolis was only about 30% than the productivity in Phoenix, thereby driving down the production costs by about 70% in Phoenix in comparison to Minneapolis. It is interesting to note EPA and DHA production costs in Albuquerque and San Diego are almost identical, despite a slightly higher productivity in San Diego than Albuquerque. This is mainly due to the higher land and electricity prices in San Diego in comparison to Albuquerque. From the economic analysis, it is concluded that economic feasibility of large-scale natural EPA and DHA production from microalgae is heavily dependent on location as location-specific climate factors influence productivity thereby resulting in a highly variable production costs.

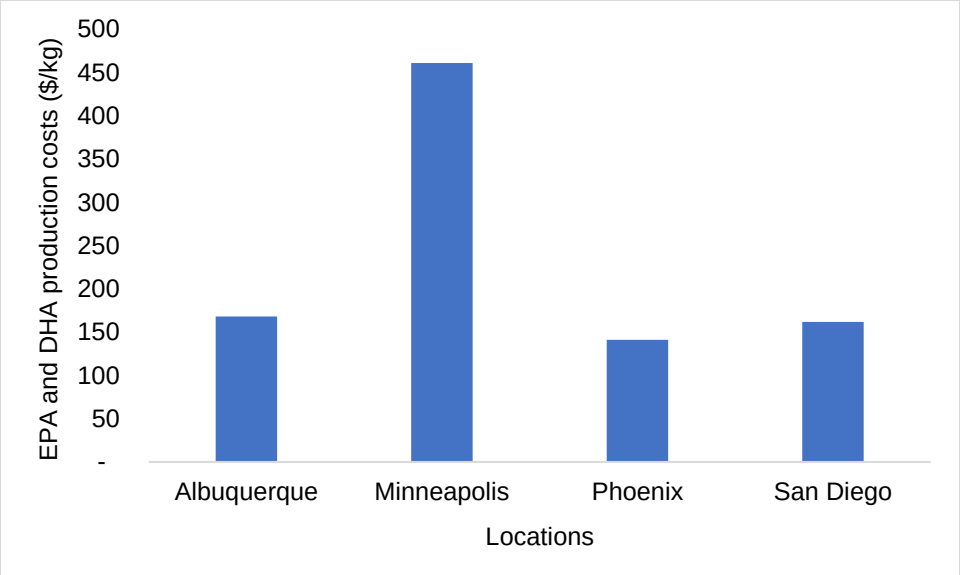

Figure 5. 6. EPA and DHA production costs for different locations incorporating geospatial variabilities

5.4.2.2 Profit and Loss (P&L) analysis

To further assess the feasibility of commercial scale natural EPA and DHA production from microalgae, a P&L analysis was conducted (performed previously to assess implications of natural astaxanthin production, described in Chapter 4 of the thesis). The P&L analysis was developed to calculate the Return on Investment (ROI) by quantifying the net revenues and expenditure of a plant [207–209]. For the P&L analysis, different scenarios were considered by varying EPA and DHA prices to 20, 40, 80, 160 and 320 \$ kg^{-1}. It was assumed that the protein-rich oil-extracted microalgae was sold in the market at a price of 33.5 \$ kg^{-1} [86]. ROIs for New Mexico (Albuquerque), Arizona (Phoenix) and California (San Diego) were determined to be 26 – 42%, 31 – 51%, and 27 – 45%, respectively. For the hypothetical plant in Minnesota (Minneapolis), the resulting ROI was found to be 12% for a market price of EPA and DHA over 160 \$ kg^{-1}, indicating the plant would not be economically as competitive as the other locations in that scenario. The detailed P&L analysis for the hypothetical plants in Arizona and Minnesota are

provided in Table 5.3 and Table 5.4, respectively. P&L analysis highlighted the economic implications of commercial scale microalgae-based natural EPA and DHA production. Results suggest that locations like New Mexico (Phoenix), Arizona (Phoenix) and California (San Diego) may indeed be conducive to natural EPA and DHA production with an available market of microalgae-based protein as biofertilizer, thereby resulting in very high ROI. From the location point of view, it can further be stated that cultivation in Minnesota is not economical due to the very low productivity potential of natural EPA and DHA production which culminates to a very high production costs in comparison to other places.

Table 5. 3. P&L analysis for natural EPA and DHA production plant in Minnesota (Minneapolis)

Market Price ($/kg)	EPA and DHA Market price	20	40	80	160	320
Market Price ($/kg)	Protein-rich algae	33.5	33.5	33.5	33.5	33.5
Quantity (kg)	EPA and DHA	2527	2527	2527	2527	2527
Quantity (kg)	Protein-rich algae	35473	35473	35473	35473	35473
Gross revenue ($)		1,238,886	1,289,426	1,390,506	1,592,666	1,996,986
VAT (23%) ($)		284,944	296,568	319,816	366,313	459,307
Total revenue ($)	Gross revenue - VAT	953,942	992,858	1,070,689	1,226,352	1,537,679
OPEX ($)		483,383	483,383	483,383	483,383	483,383
EBITDA ($)	Total revenue - OPEX	470,559	509,475	587,307	742,970	1,054,296

Depreciation ($)	10%	609,266	609,266	609,266	609,266	609,266
EBIT or EBT ($)		(138,706)	(99,791)	(21,959)	133,704	445,031
Tax ($)	0%	-	-	-	-	-
EAT ($)		(138,706)	(99,791)	(21,959)	133,704	445,031
CAD ($)		470,559	509,475	587,307	742,970	1,054,296
FCI/CAPEX ($)		6,092,656	6,092,656	6,092,656	6,092,656	6,092,656
ROI		8%	8%	10%	12%	17%
Payback period (years)		-43.9	-61.1	-277.5	45.6	13.7

Table 5. 4. P&L analysis for natural EPA and DHA production plant in Arizona (Phoenix)

Market Price ($/kg)	EPA and DHA Market price	20	40	80	160	320
Market Price ($/kg)	Protein-rich algae	33.5	33.5	33.5	33.5	33.5
Quantity (kg)	EPA and DHA	8645	8645	8645	8645	8645
Quantity (kg)	Protein-rich algae	121355	121355	121355	121355	121355
Gross revenue ($)		4,238,293	4,411,193	4,756,993	5,448,593	6,831,793
VAT (23%) ($)		974,807	1,014,574	1,094,108	1,253,176	1,571,312
Total revenue ($)	Gross revenue - VAT	3,263,485	3,396,618	3,662,884	4,195,416	5,260,480
OPEX ($)		546,973	546,973	546,973	546,973	546,973

EBITDA ($)	Total revenue - OPEX	2,716,513	2,849,646	3,115,912	3,648,444	4,713,508
Depreciation ($)	10%	612,354	612,354	612,354	612,354	612,354
EBIT or EBT ($)		2,104,159	2,237,292	2,503,558	3,036,090	4,101,154
Tax ($)	39%	820,622	872,544	976,388	1,184,075	1,599,450
EAT ($)		1,283,537	1,364,748	1,527,170	1,852,015	2,501,704
CAD ($)		1,895,891	1,977,102	2,139,524	2,464,369	3,114,058
FCI/CAPEX ($)		6,123,538	6,123,538	6,123,538	6,123,538	6,123,538
ROI		31%	32%	35%	40%	51%
Payback period (years)		4.8	4.5	4.0	3.3	2.4

5.4.3 Production scale

Scale is an important consideration for understanding the economic implications of commercial level microalgae based biorefineries. Previous literature has illustrated that the economics of scale can heavily influence microalgae production costs in different reactors systems [18,147]. In order to interpret the effects of scale-up on product costs, the hypothetical biorefinery scale was extended from its baseline case of 1 hectare to larger sizes of 5, 10, 25, 50 and 100 hectare. The results of plant size on EPA and DHA production costs are provided in Figure 5.7. This analysis shows that production costs drop significantly with the increase in scale and this trend is consistent for all the locations. When size of the refinery is expanded from the base case scenario of 1 hectare to 100 hectares, the corresponding production costs decrease by about 55-60% for the different locations. At the 100-hectare scale, EPA and DHA production costs in Minneapolis, Albuquerque, Phoenix and San Diego were obtained to be 189, 72, 63 and 75 $ kg^{-1},

respectively. From the results it is evident that the scale of microalgae biorefineries is a key factor driving production costs, and an increase in size to about 50-100 hectare diminishes microalgae-based products cost significantly, consistent with literature [18].

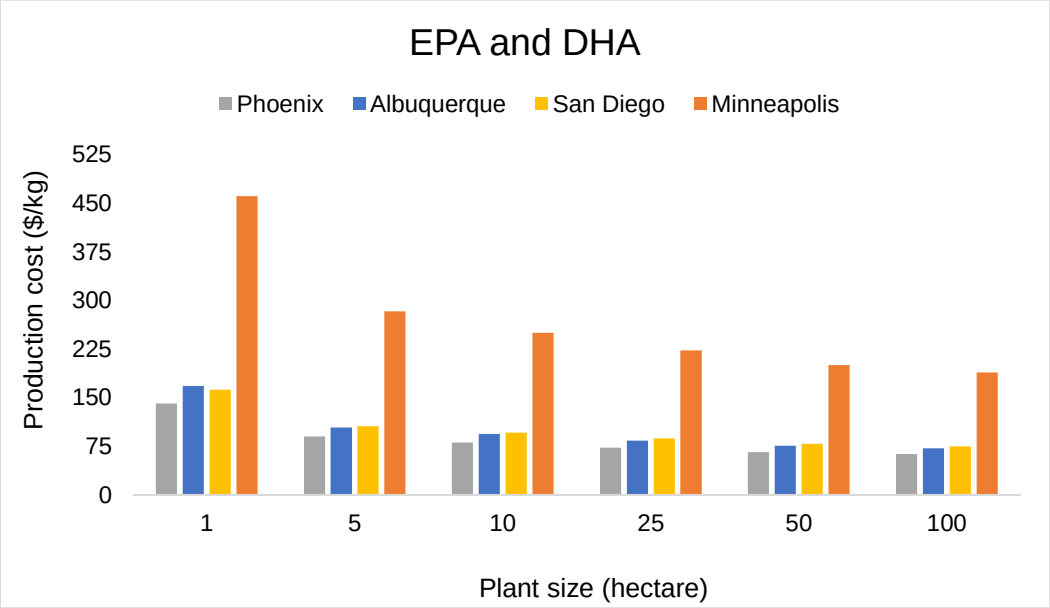

Figure 5. 7. Variation in EPA and DHA production costs with increase in microalgae biorefinery scale

5.5 Conclusion

In the present study, techno-economic analysis of microalgae-based natural EPA and DHA was carried out for four different locations in the United States. To facilitate the analysis, first a quantitative model was developed from a first-principles approach to determine EPA and DHA yield annually. The model considered geospatial variabilities to help understand the impact of local parameters on the annual productivity. This engineering model was further integrated with an economic analysis model to determine EPA and DHA production costs. At the baseline scenario, the resulting production costs ranged from 141 – 461 \$ kg^{-1} for the different regions. A 50-100 times increase in scale, lowered EPA and DHA production costs by around 60% making it economically attractive. Although the calculated costs were higher than the market price of synthetic fish oils,

natural microalgae-based EPA and DHA may be an attractive prospect in the natural and bio-based products market globally. The rising demand for fish oil for aquaculture and the current expansion of the omega-3 fatty acid market may result in microalgae-based natural fish oil becoming a viable product in the global market very soon.

Chapter 6. Conclusion

The primary goal of this study was to assess the feasibility of microalgae production on a large scale for the generation of bioproducts while considering geospatial variability. Temperature profiling, microalgae productivity modeling, and economic analysis to determine production costs were executed for both open raceway ponds and flat panel photobioreactors considering the algae species *Nannochloropsis sp.* for four separate locations- Minneapolis, Albuquerque, Phoenix, and San Diego. The present work is first of its kind that combines first principles-based engineering analysis and economic analysis of commercial scale microalgae cultivation in two different reactor systems incorporating geographic location specific climatic factors and year round production.

For open raceway ponds, microalgae productivity was found to be well corelated with daily and seasonal changes in temperature. The differences in weather patterns were found to contribute to differences in productivity observed for different geographic locations. The lowest productivity was seen in Minneapolis corresponding to the colder weather patterns of 2000 t km^{-2} $year^{-1}$. In comparison, microalgae productivity for the warmer locations were found to lie between 6000-7000 t km^{-2} $year^{-1}$. To better understand the effect of different parameters on microalgae price, an economic sensitivity analysis was performed. As expected, an increase in annual areal productivity leads to a decrease in microalgae production price (+-20%). Additionally, pond liners and covers were seen to have a significant effect on price in the case of open race way ponds. Upon evaluation of production costs, based on estimated areal productivity, electricity price and land price, a range between 502 - 1074 \$ t^{-1} was observed. The estimated productivity and microalgae costs from the present study are in accordance with those reported in the literature.

Next, microalgae productivity modeling and economic analysis were carried out considering flat panel bioreactors for the four locations. The highest performance for microalgae was found to be in Phoenix was at approximately 13000 t km^{-2} $year^{-1}$ which is about 3.42 times than the productivity in Minneapolis. Microalgae productivity in Albuquerque and Phoenix were found to be 10800 and 11500 t km^{-2} $year^{-1}$, respectively. These results reinforce the importance of location for microalgae cultivation. Economic sensitivity analysis confirmed the sensitivity of microalgae costs to productivity potential for that location. Labor costs were also seen to heavily influence microalgae costs. Changing the number of workers and thereby labor costs by ± 50% caused the microalgae cost to vary by more than ± 16% from the baseline scenario. The microalgae productivity results from the present study ranging between 3800 – 13000 t km^{-2} $year^{-1}$ productivity are well within the reported range. A broad range was observed in the cost of microalgae production in flat panel bioreactors for the separate locations, from about 9564 \$ t^{-1} in the Twin Cities (Minnesota) area to approximately 2895 \$ t^{-1} in the Phoenix (Arizona) region. Results from published articles are reasonably comparable to those obtained from the current analysis and reinforce the suitability of the novel methodology employed here. The results demonstrate the importance of reactor choice and locations for commercial scale microalgae cultivation. Microalgae productivity trends are consistent across all the locations for both the open raceway and flat panel photobioreactor systems. Although algal productivity is much higher in photobioreactors than in open raceways for the locations, algae production costs in flat panels are considerably higher than corresponding costs in open raceways primarily due to the sophisticated design specification and operation complexity of the closed photo bioreactor system in comparison to open raceways. The mathematical framework developed in the study is essential for comparing productivities and cultivation costs across systems and can further be utilized to validate experimental data regarding microalgae productivity in outdoor scenarios.

To ensure the commercial success of microalgae based biorefineries, it is critical to effectively utilize the secondary metabolites that may be extracted from microalgae. One of the most valuable secondary metabolites of microalgae is a carotenoid named astaxanthin with wide applications in the cosmetic and pharmaceutical industry. A combined heat and mass transfer model together with a biological growth kinetics model were utilized to determine microalgae productivity and corresponding astaxanthin output for a selected algal species, namely *Haematococcus pluvialis,* cultured in a hybrid bioreactor system for the four locations. Astaxanthin production in Phoenix was the highest at 1258 kg $year^{-1}$, and lowest in Minneapolis at 349 kg $year^{-1}$ which is only about 28% of the productivity potential in Phoenix. Once again, the choice of location is seen to influence microalgae productivity potential and consequently downstream applications such as astaxanthin production. Natural astaxanthin production costs for the different locations were found to vary greatly among the different locations ranging between 1365 – 4884 \$ kg^{-1}, was found to be the lowest in Phoenix at 1365 \$ kg^{-1} and highest in Minneapolis at 4884 \$ kg-1. Moreover, a profit and loss analysis was conducted, whereby ROI for New Mexico (Albuquerque), Minnesota (Minneapolis), Arizona (Phoenix) and California (San Diego) were calculated at 16.92 – 50.25%, -0.58 – 14.94%, 20.6 – 59.73%, and 17.42 – 52.92%, respectively. The higher ROIs for New Mexico (Phoenix), Arizona (Phoenix) and California (San Diego), indicate the feasibility of microalgae-based commercial scale astaxanthin production in these locations with the proper exploitation of the astaxanthin derived residual biomass. Production costs of synthetic astaxanthin are reported to be approximately 1000 \$ kg^{-1} with a market price often greater than 2000 kg^{-1} [91]. The current study suggests that although the obtained astaxanthin costs for the climatically favorable locations are still higher than those for synthetic astaxanthin, commercial production of microalgae-based natural astaxanthin is highly feasible and may

be successfully utilized to replace fossil fuel-based products in the market and meet the growing demand for natural products.

Microalgae-based natural EPA and DHA production is an attractive option to meet the demands of an expanding omega-3 market and aquaculture industry. Yet, there is a lack of detailed modeling and analysis of commercial scale natural PUFA production in literature. To bridge this gap, process models were developed to quantify annual microalgae-based EPA and DHA production for four locations. Among the locations examined, EPA and DHA productivity in Phoenix is highest at 8645 kg $year^{-1}$ and lowest in Minneapolis at 2525 kg $year^{-1}$. The economic analysis model further helped to quantify EPA and DHA production costs for the locations. Cost varied greatly among the locations, ranging from 141 – 461 \$ kg^{-1} for the locations. Interestingly, the scale of operations had a strong influence on the production costs as well. The results demonstrated that EPA and DHA production costs could be decreased by about 60% to 63 – 189 \$ kg^{-1} by considering the economies of scale. Results indicate that although current production costs of microalgae-based fish oils are higher than their synthetic counterparts, these natural products may be competitively placed in the global market, especially with continued research and optimization efforts.

Path forward

The scenario analysis developed for microalgae-based biorefineries presented in the thesis may be extended in various ways. An important next step is the validation and calibration of the microalgae growth model with experimental data. Microalgae cultivation experiments under outdoor ambient conditions is necessary to calibrate the models developed. This will also help standardize performance of the models for different bioreactor systems, diverse locations, and various microalgae strains. Other directions to be considered are expanding the models to integrate different combination of bioreactor

systems or other innovative reactor configuration for example, reactors facilitated with removable covers to minimize evaporative losses, utilization of solar energy to meet energy demands of cultivation, to predict microalgae productivity, as well as analyzing the environmental impacts of commercial scale microalgae cultivation while incorporating different variabilities. Furthermore, it will also be interesting to understand the implications of temperature control strategy on the optimal algal productivity and corresponding economic and environmental implications of such a thermal management strategy on large scale microalgae cultivation.

For microalgae-based multiproduct biorefinery, the present work mainly focused on value-added products with a high market price, like astaxanthin and natural EPA and DHA production, while treating the remaining extracted microalgae as bio-fertilizer. A possible extension of the models will be to incorporate other products in the mix including biofuels and assessing the economic and environmental implications of such scenarios. Besides biodiesel production via microalgae transesterification, hydrothermal liquefaction is one pathway which has been established as a promising pathway for biofuels production from microalgae [238,239]. Hence, this pathway needs to be incorporated in further analysis to determine microalgae-based high-value products and biofuels potential in comparison to fossil-fuel counterparts. Finally, an optimization framework may also be developed to elucidate the optimal product portfolio from microalgae-based biorefineries and to understand how the product portfolio is influenced by geospatial variability, choice of algae growth reactors and microalgal species strains.

Final remarks

Microalgae-based commercial scale biorefineries are in the nascent stages of development with the potential to play a pivotal role in the bio-products based economy. Process systems analysis will play an important part in designing and determining

sustainable microalgae-based biorefinery supply chains. In this thesis, process systems models are combined with economic analysis to understand feasibility of microalgae biorefinery at commercial scales considering geospatial factors. It is expected that the robust mathematical framework and scenario analyses developed in this thesis will be beneficial for related studies and adapted to alternate biomass feedstock-based processes and biorefinery configurations.

References

[1] V. Vandermeulen, M. Van der Steen, C. V. Stevens, G. Van Huylenbroeck, Industry expectations regarding the transition toward a biobased economy, Biofuels, Bioprod. Biorefining. (2012). doi:10.1002/bbb.1333.

[2] W. Pellerin, D.W. Taylor, Measuring the biobased economy: A Canadian perspective, Ind. Biotechnol. (2008). doi:10.1089/ind.2008.4.363.

[3] O. Edenhofer, R. Pichs-Madruga, Y. Sokona, K. Seyboth, P. Eickemeier, P. Matschoss, G. Hansen, S. Kadner, S. Schlömer, T. Zwickel, C. Von Stechow, IPCC, 2011: Summary for Policymakers. In: IPCC Special Report on Renewable Energy Sources and Climate Change Mitigation, 2011. doi:10.5860/CHOICE.49-6309.

[4] a U.S. Energy Information, Annual Energy Outlook 2013, Off. Integr. Int. Energy Anal. 1 (2013) 1–244. doi:DOE/EIA-0383(2013).

[5] R.C. Brown, T.R. Brown, Biorenewable Resources: Engineering New Products from Agriculture: Second Edition, 2014. doi:10.1002/9781118524985.

[6] A.A. Vertès, N. Qureshi, H.P. Blaschek, H. Yukawa, Biomass to Biofuels: Strategies for Global Industries, 2010. doi:10.1002/9780470750025.

[7] N. Gaurav, S. Sivasankari, G.S. Kiran, A. Ninawe, J. Selvin, Utilization of bioresources for sustainable biofuels: A Review, Renew. Sustain. Energy Rev. (2017). doi:10.1016/j.rser.2017.01.070.

[8] J. Ruane, A. Sonnino, A. Agostini, Bioenergy and the potential contribution of agricultural biotechnologies in developing countries, Biomass and Bioenergy. (2010). doi:10.1016/j.biombioe.2010.04.011.

[9] Nrel, A look back at the U. S. Department of Energy's aquatic species program: biodiesel from algae, Report. 328 (1998) 291 p. doi:10.2172/15003040.

[10] R.E. Davis, D.B. Fishman, E.D. Frank, M.C. Johnson, S.B. Jones, C.M. Kinchin, R.L. Skaggs, E.R. Venteris, M.S. Wigmosta, Integrated evaluation of cost, emissions, and resource potential for algal biofuels at the national scale, Environ. Sci. Technol. 48 (2014) 6035–6042. doi:10.1021/es4055719.

[11] R. Davis, A. Aden, P.T. Pienkos, Techno-economic analysis of autotrophic microalgae for fuel production, Appl. Energy. 88 (2011) 3524–3531. doi:10.1016/j.apenergy.2011.04.018.

[12] A. Sun, R. Davis, M. Starbuck, A. Ben-Amotz, R. Pate, P.T. Pienkos, Comparative cost analysis of algal oil production for biofuels, Energy. 36 (2011) 5169–5179. doi:10.1016/j.energy.2011.06.020.

[13] J.G.G. Jonker, a. P.C. Faaij, Techno-economic assessment of micro-algae as feedstock for renewable bio-energy production, Appl. Energy. 102 (2013) 461–475. doi:10.1016/j.apenergy.2012.07.053.

[14] J.W. Richardson, J.L. Outlaw, M. Allison, The economics of microalgae oil, AgBioForum. 13 (2010) 119–130. doi:10.1002/jctb.2338.

[15] L. Ou, R. Thilakaratne, R.C. Brown, M.M. Wright, Techno-economic analysis of transportation fuels from defatted microalgae via hydrothermal liquefaction and hydroprocessing, Biomass and Bioenergy. 72 (2015) 45–54. doi:10.1016/j.biombioe.2014.11.018.

[16] B.J. Gallagher, The economics of producing biodiesel from algae, Renew. Energy. 36 (2011) 158–162. doi:10.1016/j.renene.2010.06.016.

[17] F. Delrue, Y. Li-Beisson, P.A. Setier, C. Sahut, A. Roubaud, A.K. Froment, G. Peltier, Comparison of various microalgae liquid biofuel production pathways based on energetic, economic and environmental criteria, Bioresour. Technol. 136 (2013) 205–212. doi:10.1016/j.biortech.2013.02.091.

[18] N.H. Norsker, M.J. Barbosa, M.H. Vermuë, R.H. Wijffels, Microalgal production - A close look at the economics, Biotechnol. Adv. 29 (2011) 24–27. doi:10.1016/j.biotechadv.2010.08.005.

[19] L. Amer, B. Adhikari, J. Pellegrino, Technoeconomic analysis of five microalgae-to-biofuels processes of varying complexity, Bioresour. Technol. 102 (2011) 9350–9359. doi:10.1016/j.biortech.2011.08.010.

[20] J.R. Benemann, CO2 mitigation with microalgae systems, Energy Convers. Manag. 38 (1997) S475–S479. doi:10.1016/S0196-8904(96)00313-5.

[21] A. Demirbas, M. Fatih Demirbas, Importance of algae oil as a source of biodiesel, in: Energy Convers. Manag., 2011: pp. 163–170. doi:10.1016/j.enconman.2010.06.055.

[22] A. Demirbas, Use of algae as biofuel sources, Energy Convers. Manag. 51 (2010) 2738–2749. doi:10.1016/j.enconman.2010.06.010.

[23] S. Amin, Review on biofuel oil and gas production processes from microalgae, Energy Convers. Manag. 50 (2009) 1834–1840. doi:10.1016/j.enconman.2009.03.001.

[24] Y. Watanabe, D.O. Hall, Photosynthetic CO2 conversion technologies using a photobioreactor incorporating microalgae - energy and material balances -, Energy Convers. Manag. 37 (1996) 1321–1326. doi:10.1016/0196-

8904(95)00340-1.

[25] G. Stephanopolous, Cellulosic biofuels, Technol. Rev. (2008). doi:10.1146/annurev.arplant.043008.092125.

[26] E. de Jong, G. Jungmeier, Biorefinery Concepts in Comparison to Petrochemical Refineries, in: Ind. Biorefineries White Biotechnol., 2015. doi:10.1016/B978-0-444-63453-5.00001-X.

[27] A.G. Grima, E. Molina; Gonzàlez, Marìa Josè Ibànez; Gimènez, Algae for Biofuels and Energy, Algae Biofuels …. (2013) 99–113. doi:10.1007/978-94-007-5479-9.

[28] M.A. Borowitzka, High-value products from microalgae-their development and commercialisation, J. Appl. Phycol. (2013). doi:10.1007/s10811-013-9983-9.

[29] J. de la Noue, N. de Pauw, The potential of microalgal biotechnology: A review of production and uses of microalgae, Biotechnol. Adv. (1988). doi:10.1016/0734-9750(88)91921-0.

[30] M.J. Barbosa, R.H. Wijffels, Biofuels from Microalgae, in: Handb. Microalgal Cult. Appl. Phycol. Biotechnol., 2013: pp. 566–577. doi:10.1002/9781118567166.ch29.

[31] Nrc, Sustainable development of algal biofuels in the United States, 2012. doi:10.4162/nrp.2013.7.3.233.

[32] W.Y. Cheah, P.L. Show, J.S. Chang, T.C. Ling, J.C. Juan, Biosequestration of atmospheric CO2 and flue gas-containing CO2 by microalgae, Bioresour. Technol. (2015). doi:10.1016/j.biortech.2014.11.026.

[33] P. Spolaore, C. Joannis-Cassan, E. Duran, A. Isambert, Commercial applications of microalgae, J. Biosci. Bioeng. 101 (2006) 87–96. doi:10.1263/jbb.101.87.

[34] T.M. Mata, A.A. Martins, N.S. Caetano, Microalgae for biodiesel production and other applications: A review, Renew. Sustain. Energy Rev. 14 (2010) 217–232. doi:10.1016/j.rser.2009.07.020.

[35] L. Brennan, P. Owende, Biofuels from microalgae-A review of technologies for production, processing, and extractions of biofuels and co-products, Renew. Sustain. Energy Rev. 14 (2010) 557–577. doi:10.1016/j.rser.2009.10.009.

[36] P.M. Foley, E.S. Beach, J.B. Zimmerman, Algae as a source of renewable chemicals: Opportunities and challenges, Green Chem. (2011). doi:10.1039/c1gc00015b.

[37] P.M. Slegers, Scenario studies for algae production, 2014.

[38] R.H. Wijffels, M.J. Barbosa, An outlook on microalgal biofuels, Science (80-.). (2010). doi:10.1126/science.1189003.

[39] M.R. Tredici, Mass Production of Microalgae: Photobioreactors, in: Handb. Microalgal Cult. Biotechnol. Appl. Phycol., 2004: pp. 178–214. doi:10.1002/9780470995280.ch9.

[40] A.P. Carvalho, L.A. Meireles, F.X. Malcata, Microalgal reactors: A review of enclosed system designs and performances, Biotechnol. Prog. (2006). doi:10.1021/bp060065r.

[41] P.M. Slegers, M.B. Lösing, R.H. Wijffels, G. van Straten, A.J.B. van Boxtel, Scenario evaluation of open pond microalgae production, Algal Res. 2 (2013) 358–368. doi:10.1016/j.algal.2013.05.001.

[42] P.M. Slegers, R.H. Wijffels, G. van Straten, A.J.B. van Boxtel, Design scenarios for flat panel photobioreactors, Appl. Energy. 88 (2011) 3342–3353.

doi:10.1016/j.apenergy.2010.12.037.

[43] W.H. Thomas, D.L.R. Seibert, M. Alden, A. Neori, P. Eldridge, Yields, photosynthetic efficiencies and proximate composition of dense marine microalgal cultures. I. Introduction and Phaeodactylum tricornutum experiments, Biomass. (1984). doi:10.1016/0144-4565(84)90022-2.

[44] A.D. Ansell, J.E.G. Raymont, K.F. Lander, E. Crowley, P. Shackley, STUDIES ON THE MASS CULTURE OF PHAEODACTYLUM. II. THE GROWTH OF PHAEODACTYLUM AND OTHER SPECIES IN OUTDOOR TANKS, Limnol. Oceanogr. (1963). doi:10.4319/lo.1963.8.2.0184.

[45] M.R. Tredici, R. Materassi, From open ponds to vertical alveolar panels: the Italian experience in the development of reactors for the mass cultivation of phototrophic microorganisms, J. Appl. Phycol. (1992). doi:10.1007/BF02161208.

[46] M.A. Borowitzka, Biotechno,logy Commercial production of microalgae" ponds, tanks, and fermenters tubes, 1999.

[47] B. Crowe, S. Attalah, S. Agrawal, P. Waller, R. Ryan, J. Van Wagenen, A. Chavis, J. Kyndt, M. Kacira, K.L. Ogden, M. Huesemann, A comparison of nannochloropsis salina growth performance in two outdoor pond designs: Conventional raceways versus the arid pond with superior temperature management, Int. J. Chem. Eng. (2012). doi:10.1155/2012/920608.

[48] J. Quinn, L. de Winter, T. Bradley, Microalgae bulk growth model with application to industrial scale systems, Bioresour. Technol. 102 (2011) 5083–5092. doi:10.1016/j.biortech.2011.01.019.

[49] R. Bosma, E. Van Zessen, J.H. Reith, J. Tramper, R.H. Wijffels, Prediction of

volumetric productivity of an outdoor photobioreactor, Biotechnol. Bioeng. (2007). doi:10.1002/bit.21319.

[50] F.G. Acién Fernández, F. García Camacho, J.A. Sánchez Pérez, J.M. Fernández Sevilla, E. Molina Grima, A model for light distribution and average solar irradiance inside outdoor tubular photobioreactors for the microalgal mass culture, Biotechnol. Bioeng. (1997). doi:10.1002/(SICI)1097-0290(19970905)55:5<701::AID-BIT1>3.0.CO;2-F.

[51] F.G.A. Fernández, F.G. Camacho, J.A.S. Pérez, J.M.F. Sevilla, E.M. Grima, Modeling of biomass productivity in tubular photobioreactors for microalgal cultures: Effects of dilution rate, tube diameter, and solar irradiance, Biotechnol. Bioeng. (1998). doi:10.1002/(SICI)1097-0290(19980620)58:6<605::AID-BIT6>3.0.CO;2-M.

[52] E. Molina Grima, F. Garcı´a Camacho, J.A.S. Perez, J.M.F. Sevilla, F.G.A. Fernandez, A.C. Gomez, A mathematical model of microalgal growth in light limited chemostat cultures, J. Chem. Technol. Biotechnol. 61 (1994) 167–173.

[53] F.G. Acién Fernández, J.M. Fernández Sevilla, J.A. Sánchez Pérez, E. Molina Grima, Y. Chisti, Airlift-driven external-loop tubular photobioreactors for outdoor production of microalgae: Assessment of design and performance, Chem. Eng. Sci. (2001). doi:10.1016/S0009-2509(00)00521-2.

[54] E. Molina, J. Fernández, F.G. Acién, Y. Chisti, Tubular photobioreactor design for algal cultures, J. Biotechnol. (2001). doi:10.1016/S0168-1656(01)00353-4.

[55] L. Batan, J.C. Quinn, T.H. Bradley, Analysis of water footprint of a photobioreactor microalgae biofuel production system from blue, green and lifecycle perspectives, Algal Res. 2 (2013) 196–203. doi:10.1016/j.algal.2013.02.003.

[56] E.R. Venteris, R.L. Skaggs, A.M. Coleman, M.S. Wigmosta, An assessment of land availability and price in the coterminous United States for conversion to algal biofuel production, Biomass and Bioenergy. 47 (2012) 483–497. doi:10.1016/j.biombioe.2012.09.060.

[57] M.S. Wigmosta, A.M. Coleman, R.J. Skaggs, M.H. Huesemann, L.J. Lane, National microalgae biofuel production potential and resource demand, Water Resour. Res. 47 (2011). doi:10.1029/2010WR009966.

[58] R.C. Pate, Resource requirements for the large-scale production of algal biofuels, Biofuels. 4 (2013) 409–435. doi:10.4155/bfs.13.28.

[59] J.C. Quinn, K.B. Catton, S. Johnson, T.H. Bradley, Geographical Assessment of Microalgae Biofuels Potential Incorporating Resource Availability, Bioenergy Res. 6 (2013) 591–600. doi:10.1007/s12155-012-9277-0.

[60] E.R. Venteris, R.L. Skaggs, M.S. Wigmosta, A.M. Coleman, A national-scale comparison of resource and nutrient demands for algae-based biofuel production by lipid extraction and hydrothermal liquefaction, Biomass and Bioenergy. 64 (2014) 276–290. doi:10.1016/j.biombioe.2014.02.001.

[61] E.R. Venteris, R.C. McBride, A.M. Coleman, R.L. Skaggs, M.S. Wigmosta, Siting algae cultivation facilities for biofuel production in the united states: Trade-offs between growth rate, site constructability, water availability, and infrastructure, Environ. Sci. Technol. 48 (2014) 3559–3566. doi:10.1021/es4045488.

[62] A.M. Coleman, J.M. Abodeely, R.L. Skaggs, W.A. Moeglein, D.T. Newby, E.R. Venteris, M.S. Wigmosta, An integrated assessment of location-dependent scaling for microalgae biofuel production facilities, Algal Res. 5 (2014) 79–94. doi:10.1016/j.algal.2014.05.008.

[63] R. Pate, G. Klise, B. Wu, Resource demand implications for US algae biofuels production scale-up, Appl. Energy. 88 (2011) 3377–3388. doi:10.1016/j.apenergy.2011.04.023.

[64] J.C. Quinn, R. Davis, The potentials and challenges of algae based biofuels: A review of the techno-economic, life cycle, and resource assessment modeling, Bioresour. Technol. 184 (2015) 444–452. doi:10.1016/j.biortech.2014.10.075.

[65] E. Nogueira Junior, M. Kumar, S. Pankratz, A.O. Oyedun, A. Kumar, Development of life cycle water footprints for the production of fuels and chemicals from algae biomass, Water Res. 140 (2018) 311–322. doi:10.1016/J.WATRES.2018.04.046.

[66] L. Batan, J. Quinn, B. Willson, T. Bradley, Net energy and greenhouse gas emission evaluation of biodiesel derived from microalgae, Environ. Sci. Technol. 44 (2010) 7975–7980. doi:10.1021/es102052y.

[67] C.F. Murphy, D.T. Allen, Energy-Water Nexus for Mass Cultivation of Algae, Environ. Sci. Technol. 45 (2011) 5861–5868. doi:10.1021/es200109z.

[68] J. Yang, M. Xu, X. Zhang, Q. Hu, M. Sommerfeld, Y. Chen, Life-cycle analysis on biodiesel production from microalgae: Water footprint and nutrients balance, Bioresour. Technol. 102 (2011) 159–165. doi:10.1016/j.biortech.2010.07.017.

[69] M. Min, B. Hu, M.J. Mohr, A. Shi, J. Ding, Y. Sun, Y. Jiang, Z. Fu, R. Griffith, F. Hussain, D. Mu, Y. Nie, P. Chen, W. Zhou, R. Ruan, Swine manure-based pilot-scale algal biomass production system for fuel production and wastewater treatment--a case study., Appl. Biochem. Biotechnol. 172 (2014) 1390–406. doi:10.1007/s12010-013-0603-6.

[70] W. Zhou, B. Hu, Y. Li, M. Min, M. Mohr, Z. Du, P. Chen, R. Ruan, Mass cultivation of microalgae on animal wastewater: A sequential two-stage cultivation process for energy crop and omega-3-rich animal feed production, Appl. Biochem. Biotechnol. 168 (2012) 348–363. doi:10.1007/s12010-012-9779-4.

[71] R. Craggs, D. Sutherland, H. Campbell, Hectare-scale demonstration of high rate algal ponds for enhanced wastewater treatment and biofuel production, J. Appl. Phycol. 24 (2012) 329–337. doi:10.1007/s10811-012-9810-8.

[72] J.B.K. Park, R.J. Craggs, A.N. Shilton, Wastewater treatment high rate algal ponds for biofuel production, Bioresour. Technol. 102 (2011) 35–42. doi:10.1016/j.biortech.2010.06.158.

[73] S. Chinnasamy, A. Bhatnagar, R.W. Hunt, K.C. Das, Microalgae cultivation in a wastewater dominated by carpet mill effluents for biofuel applications, Bioresour. Technol. 101 (2010) 3097–3105. doi:10.1016/j.biortech.2009.12.026.

[74] M.F. Demirbas, Biofuels from algae for sustainable development, Appl. Energy. 88 (2011) 3473–3480. doi:10.1016/j.apenergy.2011.01.059.

[75] E.P. Resurreccion, L.M. Colosi, M.A. White, A.F. Clarens, Comparison of algae cultivation methods for bioenergy production using a combined life cycle assessment and life cycle costing approach, Bioresour. Technol. 126 (2012) 298–306. doi:10.1016/j.biortech.2012.09.038.

[76] J.W. Richardson, M.D. Johnson, X. Zhang, P. Zemke, W. Chen, Q. Hu, A financial assessment of two alternative cultivation systems and their contributions to algae biofuel economic viability, Algal Res. 4 (2014) 96–104. doi:10.1016/j.algal.2013.12.003.

[77] G. Markou, E. Nerantzis, Microalgae for high-value compounds and biofuels production: A review with focus on cultivation under stress conditions, Biotechnol. Adv. (2013). doi:10.1016/j.biotechadv.2013.07.011.

[78] E. Molina Grima, E.H. Belarbi, F.G. Acién Fernández, a. Robles Medina, Y. Chisti, Recovery of microalgal biomass and metabolites: Process options and economics, Biotechnol. Adv. 20 (2003) 491–515. doi:10.1016/S0734-9750(02)00050-2.

[79] S. Leu, S. Boussiba, Advances in the Production of High-Value Products by Microalgae, Ind. Biotechnol. 10 (2014) 169–183. doi:10.1089/ind.2013.0039.

[80] H.W. Yen, I.C. Hu, C.Y. Chen, S.H. Ho, D.J. Lee, J.S. Chang, Microalgae-based biorefinery - From biofuels to natural products, Bioresour. Technol. (2013). doi:10.1016/j.biortech.2012.10.099.

[81] K.W. Chew, J.Y. Yap, P.L. Show, N.H. Suan, J.C. Juan, T.C. Ling, D.J. Lee, J.S. Chang, Microalgae biorefinery: High value products perspectives, Bioresour. Technol. (2017). doi:10.1016/j.biortech.2017.01.006.

[82] M.F. De Jesus Raposo, R.M.S.C. De Morais, A.M.M.B. De Morais, Health applications of bioactive compounds from marine microalgae, Life Sci. (2013). doi:10.1016/j.lfs.2013.08.002.

[83] P. Spolaore, C. Joannis-Cassan, E. Duran, A. Isambert, Commercial applications of microalgae, J. Biosci. Bioeng. (2006). doi:10.1263/jbb.101.87.

[84] M. Koller, A. Muhr, G. Braunegg, Microalgae as versatile cellular factories for valued products, Algal Res. (2014). doi:10.1016/j.algal.2014.09.002.

[85] The biochemistry of the carotenoids: volume II, animals: T.W. Goodwin Chapman

and Hall; London, 1984 224 pages. £25.00, FEBS Lett. (1985). doi:10.1016/0014-5793(85)80904-2.

[86] G. Panis, J.R. Carreon, Commercial astaxanthin production derived by green alga Haematococcus pluvialis: A microalgae process model and a techno-economic assessment all through production line, Algal Res. (2016). doi:10.1016/j.algal.2016.06.007.

[87] K.H.M. Cardozo, T. Guaratini, M.P. Barros, V.R. Falcão, A.P. Tonon, N.P. Lopes, S. Campos, M.A. Torres, A.O. Souza, P. Colepicolo, E. Pinto, Metabolites from algae with economical impact, Comp. Biochem. Physiol. - C Toxicol. Pharmacol. (2007). doi:10.1016/j.cbpc.2006.05.007.

[88] A. Molino, A. Iovine, P. Casella, S. Mehariya, S. Chianese, A. Cerbone, J. Rimauro, D. Musmarra, Microalgae Characterization for Consolidated and New Application in Human Food, Animal Feed and Nutraceuticals, Int. J. Environ. Res. Public Health. 15 (2018) 2436. doi:10.3390/ijerph15112436.

[89] M.M.R. Shah, Y. Liang, J.J. Cheng, M. Daroch, Astaxanthin-producing green microalga Haematococcus pluvialis: From single cell to high value commercial products, Front. Plant Sci. (2016). doi:10.3389/fpls.2016.00531.

[90] R.T. Lorenz, G.R. Cysewski, Commercial potential for Haematococcus microalgae as a natural source of astaxanthin, Trends Biotechnol. (2000). doi:10.1016/S0167-7799(00)01433-5.

[91] J. Li, D. Zhu, J. Niu, S. Shen, G. Wang, An economic assessment of astaxanthin production by large scale cultivation of Haematococcus pluvialis, Biotechnol. Adv. (2011). doi:10.1016/j.biotechadv.2011.04.001.

[92] M. Guerin, M.E. Huntley, M. Olaizola, Haematococcus astaxanthin: Applications for human health and nutrition, Trends Biotechnol. (2003). doi:10.1016/S0167-7799(03)00078-7.

[93] P. Pérez-López, S. González-García, C. Jeffryes, S.N. Agathos, E. McHugh, D. Walsh, P. Murray, S. Moane, G. Feijoo, M.T. Moreira, Life cycle assessment of the production of the red antioxidant carotenoid astaxanthin by microalgae: From lab to pilot scale, J. Clean. Prod. (2014). doi:10.1016/j.jclepro.2013.07.011.

[94] J. Ruiz, G. Oliveri, J. de Vree, R. Bosma, P. Willems, J.H. Reith, M.H.M. Eppink, D.M.M. Kleinegris, R.H. Wijffels, M.J. Barbosa, Towards industrial products from microalgae, Energy Environ. Sci. 9 (2016) 3036–3043. doi:10.1039/c6ee01493c.

[95] K.W. Chew, J.Y. Yap, P.L. Show, N.H. Suan, J.C. Juan, T.C. Ling, D.J. Lee, J.S. Chang, Microalgae biorefinery: High value products perspectives, Bioresour. Technol. (2017). doi:10.1016/j.biortech.2017.01.006.

[96] G. Lenihan-Geels, K.S. Bishop, L.R. Ferguson, Alternative sources of omega-3 fats: Can we find a sustainable substitute for fish?, Nutrients. (2013). doi:10.3390/nu5041301.

[97] https://www.iffo.net/, (n.d.).

[98] M.S. Chauton, K.I. Reitan, N.H. Norsker, R. Tveterås, H.T. Kleivdal, A techno-economic analysis of industrial production of marine microalgae as a source of EPA and DHA-rich raw material for aquafeed: Research challenges and possibilities, Aquaculture. (2015). doi:10.1016/j.aquaculture.2014.10.038.

[99] R. Shields, I. Lupatsch, 5 Algae for aquaculture and animal feeds, in: Microalgal Biotechnol. Integr. Econ., 2013. doi:10.1515/9783110298321.79.

[100] J. Benemann, Microalgae for biofuels and animal feeds, Energies. (2013). doi:10.3390/en6115869.

[101] G.S. Burr, F.T. Barrows, G. Gaylord, W.R. Wolters, Apparent digestibility of macro-nutrients and phosphorus in plant-derived ingredients for Atlantic salmon, Salmo salar and Arctic charr, Salvelinus alpinus, Aquac. Nutr. (2011). doi:10.1111/j.1365-2095.2011.00855.x.

[102] A.T.T.--a Focus, H. Committee, R. Needs, F. Cell, H. Technologies, C. Isbn, T. Pdf, N.A. Press, N. Academy, Transitions to alternative transportation technologies: a focus on hydrogen, 2008. http://scholar.google.com/scholar?hl=en&btnG=Search&q=intitle:Transitions+to+alternative+transportation+technologies+-+a+focus+on+hydrogen#0%5Cnhttp://scholar.google.com/scholar?hl=en&btnG=Search&q=intitle:Transitions+to+alternative+transportation+technolog.

[103] Pnnl, S. Jones, Y. Zhu, D. Anderson, R.T. Hallen, D.C. Elliott, Process Design and Economics for the Conversion of Algal Biomass to Hydrocarbons : Whole Algae Hydrothermal Liquefaction and Upgrading, (2014) 69. doi:10.2172/1126336.

[104] P.T. Pienkos, A. Darzins, The promise and challenges of microalgal-derived biofuels, Biofuels, Bioprod. Biorefining. 3 (2009) 431–440. doi:10.1002/bbb.159.

[105] J.W. Richardson, M.D. Johnson, J.L. Outlaw, Economic comparison of open pond raceways to photo bio-reactors for profitable production of algae for transportation fuels in the Southwest, Algal Res. 1 (2012) 93–100. doi:10.1016/j.algal.2012.04.001.

[106] R. Thilakaratne, M.M. Wright, R.C. Brown, A techno-economic analysis of

microalgae remnant catalytic pyrolysis and upgrading to fuels, Fuel. 128 (2014) 104–112. doi:10.1016/j.fuel.2014.02.077.

[107] J.R. Benemann, W.J. Oswald, Systems and Economic Analysis of Microalgae Ponds for Conversion of CO2 to Biomass, Final Rep. to Dep. Energy, Pittsburgh Energy Technol. Cent. (1996) DOE/PC/93204-T5. doi:10.2172/493389.

[108] T.J. Lundquist, I.C. Woertz, N.W.T. Quinn, J.R. Benemann, A Realistic Technology and Engineering Assessment of Algae Biofuel Production, Energy. October (2010) 1. http://digitalcommons.calpoly.edu/cenv_fac/188/.

[109] L. Axelsson, M. Franzén, M. Ostwald, G. Berndes, G. Lakshmi, N.H. Ravindranath, Perspective: Jatropha cultivation in southern India: Assessing farmers' experiences, Biofuels, Bioprod. Biorefining. 6 (2012) 246–256. doi:10.1002/bbb.

[110] M. Brandenberger, J. Matzenberger, F. Vogel, C. Ludwig, Producing synthetic natural gas from microalgae via supercritical water gasification: A techno-economic sensitivity analysis, Biomass and Bioenergy. 51 (2013) 26–34. doi:10.1016/j.biombioe.2012.12.038.

[111] J.A. Gomez, K. Höffner, P.I. Barton, From sugars to biodiesel using microalgae and yeast, Green Chem. (2015) 461–475. doi:10.1039/C5GC01843A.

[112] P.J.L.B. Williams, L.M.L. Laurens, Microalgae as biodiesel & biomass feedstocks: Review & analysis of the biochemistry, energetics & economics, Energy Environ. Sci. 3 (2010) 554. doi:10.1039/b924978h.

[113] S. Nagarajan, S.K. Chou, S. Cao, C. Wu, Z. Zhou, An updated comprehensive techno-economic analysis of algae biodiesel, Bioresour. Technol. 145 (2013)

150–156. doi:10.1016/j.biortech.2012.11.108.

[114] R. Davis, C. Kinchin, J. Markham, E.C.D. Tan, L.M.L. Laurens, Process Design and Economics for the Conversion of Algal Biomass to Biofuels : Algal Biomass Fractionation to Lipid- Products Process Design and Economics for the Conversion of Algal Biomass to Biofuels : Algal Biomass Fractionation to Lipid- and Carbohyd, (2014) NREL/TP-5100-62368.

[115] M.Q.W. Ryan Davis , Daniel Fishman , Edward D. Frank , Mark S. Wigmosta ,Andy Aden , Andre M. Coleman , Philip T. Pienkos , Richard J. Skaggs, Erik R. Venteris, Renewable Diesel from Algal Lipids: An Integrated Baseline for Cost, Emissions, and Resource Potential from a Harmonized Model, J. Chem. Inf. Model. 53 (2013) 1689–1699. doi:10.1017/CBO9781107415324.004.

[116] B. Schlarb, Algal research in the uk, Technol. Rev. (2011). http://www.bbsrc.ac.uk/organisation/policies/reviews/scientific-areas/1107-algal-research.aspx.

[117] O. Jorquera, A. Kiperstok, E.A. Sales, M. Embiruçu, M.L. Ghirardi, Comparative energy life-cycle analyses of microalgal biomass production in open ponds and photobioreactors, Bioresour. Technol. 101 (2010) 1406–1413. doi:10.1016/j.biortech.2009.09.038.

[118] R.M. Handler, C.E. Canter, T.N. Kalnes, F.S. Lupton, O. Kholiqov, D.R. Shonnard, P. Blowers, Evaluation of environmental impacts from microalgae cultivation in open-air raceway ponds: Analysis of the prior literature and investigation of wide variance in predicted impacts, Algal Res. 1 (2012) 83–92. doi:10.1016/j.algal.2012.02.003.

[119] P.K. Campbell, T. Beer, D. Batten, Life cycle assessment of biodiesel production

from microalgae in ponds, Bioresour. Technol. 102 (2010) 50–56. doi:10.1016/j.biortech.2010.06.048.

[120] S. Abu-Ghosh, D. Fixler, Z. Dubinsky, D. Iluz, Energy-input analysis of the life-cycle of microalgal cultivation systems and best scenario for oil-rich biomass production, Appl. Energy. 154 (2014) 1082–1088. doi:10.1016/j.apenergy.2015.02.086.

[121] C.M. Beal, L.N. Gerber, D.L. Sills, M.E. Huntley, S.C. Machesky, M.J. Walsh, J.W. Tester, I. Archibald, J. Granados, C.H. Greene, Algal biofuel production for fuels and feed in a 100-ha facility: A comprehensive techno-economic analysis and life cycle assessment, Algal Res. 10 (2015) 266–279. doi:10.1016/j.algal.2015.04.017.

[122] M.E. Huntley, Z.I. Johnson, S.L. Brown, D.L. Sills, L. Gerber, I. Archibald, S.C. Machesky, J. Granados, C. Beal, C.H. Greene, Demonstrated large-scale production of marine microalgae for fuels and feed, Algal Res. 10 (2015) 249–265. doi:10.1016/j.algal.2015.04.016.

[123] A.F. Clarens, E.P. Resurreccion, M.A. White, L.M. Colosi, Environmental life cycle comparison of algae to other bioenergy feedstocks, Environ. Sci. Technol. 44 (2010) 1813–1819. doi:10.1021/es902838n.

[124] L. Lardon, A. Hélias, B. Sialve, J.-P. Steyer, O. Bernard, Life-Cycle Assessment of Biodiesel Production from Microalgae, Environ. Sci. Technol. 43 (2009) 6475–6481. doi:10.1021/es900705j.

[125] A.L. Stephenson, E. Kazamia, J.S. Dennis, C.J. Howe, S.A. Scott, A.G. Smith, Life-cycle assessment of potential algal biodiesel production in the united kingdom: A comparison of raceways and air-lift tubular bioreactors, Energy and

Fuels. 24 (2010) 4062–4077. doi:10.1021/ef1003123.

[126] K.L. Kadam, Environmental implications of power generation via coal-microalgae cofiring, Energy. 27 (2002) 905–922. doi:10.1016/S0360-5442(02)00025-7.

[127] M.A. Borowitzka, Commercial production of microalgae: ponds, tanks, tubes and fermenters, in: J. Biotechnol., 1999: pp. 313–321. doi:10.1016/S0168-1656(99)00083-8.

[128] J.N. Rogers, J.N. Rosenberg, B.J. Guzman, V.H. Oh, L.E. Mimbela, A. Ghassemi, M.J. Betenbaugh, G. a. Oyler, M.D. Donohue, A critical analysis of paddlewheel-driven raceway ponds for algal biofuel production at commercial scales, Algal Res. 4 (2013) 76–88. doi:10.1016/j.algal.2013.11.007.

[129] Y. Chisti, Biodiesel from microalgae., Biotechnol. Adv. 25 (2007) 294–306. doi:10.1016/j.biotechadv.2007.02.001.

[130] M. Marsullo, A. Mian, A.V. Ensinas, G. Manente, A. Lazzaretto, F. Marechal, Dynamic Modeling of the Microalgae Cultivation Phase for Energy Production in Open Raceway Ponds and Flat Panel Photobioreactors, Front. Energy Res. 3 (2015) 1–18. doi:10.3389/fenrg.2015.00041.

[131] S. Boussiba, A. Vonshak, Z. Cohen, Y. Avissar, A. Richmond, Lipid and biomass production by the halotolerant microalga Nannochloropsis salina, Biomass. 12 (1987) 37–47. doi:10.1016/0144-4565(87)90006-0.

[132] Climate Data Online, (n.d.). http://www.ncdc.noaa.gov/ (accessed September 20, 2015).

[133] Q. Béchet, A. Shilton, J.B.K. Park, R.J. Craggs, B. Guieysse, Universal temperature model for shallow algal ponds provides improved accuracy., Environ.

Sci. Technol. 45 (2011) 3702–9. doi:10.1021/es1040706.

[134] A.D. Yang, Modeling and evaluation of CO2 supply and utilization in slgal ponds, Ind. Eng. Chem. Res. 50 (2011) 11181–11192. doi:10.1021/Ie200723w.

[135] B. Ketheesan, N. Nirmalakhandan, Modeling microalgal growth in an airlift-driven raceway reactor, Bioresour. Technol. 136 (2013) 689–696. doi:10.1016/j.biortech.2013.02.028.

[136] A.K. Pegallapati, N. Nirmalakhandan, Modeling algal growth in bubble columns under sparging with CO2-enriched air, Bioresour. Technol. 124 (2012) 137–145. doi:10.1016/j.biortech.2012.08.026.

[137] J. a Raven, R.J. Geider, Temperature and algal growth, New Phytol. 110 (1988) 441–461. doi:10.1111/j.1469-8137.1988.tb00282.x.

[138] W. Gerbens-Leenes, A.Y. Hoekstra, T.H. van der Meer, The water footprint of bioenergy., Proc. Natl. Acad. Sci. U. S. A. 106 (2009) 10219–23. doi:10.1073/pnas.0812619106.

[139] R.. Andersen, Algal Culturing Techniques, Elsevier Academic Press, Amsterdam, 2005, n.d.

[140] R. Hase, H. Oikawa, C. Sasao, M. Morita, Y. Watanabe, Photosynthetic production of microalgal biomass in a raceway system under greenhouse conditions in Sendai city, J. Biosci. Bioeng. 89 (2000) 157–163. doi:10.1016/S1389-1723(00)88730-7.

[141] B. Ketheesan, N. Nirmalakhandan, Development of a new airlift-driven raceway reactor for algal cultivation, Appl. Energy. 88 (2011) 3370–3376. doi:10.1016/j.apenergy.2010.12.034.

[142] S.C. James, V. Boriah, Modeling algae growth in an open-channel raceway., J. Comput. Biol. 17 (2010) 895–906. doi:10.1089/cmb.2009.0078.

[143] A. Richmond, Handbook of microalgal culture: biotechnology and applied phycology/edited by Amos Richmond., 2004. doi:10.1002/9780470995280.

[144] A. Packer, Y. Li, T. Andersen, Q. Hu, Y. Kuang, M. Sommerfeld, Growth and neutral lipid synthesis in green microalgae: A mathematical model, Bioresour. Technol. 102 (2011) 111–117. doi:10.1016/j.biortech.2010.06.029.

[145] C. Moler, MATLAB, MathWorks, Inc. (2015).

[146] J.E. Coons, D.M. Kalb, T. Dale, B.L. Marrone, Getting to low-cost algal biofuels: A monograph on conventional and cutting-edge harvesting and extraction technologies, Algal Res. 6 (2014) 250–270. doi:10.1016/j.algal.2014.08.005.

[147] F.G. Acién, J.M. Fernández, J.J. Magán, E. Molina, Production cost of a real microalgae production plant and strategies to reduce it., Biotechnol. Adv. 30 (2012) 1344–53. doi:10.1016/j.biotechadv.2012.02.005.

[148] United States Department of Agriculture, Land Values 2015 Summary, n.d. http://www.usda.gov/nass/PUBS/TODAYRPT/land0815.pdf.

[149] U.S. Energy Information Adinistration, Electric Power Monthly with Data for October 2015, 2015. http://www.eia.gov/electricity/monthly/pdf/epm.pdf.

[150] V. Vasudevan, R.W. Stratton, M.N. Pearlson, G.R. Jersey, A.G. Beyene, J.C. Weissman, M. Rubino, J.I. Hileman, Environmental performance of algal biofuel technology options, Environ. Sci. Technol. 46 (2012) 2451–2459. doi:10.1021/es2026399.

[151] A. Richmond, E. Lichtenberg, B. Stahl, A. Vonshak, Quantitative assessment of

the major limitations on productivity of Spirulina platensis in open raceways, J. Appl. Phycol. 2 (1990) 195–206. doi:10.1007/BF02179776.

[152] K. Zhang, N. Kurano, S. Miyachi, Outdoor culture of a cyanobacterium with a vertical flat-plate photobioreactor: effects on productivity of the reactor orientation, distance setting between the plates, and culture temperature, Appl. Microbiol. Biotechnol. 52 (1999) 781–786. doi:10.1007/s002530051591.

[153] I.R. Davison, Environmental Effects on Algal Photosynthesis: Temperature, J. Phycol. 27 (1991) 2–8. doi:10.1111/1529-8817.ep10868724.

[154] J. Doucha, F. Straka, K. Lívanský, Utilization of flue gas for cultivation of microalgae (Chlorella sp.) in an outdoor open thin-layer photobioreactor, J. Appl. Phycol. 17 (2005) 403–412. doi:10.1007/s10811-005-8701-7.

[155] J.C. Weissman, D.M. Tillet, R.P. Goebel, Design and Operation of an Outdoor Microalgae Test Facility Final Subcontract Report Design and Operation of an Facility, Energy. 8 (1989) 2266–2284. http://www.pubmedcentral.nih.gov/articlerender.fcgi?artid=2758755&tool=pmcentrez&rendertype=abstract.

[156] R. Davis, A. Aden, P.T. Pienkos, Techno-economic analysis of autotrophic microalgae for fuel production, Appl. Energy. 88 (2011) 3524–3531. doi:10.1016/j.apenergy.2011.04.018.

[157] W.H. Thomas, D.L.R. Seibert, M. Alden, P. Eldridge, A. Neori, Yields, Photosynthetic Efficiencies, and Proximate Chemical Composition of Dense Cultures of Marine Microalgae, 1983. http://www.google.com/url?sa=t&rct=j&q=yields%252C photosynthetic efficiencies and proximate composition of dense marine microalgal cultures. i. introduction

and phaeodactylum tricornutum experi-ments&source=web&cd=1&ved=0CCMQFjAA&url=http%253A%252F%252Fwww.nrel.

[158] E. Stephens, I.L. Ross, Z. King, J.H. Mussgnug, O. Kruse, C. Posten, M.A. Borowitzka, B. Hankamer, An economic and technical evaluation of microalgal biofuels, Nat. Biotechnol. 28 (2010) 126–128. doi:10.1038/nbt0210-126.

[159] F. Delrue, P.-A. Setier, C. Sahut, L. Cournac, A. Roubaud, G. Peltier, A.-K. Froment, An economic, sustainability, and energetic model of biodiesel production from microalgae., Bioresour. Technol. 111 (2012) 191–200. doi:10.1016/j.biortech.2012.02.020.

[160] R. Davis, J. Markham, C. Kinchin, N. Grundl, E.C.D. Tan, D. Humbird, R. Davis, J. Markham, C. Kinchin, N. Grundl, E.C.D. Tan, D. Humbird, Process Design and Economics for the Production of Algal Biomass : Algal Biomass Production in Open Pond Systems and Processing Through Dewatering for Downstream Conversion Process Design and Economics for the Production of Algal Biomass : Algal Biomass P, (2016).

[161] IEA Bioenergy, State of Technology Review - Algae Bioenergy, 2017. doi:10.13140/RG.2.2.11770.90560.

[162] L. Xu, P.J. Weathers, X.R. Xiong, C.Z. Liu, Microalgal bioreactors: Challenges and opportunities, Eng. Life Sci. 9 (2009) 178–189. doi:10.1002/elsc.200800111.

[163] S. Banerjee, S. Ramaswamy, Dynamic process model and economic analysis of microalgae cultivation in open raceway ponds, Algal Res. 26 (2017) 330–340. doi:10.1016/j.algal.2017.08.011.

[164] C.H. Endres, A. Roth, T.B. Brück, Modeling Microalgae Productivity in Industrial-Scale Vertical Flat Panel Photobioreactors, Environ. Sci. Technol. 52 (2018) 5490–5498. doi:10.1021/acs.est.7b05545.

[165] J.C.M. Pires, M.C.M. Alvim-Ferraz, F.G. Martins, Photobioreactor design for microalgae production through computational fluid dynamics: A review, Renew. Sustain. Energy Rev. 79 (2017) 248–254. doi:10.1016/j.rser.2017.05.064.

[166] S. Banerjee, S. Ramaswamy, Dynamic process model and economic analysis of microalgae cultivation in flat panel photobioreactors, Algal Res. (2019). doi:10.1016/j.algal.2019.101445.

[167] National Solar Radiation Database, National Renewable Energy Laboratory, (n.d.). redc.nrel.gov/solar/old_data/nsrdb/ (accessed April 20, 2017).

[168] Q. Béchet, A. Shilton, O.B. Fringer, R. Munoz, B. Guieysse, Mechanistic modeling of broth temperature in outdoor photobioreactors, Environ. Sci. Technol. 44 (2010) 2197–2203. doi:10.1021/es903214u.

[169] C.H. Endres, A. Roth, T.B. Bruck, Thermal Reactor Model for Large-Scale Algae Cultivation in Vertical Flat Panel Photobioreactors, Environ. Sci. Technol. 50 (2016) 3920–3927. doi:10.1021/acs.est.5b05414.

[170] M.R. Tredici, L. Rodolfi, N. Biondi, N. Bassi, G. Sampietro, Techno-economic analysis of microalgal biomass production in a 1-ha Green Wall Panel (GWP®) plant, Algal Res. 19 (2016) 253–263. doi:10.1016/j.algal.2016.09.005.

[171] U.S.E. Information Association, Electric Power Monthly with Data for March 2017, 2017. doi:10.2172/123200.

[172] USDA, Land Values 2016 Summary, (2016). doi:ISSN:1949-0372.

[173] M.S. Peters, K.D. Timmerhaus, Plant Design and Economics for Chemical Engineers, 1991.

[174] M.R. Tredici, N. Bassi, M. Prussi, N. Biondi, L. Rodolfi, G. Chini Zittelli, G. Sampietro, Energy balance of algal biomass production in a 1-ha “Green Wall Panel” plant: How to produce algal biomass in a closed reactor achieving a high Net Energy Ratio, Appl. Energy. 154 (2015) 1103–1111. doi:10.1016/j.apenergy.2015.01.086.

[175] M.A. Borowitzka, Techno-Economic Modeling for Biofuels from Microalgae, in: Algae Biofuels …, 2013: pp. 99–113. doi:10.1007/978-94-007-5479-9.

[176] R.R. Ambati, P.S. Moi, S. Ravi, R.G. Aswathanarayana, Astaxanthin: Sources, extraction, stability, biological activities and its commercial applications - A review, Mar. Drugs. (2014). doi:10.3390/md12010128.

[177] S. Davinelli, M.E. Nielsen, G. Scapagnini, Astaxanthin in skin health, repair, and disease: A comprehensive review, Nutrients. (2018). doi:10.3390/nu10040522.

[178] E. Del Río, F.G. Acién, M.C. García-Malea, J. Rivas, E. Molina-Grima, M.G. Guerrero, Efficiency assessment of the one-step production of astaxanthin by the microalga Haematococcus pluvialis, Biotechnol. Bioeng. (2008). doi:10.1002/bit.21770.

[179] S. Boussiba, A. Vonshak, Astaxanthin accumulation in the green alga haematococcus pluvialis, Plant Cell Physiol. (1991). doi:10.1093/oxfordjournals.pcp.a078171.

[180] S. Boussiba, Carotenogenesis in the green alga Haematococcus pluvialis: Cellular physiology and stress response, Physiol. Plant. (2000).

doi:10.1034/j.1399-3054.2000.108002111.x.

[181] C. Aflalo, Y. Meshulam, A. Zarka, S. Boussiba, On the relative efficiency of two- vs. one-stage production of astaxanthin by the green alga Haematococcus pluvialis, Biotechnol. Bioeng. (2007). doi:10.1002/bit.21391.

[182] M. Harker, A.J. Tsavalos, A.J. Young, Factors responsible for astaxanthin formation in the chlorophyte Haematococcus pluvialis, Bioresour. Technol. (1996). doi:10.1016/0960-8524(95)00002-X.

[183] P. He, J. Duncan, J. Barber, Astaxanthin accumulation in the green alga haematococcus pluvialis: Effects of cultivation parameters, J. Integr. Plant Biol. (2007). doi:10.1111/j.1744-7909.2007.00468.x.

[184] B. Wang, Y. Li, N. Wu, C.Q. Lan, CO2 bio-mitigation using microalgae, Appl. Microbiol. Biotechnol. (2008). doi:10.1007/s00253-008-1518-y.

[185] J. Fábregas, A. Otero, A. Maseda, A. Domínguez, Two-stage cultures for the production of astaxanthin from Haematococcus pluvialis, J. Biotechnol. (2001). doi:10.1016/S0168-1656(01)00289-9.

[186] A.I. Barros, A.L. Gonçalves, M. Simões, J.C.M. Pires, Harvesting techniques applied to microalgae: A review, Renew. Sustain. Energy Rev. (2015). doi:10.1016/j.rser.2014.09.037.

[187] G. Singh, S.K. Patidar, Microalgae harvesting techniques: A review, J. Environ. Manage. (2018). doi:10.1016/j.jenvman.2018.04.010.

[188] K.K. Sharma, S. Garg, Y. Li, A. Malekizadeh, P.M. Schenk, Critical analysis of current microalgae dewatering techniques, Biofuels. (2013). doi:10.4155/bfs.13.25.

[189] D. Han, Y. Li, Q. Hu, Astaxanthin in microalgae: Pathways, functions and biotechnological implications, Algae. (2013). doi:10.4490/algae.2013.28.2.131.

[190] F. Fasaei, J.H. Bitter, P.M. Slegers, A.J.B. van Boxtel, Techno-economic evaluation of microalgae harvesting and dewatering systems, Algal Res. (2018). doi:10.1016/j.algal.2017.11.038.

[191] J.J. Milledge, S. Heaven, A review of the harvesting of micro-algae for biofuel production, Rev. Environ. Sci. Biotechnol. (2013). doi:10.1007/s11157-012-9301-z.

[192] J.J. Milledge, S. Heaven, Disc Stack Centrifugation Separation and Cell Disruption of Microalgae: A Technical Note, Environ. Nat. Resour. Res. (2011). doi:10.5539/enrr.v1n1p17.

[193] E. Molina Grima, E.H. Belarbi, F.G. Acién Fernández, A. Robles Medina, Y. Chisti, Recovery of microalgal biomass and metabolites: Process options and economics, Biotechnol. Adv. (2003). doi:10.1016/S0734-9750(02)00050-2.

[194] R. Sarada, R. Vidhyavathi, D. Usha, G.A. Ravishankar, An efficient method for extraction of astaxanthin from green alga Haematococcus pluvialis, J. Agric. Food Chem. (2006). doi:10.1021/jf060737t.

[195] H.C. Greenwell, L.M.L. Laurens, R.J. Shields, R.W. Lovitt, K.J. Flynn, Placing microalgae on the biofuels priority list: A review of the technological challenges, J. R. Soc. Interface. (2010). doi:10.1098/rsif.2009.0322.

[196] M.F.J. Raposo, A.M.M.B. Morais, R.M.S.C. Morais, Effects of spray-drying and storage on astaxanthin content of Haematococcus pluvialis biomass, World J. Microbiol. Biotechnol. (2012). doi:10.1007/s11274-011-0929-6.

[197] M.M. Mendes-Pinto, M.F.J. Raposo, J. Bowen, A.J. Young, R. Morais, Evaluation of different cell disruption process on encysted cells of Haematococcus pluvialis, J. Appl. Phycol. (2001).

[198] R.L. Mendes, B.P. Nobre, M.T. Cardoso, A.P. Pereira, A.F. Palavra, Supercritical carbon dioxide extraction of compounds with pharmaceutical importance from microalgae, Inorganica Chim. Acta. (2003). doi:10.1016/S0020-1693(03)00363-3.

[199] H.W. Yen, S.C. Yang, C.H. Chen, Jesisca, J.S. Chang, Supercritical fluid extraction of valuable compounds from microalgal biomass, Bioresour. Technol. (2015). doi:10.1016/j.biortech.2014.10.030.

[200] F. Sahena, I.S.M. Zaidul, S. Jinap, A.A. Karim, K.A. Abbas, N.A.N. Norulaini, A.K.M. Omar, Application of supercritical CO2 in lipid extraction - A review, J. Food Eng. (2009). doi:10.1016/j.jfoodeng.2009.06.026.

[201] J. Wisniak, E. Korin, Supercritical Fluid Extraction of Lipids and Other Materials from Algae, in: Single Cell Oils, 2005. doi:10.1201/9781439822364.ch14.

[202] D. Rakhuba, G. Novik, E.S. Dey, Application of supercritical carbon dioxide (scCO2) for the extraction of glycolipids from Lactobacillus plantarum B-01, J. Supercrit. Fluids. (2009). doi:10.1016/j.supflu.2008.11.016.

[203] J.O. Valderrama, M. Perrut, W. Majewski, Extraction of Astaxantine and phycocyanine from microalgae with supercritical carbon dioxide, in: J. Chem. Eng. Data, 2003. doi:10.1021/je020128r.

[204] F.K. Kazi, J.A. Fortman, R.P. Anex, D.D. Hsu, A. Aden, A. Dutta, G. Kothandaraman, Techno-economic comparison of process technologies for biochemical ethanol production from corn stover, Fuel. (2010).

doi:10.1016/j.fuel.2010.01.001.

[205] M. von Sivers, G. Zacchi, A techno-economical comparison of three processes for the production of ethanol from pine, Bioresour. Technol. (1995). doi:10.1016/0960-8524(94)00094-H.

[206] C. Lohrey, V. Kochergin, Biodiesel production from microalgae: Co-location with sugar mills, Bioresour. Technol. (2012). doi:10.1016/j.biortech.2011.12.035.

[207] W. Murdoch, S. Polasky, K.A. Wilson, H.P. Possingham, P. Kareiva, R. Shaw, Maximizing return on investment in conservation, Biol. Conserv. (2007). doi:10.1016/j.biocon.2007.07.011.

[208] R. Masters, E. Anwar, B. Collins, R. Cookson, S. Capewell, Return on investment of public health interventions: A systematic review, J. Epidemiol. Community Health. (2017). doi:10.1136/jech-2016-208141.

[209] G. Psacharopoulos, H.A. Patrinos, Returns to investment in education: A further update, Educ. Econ. (2004). doi:10.1080/0964529042000239140.

[210] No Title, Cyanotech Corp. (2019) https://www.cyanotech.com/.

[211] No Title, Algatech. (2019) https://www.algatech.com/.

[212] J. Kinderlerer, Fish oil, Br. Food J. (1989). doi:10.1108/00070709010134693.

[213] A.G.J. Tacon, M. Metian, Global overview on the use of fish meal and fish oil in industrially compounded aquafeeds: Trends and future prospects, Aquaculture. (2008). doi:10.1016/j.aquaculture.2008.08.015.

[214] P.M. Kris-Etherton, W.S. Harris, L.J. Appel, Fish consumption, fish oil, omega-3 fatty acids, and cardiovascular disease, Circulation. (2002).

doi:10.1161/01.CIR.0000038493.65177.94.

[215] R.L. Naylor, R.W. Hardy, D.P. Bureau, A. Chiu, M. Elliott, A.P. Farrell, I. Forster, D.M. Gatlin, R.J. Goldburg, K. Hua, P.D. Nichols, Feeding aquaculture in an era of finite resources, Proc. Natl. Acad. Sci. U. S. A. (2009). doi:10.1073/pnas.0905235106.

[216] H. Kleivdal, M.S. Chauton, I. Reitan, Industrial production of marine microalgae as a source of EPA and DHA rich raw material in fish feed - Basis, Knowledge status and possibilities, (2013) 1–88.

[217] A. Bertrand, F. Gerlotto, S. Bertrand, M. Gutiérrez, L. Alza, A. Chipollini, E. Díaz, P. Espinoza, J. Ledesma, R. Quesquén, S. Peraltilla, F. Chavez, Schooling behaviour and environmental forcing in relation to anchoveta distribution: An analysis across multiple spatial scales, Prog. Oceanogr. (2008). doi:10.1016/j.pocean.2008.10.018.

[218] P. Fréon, J.C. Sueiro, F. Iriarte, O.F. Miro Evar, Y. Landa, J.F. Mittaine, M. Bouchon, Harvesting for food versus feed: A review of Peruvian fisheries in a global context, Rev. Fish Biol. Fish. (2014). doi:10.1007/s11160-013-9336-4.

[219] Food and Agricultural Organization of the United Nations, (n.d.). http://www.fao.org/home/en/.

[220] T.C. Adarme-Vega, D.K.Y. Lim, M. Timmins, F. Vernen, Y. Li, P.M. Schenk, Microalgal biofactories: a promising approach towards sustainable omega-3 fatty acid production, Microb. Cell Fact. (2012). doi:10.1186/1475-2859-11-96.

[221] T.C. Adarme-Vega, S.R. Thomas-Hall, P.M. Schenk, Towards sustainable sources for omega-3 fatty acids production, Curr. Opin. Biotechnol. (2014).

doi:10.1016/j.copbio.2013.08.003.

[222] A.M. de O. Finco, L.D.G. Mamani, J.C. de Carvalho, G.V. de Melo Pereira, V. Thomaz-Soccol, C.R. Soccol, Technological trends and market perspectives for production of microbial oils rich in omega-3, Crit. Rev. Biotechnol. 8551 (2016) 1–16. doi:10.1080/07388551.2016.1213221.

[223] A. Skrede, L.T. Mydland, O. Ahlstrem, K.I. Reitan, H.R. Gislered, M. Overland, Evaluation of microalgae as sources of digestible nutrients for monogastric animals, J. Anim. Feed Sci. (2011). doi:10.22358/jafs/66164/2011.

[224] J. Camacho-Rodríguez, M.C. Cerón-García, C. V. González-López, J.M. Fernández-Sevilla, A. Contreras-Gómez, E. Molina-Grima, A low-cost culture medium for the production of Nannochloropsis gaditana biomass optimized for aquaculture, Bioresour. Technol. (2013). doi:10.1016/j.biortech.2013.06.083.

[225] V. Patil, T. Källqvist, E. Olsen, G. Vogt, H.R. Gislerød, Fatty acid composition of 12 microalgae for possible use in aquaculture feed, Aquac. Int. (2007). doi:10.1007/s10499-006-9060-3.

[226] A.J. Dassey, C.S. Theegala, Harvesting economics and strategies using centrifugation for cost effective separation of microalgae cells for biodiesel applications, Bioresour. Technol. (2013). doi:10.1016/j.biortech.2012.10.061.

[227] M.L. Gerardo, S. Van Den Hende, H. Vervaeren, T. Coward, S.C. Skill, Harvesting of microalgae within a biorefinery approach: A review of the developments and case studies from pilot-plants, Algal Res. (2015). doi:10.1016/j.algal.2015.06.019.

[228] X.J. Ji, L.J. Ren, H. Huang, Omega-3 biotechnology: A green and sustainable process for omega-3 fatty acids production, Front. Bioeng. Biotechnol. (2015).

doi:10.3389/fbioe.2015.00158.

[229] E. Günerken, E. D'Hondt, M.H.M. Eppink, L. Garcia-Gonzalez, K. Elst, R.H. Wijffels, Cell disruption for microalgae biorefineries, Biotechnol. Adv. (2015). doi:10.1016/j.biotechadv.2015.01.008.

[230] E.M. Spiden, B.H.J. Yap, D.R.A. Hill, S.E. Kentish, P.J. Scales, G.J.O. Martin, Quantitative evaluation of the ease of rupture of industrially promising microalgae by high pressure homogenization, Bioresour. Technol. (2013). doi:10.1016/j.biortech.2013.04.074.

[231] M. Mubarak, A. Shaija, T. V. Suchithra, A review on the extraction of lipid from microalgae for biodiesel production, Algal Res. (2015). doi:10.1016/j.algal.2014.10.008.

[232] R.R. Kumar, P.H. Rao, M. Arumugam, Lipid extraction methods from microalgae: A comprehensive review, Front. Energy Res. (2015). doi:10.3389/fenrg.2014.00061.

[233] R. Halim, M.K. Danquah, P.A. Webley, Extraction of oil from microalgae for biodiesel production: A review, Biotechnol. Adv. (2012). doi:10.1016/j.biotechadv.2012.01.001.

[234] J.-C. Lee, B. Lee, J. Heo, H.-W. Kim, H. Lim, Techno-economic assessment of conventional and direct-transesterification processes for microalgal biomass to biodiesel conversion, Bioresour. Technol. 294 (2019) 122173. doi:10.1016/j.biortech.2019.122173.

[235] C. Ratledge, H. Streekstra, Z. Cohen, J. Fichtali, Downstream Processing, Extraction, and Purification of Single Cell Oils, in: Single Cell Oils Microb. Algal

Oils Second Ed., 2010. doi:10.1016/B978-1-893997-73-8.50013-X.

[236] K. Ochsenreither, C. Glück, T. Stressler, L. Fischer, C. Syldatk, Production strategies and applications of microbial single cell oils, Front. Microbiol. (2016). doi:10.3389/fmicb.2016.01539.

[237] T. Dong, E.P. Knoshaug, P.T. Pienkos, L.M.L. Laurens, Lipid recovery from wet oleaginous microbial biomass for biofuel production: A critical review, Appl. Energy. (2016). doi:10.1016/j.apenergy.2016.06.002.

[238] D. López Barreiro, W. Prins, F. Ronsse, W. Brilman, Hydrothermal liquefaction (HTL) of microalgae for biofuel production: State of the art review and future prospects, Biomass and Bioenergy. (2013). doi:10.1016/j.biombioe.2012.12.029.

[239] Y. Guo, T. Yeh, W. Song, D. Xu, S. Wang, A review of bio-oil production from hydrothermal liquefaction of algae, Renew. Sustain. Energy Rev. (2015). doi:10.1016/j.rser.2015.04.049.

[240] F.P. Incropera, D.P. DeWitt, T.L. Bergman, A.S. Lavine, Fundamentals of Heat and Mass Transfer, 2007. doi:10.1016/j.applthermaleng.2011.03.022.

[241] J. Taine, J.-P. Petit, Transferts thermiques : introduction aux sciences des transferts\r(Cours et exercices corrigés) (Sciences Sup) 3° Ed, 2003.

[242] R. Tang, Y. Etzion, Comparative studies on the water evaporation rate from a wetted surface and that from a free water surface, Build. Environ. 39 (2004) 77–86. doi:10.1016/j.buildenv.2003.07.007.

[243] T. Legović, a. Cruzado, A model of phytoplankton growth on multiple nutrients based on the Michaelis-Menten-Monod uptake, Droop's growth and Liebig's law, Ecol. Modell. 99 (1997) 19–31. doi:10.1016/S0304-3800(96)01919-9.

[244] R.J. Geider, H.L. MacIntyre, T.M. Kana, Dynamic model of phytoplankton growth and acclimation: Responses of the balanced growth rate and the chlorophyll a:carbon ratio to light, nutrient-limitation and temperature, Mar. Ecol. Prog. Ser. 148 (1997) 187–200. doi:10.3354/meps148187.

[245] J.A. Duffie, W.A. Beckman, Solar Engineering of Thermal Processes: Fourth Edition, 2013. doi:10.1002/9781118671603.

[246] J.H. de Vree, R. Bosma, M. Janssen, M.J. Barbosa, R.H. Wijffels, Comparison of four outdoor pilot-scale photobioreactors, Biotechnol. Biofuels. 8 (2015) 215. doi:10.1186/s13068-015-0400-2.

Appendix

Chapter 2. Dynamic Process Model and Economic Analysis of Microalgae Cultivation in Open Raceway Ponds

A1. Details of heat and mass transfer model in microalgae growth ponds

Radiation from pond water

Radiative heat flux transfer from the pond water surface was computed by Stefan-Boltzmann power law [240] according to the following equation:

$$Q_{radiation,water} = -\varepsilon_{water}\sigma S T_{water}^{4} \quad (1)$$

where ε_{water} was the water emissivity, σ was the Stefan-Boltzmann constant (W m^{-2} K^{-4}) and S was the surface area of the raceway pond (m^2).

Radiation from Sun

Flux received by the raceway pond from solar radiation was computed on the basis of the total solar irradiance at the ground I (W m^{-2}) and was given by the following equation:

$$Q_{radiation,sun} = IS\left(1 - \varepsilon_{photosynthesis}\right) \quad (2)$$

where $\varepsilon_{photosynthesis}$ was the efficiency of photosynthesis i.e the fraction of solar energy converted by algae during photosynthesis. It was assumed that conversion efficiency of microalgae was 2.5% [133]. It is important to note that it was assumed that the raceway ponds were not located in the shade of external elements (like trees or buildings) and thus a 'shadow function' was not included in the above equation. Amount of solar irradiance that was reflected was assumed to be negligible in the present study.

Radiation from air

Radiative heat flux from air was computed by Stefan-Boltzmann power law [240] according to the following equation:

$$Q_{radiation,air} = \varepsilon_{water}\varepsilon_{air}\sigma S T_{air}^4 \quad (3)$$

where ε_{air} was the emissivity of air with a value of 0.8 [133], T_{air} was the air temperature. Reflection from water was assumed to be negligible in the present study.

Evaporation from pond

The evaporative heat transfer from the pond water surface was given by the following equation:

$$Q_{evaporation} = -m_{water,evaporated} L_{water} S \quad (4)$$

where $m_{water,evaporated}$ was the rate of water evaporation from the raceway pond (kg s^{-1} m^{-2}), L_{water} was the latent heat of water (J kg^{-1}). By the Buckingham theorem and heat transfer correlations, the rate of evaporation was determined from the following correlation (based on turbulent flow) which involved three dimensionless numbers [241]

$$Sh_L = 0.035 {Re_L}^{0.8} {Sch_L}^{0.33} \quad (5)$$

$$i)\ Sh_L = Sherwood\ number = \frac{K_{mass\ transfer} L}{D_{water,air}} \quad (6)$$

$$ii)\ Re_L = Reynolds\ number = L v_{air} / \nu_{air} \quad (7)$$

$$iii)\ Sch_L = Schmidt\ number = \nu_{air} / D_{water,air} \quad (8)$$

where $K_{mass\ transfer}$ was the mass transfer coefficient (m s^{-1}), L was the characteristic pond length (m) (that is, the length of the pond), $D_{water,air}$ was the diffusion coefficient of water vapor in air (m^2 s^{-1}), v_{air} was the velocity of wind (m s^{-1}), and ν_{air} was the kinematic viscosity of air (m^2 s^{-1}).

The mass transfer coefficient ($K_{mass\ transfer}$) was determined using the above equations and the rate of water evaporation was then given by the following equation:

$$m_{water,evaporated} = K_{mass\ transfer}(\frac{P_{water}}{T_{water}} - \text{RH}*\frac{P_{air}}{T_{air}})\frac{M_{water}}{R_{universal}} \quad (9)$$

where P_{water} and P_{air} were the saturated vapor pressures at T_{water} and T_{air} respectively, RH was air relative humidity over raceway pond, M_{water} was the molecular weight of water (kg mol^{-1}) and $R_{universal}$ was the Universal Gas Constant. The saturated vapor pressures were computed using the following equations [242]

$$P_{water} = 3385.5\exp\left[-8.0929 + 0.97608(T_{water} + 42.607 - 273.15)^{0.5}\right] \quad (10)$$

$$P_{air} = 3385.5\exp\left[-8.0929 + 0.97608(T_{air} + 42.607 - 273.15)^{0.5}\right] \quad (11)$$

As there is no clear consensus as to which elevation is most appropriate to quantify the velocity of wind, the wind velocity data obtained from [132] was directly used in the model.

Convection from pond water surface

The heat flux, due to convection from the pond water surface, was computed using the following equation:

$$Q_{convection} = -h_{convection}(T_{water} - T_{air})S \quad (12)$$

where $h_{convection}$ was the convective heat transfer coefficient (W m^{-2} K^{-1}). By applying the Buckingam theorem and convective heat transfer correlations, the convective heat transfer coefficient was determined by the following equations (based on turbulent flow) and it involved three dimensionless numbers [241]

$$Nu_L = 0.035{Re_L}^{0.8}Pr^{0.33} \quad (13)$$

$$Nu_L = Nusselt\ number = h_{convection}L/k_{air} \quad (14)$$

$$\text{Pr} = Prandtl\ number = \nu_{air}/\alpha_{air} \quad (15)$$

where k_{air} was the thermal conductivity of air (W m^{-1} K^{-1}) and α_{air} was the thermal diffusivity of air (m^2 s^{-1}).

Conduction

The conductive heat flux between the bottom surface of the pond and the soil underneath was derived by Fourier's law

$$Q_{conduction} = k_{soil} S \frac{dT_{soil}}{dz} (at\ z = 0) \quad (16)$$

where k_{soil} was the thermal conductivity of soil (W m^{-1} K^{-1}), T_{soil} was the temperature of soil (K) and z was the depth of soil (m). In order to determine the soil temperature gradient, the soil temperature profile was quantified by solving the following conductive heat transfer equation in the soil underneath the raceway pond. It was assumed that the soil temperature was a function of time *t* and depth *z*.

$$C_{p_{soil}} \rho_{soil} \frac{dT_{soil}}{dt} = k_{soil} \frac{d^2 T_{soil}}{dz^2} \quad (17)$$

where $C_{p_{soil}}$ was the specific heat capacity of soil (J kg^{-1} K^{-1}) and ρ_{soil} was the density of soil (kg m^{-3}).

The boundary conditions required to solve the above heat transfer equation were as follows:

Boundary Conditions: $$T_{soil}(t, z = 0) = T_{water} \quad (18)$$

$$T_{soil}(t, z = z_{ref}) = T_{soil_{z=z_{ref}}} \quad (19)$$

Initial condition: $$\frac{d^2 T_{soil}}{dz^2} (t = 0) = 0 \quad (20)$$

where $T_{soil_{z=z_{ref}}}$ was the temperature of soil at a reference depth (z_{ref}) such that $T_{soil_{z=z_{ref}}}$ remained constant throughout the year at depth z_{ref}. The reference depth was computed using the following equation:

$$z_{ref} = 4400\ (\alpha_{soil})^{0.5} \quad (21)$$

where α_{soil} was the thermal diffusivity of soil ($m^2\ s^{-1}$). Thus, the soil temperature gradient was quantified and henceforth the conductive heat exchange between pond bottom surface and soil was determined.

Incoming water

Water loss due to evaporation was replenished by pumping in water so as to maintain constant raceway volume. Energy input from this inflow water was computed using the following equation:

$$Q_{incoming\ water} = q_{incoming\ water} * \rho_{water} * C_{p_{water}} * (T_{incoming\ water} - T_{water}) \quad (22)$$

where $Q_{incoming\ water}$ was the volumetric inflow of water ($m^3\ s^{-1}$) and $T_{incoming\ water}$ was the temperature of the inflow water. $Q_{incoming\ water}$ was essentially calculated from the rate of water evaporation from the growth pond.

S2. Details of growth kinetics model

Modeling of distribution of light

The Beer-Lambert law was used in the model to estimate the average light intensity in the pond and bulk culture, according to the following equation [52]:

$$I_{average} = I(1 - \exp(-XDK_a))/XDK_a \quad (23)$$

where I was the intensity of the incident light, $I_{average}$ was the average light intensity within the culture medium, D was the depth of the culture (m), X was the biomass concentration (kg m^{-3}) and K_a was the extinction coefficient of the biomass due to light (m^2 kg^{-1}). K_a was estimated by the following empirical relation where X_p was the fraction of pigment in microalgae. X_p generally ranges from 2% to 3% for dry microagal biomass [52]. In this particular study, X_p was assumed to be 2.5%

$$K_a = 1.7356X_p + 0.0199 \quad (24)$$

Nitrogen Uptake Modeling

The uptake of nitrogen by the microalgae was computed by solving the following set of equations [48,135]:

$$\frac{dN_{biomass}}{dt} = \left(\frac{N_{calculated\ specific\ uptake\ rate}}{N_{biomass}} - RR_N\right) N_{biomass} = R_{nitrogen\ uptake} \quad (25)$$

where $N_{biomass}$ was the cell quota of nitrogen in algal biomass (kg kg^{-1}), $N_{calculated\ specific\ uptake\ rate}$ was the calculated specific uptake rate of nitrogen (kg kg^{-1} day^{-1}), RR_N was respiration constant of nitrogen (day^{-1}) and $R_{nitrogen\ uptake}$ was the specific uptake rate of nitrogen (day^{-1}). The $N_{calculated\ specific\ uptake\ rate}$ was related to the maximum specific uptake $N_{max\ specific\ uptake\ rate}$ (kg kg^{-1} day^{-1}), uptake of internal nitrogen concentration efficiency ($\eta_{nitrogen,internal}$) and uptake of external nitrogen concentration efficiency ($\eta_{nitrogen,external}$) by the following equation:

$$N_{calculated\ specific\ uptake\ rate} = N_{max\ specific\ uptake\ rate} * \eta_{nitrogen,internal} * \eta_{nitrogen,external} \quad (26)$$

The $\eta_{nitrogen,internal}$ was defined by the following equation where $N_{biomass,minimum}$ was the minimum level of nitrogen present internally below which the cells do not grow (kg/kg).

$$\eta_{nitrogen,internal} = 1 - \frac{N_{biomass,minimum}}{N_{biomass}} \quad (27)$$

The $\eta_{nitrogen,external}$ was treated as a Michaelis-Menten kinetic function and was computed according to the following equation [143,243,244]:

$$\eta_{nitrogen,external} = N_{medium}/(N_{medium} + HSC_{nitrogen\ uptake}) \quad (28)$$

where N_{medium} was the concentration of nitrogen in the medium (kg m^{-3}) and $HSC_{nitrogen\ uptake}$ was the half-saturation constant of uptake of nitrogen (kg m^{-3}).

Phosphorus Uptake Modeling

The uptake of phosphorus by the microalgae was evaluated similarly to the nitrogen uptake. The governing equations are as follows:

$$\frac{dP_{biomass}}{dt} = \left(\frac{P_{calculated\ specific\ uptake\ rate}}{P_{biomass}} - RR_P\right) P_{biomass} = R_{phosphorus\ uptake} \quad (29)$$

where $P_{biomass}$ was the cell quota of nitrogen in algal biomass (kg kg^{-1}), $P_{calculated\ specific\ uptake\ rate}$ was the calculated specific uptake rate of nitrogen (kg kg^{-1} day^{-1}), RR_P was respiration constant of nitrogen (day^{-1}) and $R_{phosphorus\ uptake}$ was the specific uptake rate of nitrogen (day^{-1}). The $P_{calculated\ specific\ uptake\ rate}$ was related to the maximum specific uptake $P_{max\ specific\ uptake\ rate}$ (kg kg^{-1} day^{-1}), uptake of internal nitrogen concentration efficiency ($\eta_{phosphorus,internal}$) and uptake of external nitrogen concentration efficiency ($\eta_{phosphorus,external}$) by the following equation:

$$P_{calculated\ specific\ uptake\ rate} = P_{max\ specific\ uptake\ rate} * \eta_{phosphorus,internal} * \eta_{phosphorus,\ external} \quad (30)$$

The $\eta_{phosphorus,internal}$ was defined by the following equation where $P_{biomass,minimum}$ was the minimum level of nitrogen present internally below which the cells do not grow (kg kg^{-1}).

$$\eta_{phosphorus,internal} = 1 - \frac{P_{biomass,minimum}}{P_{biomass}} \quad (31)$$

The $\eta_{phosphorous,external}$ was treated as a Michaelis-Menten kinetics function and was computed according to the following equation:

$$\eta_{phosphorus,\ external} = P_{medium}/(P_{medium} + HSC_{phosphorus\ uptake}) \quad (32)$$

where P_{medium} was the concentration of phosphorous in the medium (kg m^{-3}) and $HSC_{phosphorous\ uptake}$ was the half-saturation constant of uptake of phosphorous (kg m^{-3}).

Carbon dioxide uptake modeling

The transfer and uptake of CO_2 by microalgae is a complex process and was modeled by coupling of three separate phenomena which are transfer of atmospheric CO_2 to the growth media, modeling of CO_2 transfer by sparging from gas phase to liquid phase (bulk culture medium) and uptake by microalgae during the growth phase. The following set of equations describing carbon dioxide uptake was based on literature and were used in the model [130,134,135,141].

CO_2 transfer from atmosphere across free surface

Across the free surface of the pond water, there was mass transfer of CO_2 from atmosphere to the growth medium. The transfer of CO_2 was modeled by the following equation:

$$M_{air} = K\left(C_{CO2,air} - C_{CO2,dissolved}\right)V \quad (33)$$

where M_{air} was the mass of CO_2 transferred (mol s^{-1}), K was the surface mass transfer coefficient (day^{-1}), $C_{CO2,air}$ was the concentration of CO_2 in the air (mol m^{-3}) and $C_{CO2,dissolved}$ was the concentration of the dissolved CO_2 in the culture media. However, the transfer of CO_2 from the atmosphere to the culture media across the free surface was assumed insignificant and CO_2 required for microalgae growth was supplied from an external source.

CO_2 transfer from gas phase to bulk culture medium

The mass transfer of CO_2 from the sparging gas phase to the bulk culture medium was obtained by solving the following equations as obtained in literature [134–136].

An elemental height dz of the pond depth was assumed and transfer of CO_2 within the element was expressed by the following equation:

$$\frac{d}{dt}\left[\left(\frac{p\varepsilon_{gas\ holdup}A_{cs}dz}{RT_{water}}\right)y\right] = M_{in} - M_{out} - dM_t = G_{molar\ flow}y - G_{molar\ flow}(y + dy) - dM_t \quad (34)$$

The rate of transfer of CO_2 from the gas phase to the bulk culture medium (dM_t) was estimated by the following equation:

$$dM_t = K_{CO2}\left(1 - \varepsilon_{gas\ holdup}\right)A_{cs}\left({C_{CO2}}^{*} - C_{CO2,dissolved}\right)dz \quad (35)$$

where, K_{CO2} was the mass transfer coefficient from the gas phase to the liquid phase, and ${C_{CO2}}^{*}$ was the concentration of dissolved CO_2 in the liquid phase which was in equilibrium with the concentration of CO_2 in the gas phase. K_{CO2} was estimated by the following equation:

$$\frac{K_{CO2}}{K_{O2}} = \sqrt{\frac{D_{CO2}}{D_{O2}}} \qquad (36)$$

As the residence times of the gas in the culture medium was small, pseudo steady state conditions were assumed. Thus, the following equation was obtained by combining equation 34 and 35:

$$\frac{dy}{dz} = -\left(\frac{K_{CO2}(1 - \varepsilon_{gas\ holdup})A_{cs}}{G_{molar\ flow}}\right)(C_{CO2}{}^{*} - C_{CO2,dissolved}) \quad (37)$$

The saturation concentration of CO_2 ($C_{CO2}{}^{*}$) was computed using Henry's Law according to the following:

$$C_{CO2}{}^{*} = \frac{py}{RT_{water}H} \qquad (38)$$

where, H is the Henry's constant and p is the partial pressure of CO_2 in the sparging gas phase (atmosphere).

Combining equations 37 and 38 and then integrating within the proper limits, the following equation was obtained:

$$y_{out} = \frac{RT_{water}H}{p}(C_{CO2,dissolved} + (\frac{y_{in}p}{RT_{water}H} -$$

$$C_{CO2,dissolved})\exp(\frac{-K_{CO2}(1-\varepsilon_{gas\ holdup})A_{cs}z*p*1000}{G_{molar\ flow}RT_{water}H})) \qquad (39)$$

Thus, the moles of CO_2 transferred from the gas phase to the culture medium ($M_{CO2,transfer}$) was given by the following equation:

$$M_{CO2,transfer} = G_{molar\ flow}(y_{in} - y_{out}) = G_{molar\ flow}(y_{in} - \frac{RT_{water}H}{p}(C_{CO2,dissolved} +$$

$$(\frac{y_{in}p}{RT_{water}H} - C_{CO2,dissolved})\exp(\frac{-K_{CO2}(1-\varepsilon_{gas\ holdup})A_{cs}z*p*1000}{G_{molar\ flow}RT_{water}H}))) \quad (40)$$

Uptake of Carbon by microalgae

The bio uptake of carbon by microalgae during the growth phase was modeled in a similar way described in the literature [134,136]. The dissociation of CO_2 in water was given by the following equations:

$$CO_{2,gas} + H_2O \leftrightarrow H_2CO_3^* \overset{K_1}{\Leftrightarrow} HCO_3^- + H^+ \quad (41)$$

$$HCO_3^- \overset{K_2}{\Leftrightarrow} CO_3^{2-} + H^+ \quad (42)$$

where, K_1 and K_2 were the dissociation constants of $H_2CO_3^*$ and HCO_3 respectively. The total dissolved concentration of carbon in the medium could be obtained by adding the concentration of [H_2CO_3], [HCO_3^-], and [CO_3^{2-}], respectively. Several studies considered the total dissolved concentration of carbon species in water to determine the carbon uptake by microalgae [130,134]. In this study, it was assumed that the pH of the solution was between 7.67-6.83 where the dominant species was bicarbonate [136]. Thus, the bio uptake of carbon by microalgae was assumed to take place only in the form of bicarbonate and the concentration of dissolved CO_2 ($C_{CO2,dissolved}$) was essentially the concentration of bicarbonate in the solution.

Assuming the culture medium was thoroughly mixed, molar balance of dissolved carbon in the culture medium provided the following equation:

$$\left(1 - \varepsilon_{gas\ holdup}\right)V\frac{dC_{CO2,dissolved}}{dt} = M_{CO2,transfer} - M_{carbon\ uptake,algae} \quad (43)$$

The carbon uptake rate by microalgae ($M_{carbon\ uptake,algae}$) was estimated utilizing the following equation:

$$M_{carbon\ uptake,algae} = \left(1 - \varepsilon_{gas\ holdup}\right)V\left(\frac{1}{Y_{algae}}\right)\left(\frac{dX}{dt}\right)\left(\frac{1}{MW_{bicarbonate\ ion}}\right) \quad (44)$$

where, X is the biomass concentration (kg m^{-3}). Thus, combining equations 40, 43 and 44, the main governing equation was obtained as follows:

$$\left(1 - \varepsilon_{gas\ holdup}\right)V\frac{dC_{CO2,dissolved}}{dt} = G_{molar\ flow}\left(y_{in} - \frac{RT_{water}H}{p}\left(C_{CO2,dissolved} + \left(\frac{y_{in}p}{RT_{water}H} - C_{CO2,dissolved}\right)\exp\left(\frac{-K_{CO2}\left(1-\varepsilon_{gas\ holdup}\right)A_{cs}z*p*1000}{G_{molar\ flow}RT_{water}H}\right)\right)\right) - \left(1 - \varepsilon_{gas\ holdup}\right)V\left(\frac{1}{Y_{algae}}\right)\left(\frac{dX}{dt}\right)\left(\frac{1}{MW_{bicarbonate\ ion}}\right) \quad (45)$$

Modeling carbon uptake by microalgae in the growth phase was provided in greater detail in literature [130,134–136,141].

Temperature dependence

The temperature dependence of microalgae growth was modeled by the following equation [136]:

$$f(T) = 1.066^{T_{water}-293.15} \quad (46)$$

Chapter 3. Dynamic process model and economic analysis of microalgae cultivation in flat panel photobioreactors

S1. Light distribution in single flat panel photobioreactor

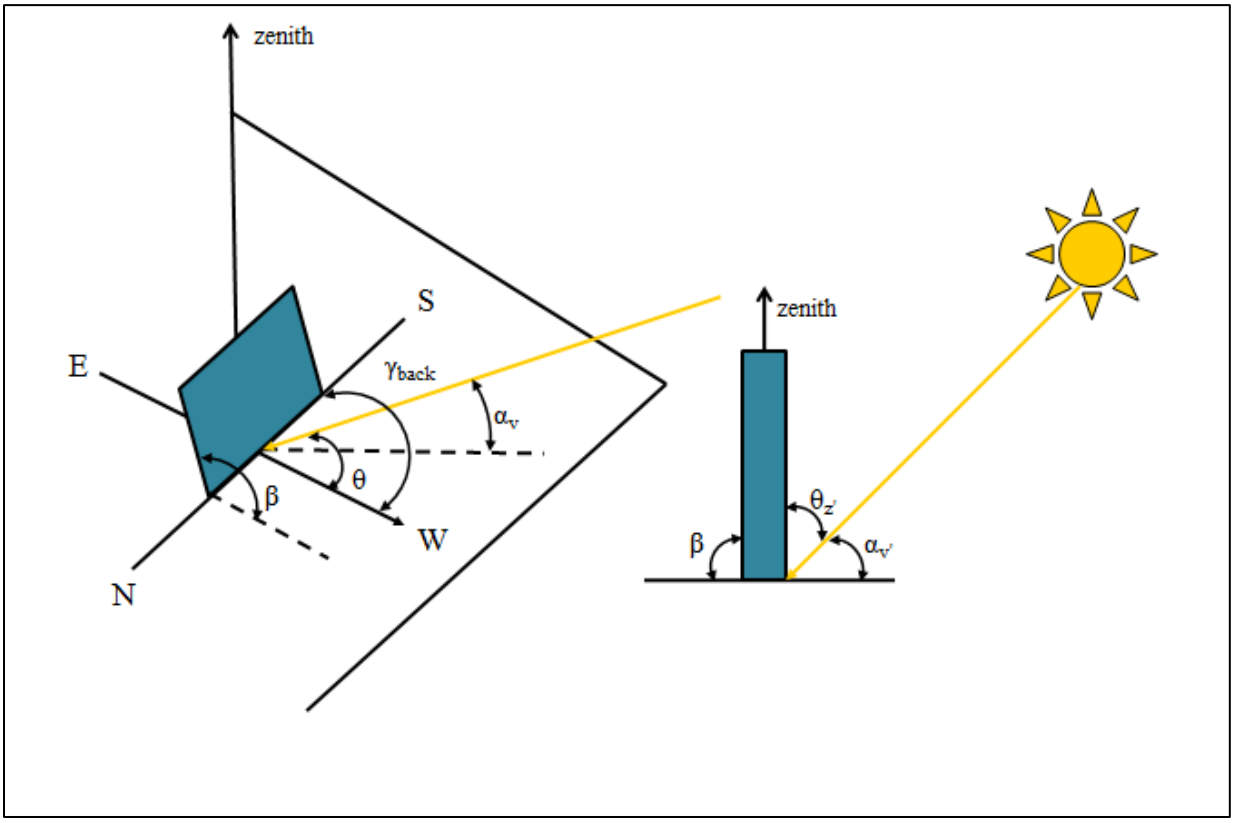

Figure S1. Parameters for sunlight irradiation used in the model [42]

The solar incidence angle θ (in degrees) is a function of the angle of solar declination δ (in degrees), the latitude of the location of the photobioreactor φ (in degrees), the inclination of the photobioreactor with respect to the ground β (in degrees), the azimuthal angle γ (in degrees) as well as the solar hour angle ω (in degrees) [42]. The solar incidence angle is given by the following equation

$$\cos(\theta) = \sin(\delta)\sin(\varphi)\cos(\beta) - \sin(\delta)\cos(\varphi)\sin(\beta)\cos(\gamma) + \cos(\delta)\cos(\varphi)\cos(\beta)\cos(\omega) + \cos(\delta)\sin(\varphi)\sin(\beta)\cos(\gamma)\cos(\omega) + \cos(\delta)\sin(\beta)\sin(\gamma)\sin(\omega) \quad (1)$$

For both the sides of the flat panel photobioreactor, the angle of incidence is calculated based on the solar azimuthal and inclination angle for the front and back sides of the reactor. The azimuthal angle and the angle of inclination of the reactor, for the front and back side, are computed using the following equations:

$$\beta_{back\ side} = 180 - \beta_{front\ side} \quad (2)$$

$$\gamma_{back\ side} = 180 + \gamma_{front\ side} \quad (3)$$

The angle of solar declination δ is computed by the following equation:

$$\delta = 23.45 \sin\left(\frac{360(N + 284)}{365}\right) \quad (4)$$

where, N is the number of the day in the year.

The solar hour angle ω, is given by the following equation:

$$\omega = 15(t_{solar} - 12) \quad (5)$$

where, t_{solar} is a function of the actual time t (h), longitude of the location of the reactor λ (in degrees), meridian of the location of the reactor κ (in degrees) and the equation of time e. The solar time (t_{solar}) is computed by the following equations:

$$\zeta = \frac{(N-1)360}{365} \quad (6)$$

$$e = 0.017 + 0.43\cos(\zeta) - 7.35\sin(\zeta) - 3.35e^{-2}\cos(2\zeta) - 9.37\sin(2\zeta) \quad (7)$$

$$t_{solar} = t + \frac{4(\lambda - \kappa) + e}{60} \quad (8)$$

The solar zenith angle θ_z (in degrees) and the angle of elevation of the Sun α_v (in degrees) are complementary to each other and the calculated by the following equations:

$$\cos(\theta_z) = \sin(\varphi)\sin(\delta) + \cos(\varphi)\cos(\delta)\cos(\omega) \qquad (9)$$

$$\alpha_v = 90 - \theta_z \qquad (10)$$

The azimuthal angle γ (in degrees) is given by the following equation:

$$\cos(\gamma) = \frac{\sin(\delta)\cos(\varphi) - \cos(\delta)\cos(\omega)\sin(\varphi)}{\cos(\alpha_v)} \qquad (11)$$

In order to model the solar irradiance on flat panel photobioreactor the direct and diffuse solar irradiance were considered. As solar irradiance data are measured perpendicular to the surface of the earth, geometric factors are introduced to obtain solar irradiance on the front and back sides of the photobioreactor based on its inclination with respect to the surface of the earth. The front side and back side geometric factors for the reactor for direct solar irradiance are computed by the following set of equations:

$$G_{direct,front\ side}(t) = \frac{\cos[\theta(\beta_{front\ side}, \gamma_{front\ side})]}{\cos(\theta_z)} \qquad (12)$$

$$G_{direct,back\ side}(t) = \frac{\cos[\theta(\beta_{back\ side}, \gamma_{back\ side})]}{\cos(\theta_z)} \qquad (13)$$

The geometric factors for the diffuse solar irradiance are a function of the angle of inclination of the reactor with respect to the ground, β (in degrees). The geometric factors for the front side and back side of the reactor for diffuse solar irradiance are computed by the following equations:

$$G_{diffuse,front\ side} = \frac{1 + \cos(\beta_{front\ side})}{2} \qquad (14)$$

$$G_{diffuse,back\ side} = \frac{1 + \cos(\beta_{back\ side})}{2} \quad (15)$$

The geometric factors for the ground reflected diffuse solar irradiance for the photobioreactor is a function of the reflectivity of the ground surface ρ. Following the same approach as above the geometric factors are computed by the following equations:

$$G_{reflect,front\ side} = \rho \frac{1 - \cos(\beta_{front\ side})}{2} \quad (16)$$

$$G_{reflect,back\ side} = \rho \frac{1 - \cos(\beta_{back\ side})}{2} \quad (17)$$

The total solar irradiance on the front and back side of the photobioreactor (I_0) (W/m^2) is computed by the following equations:

$$I_{0,front\ side}(t) = \left(G_{direct,front\ side}(t) + G_{reflect,front\ side}\right) I_{direct}(t) + \left(G_{diffuse,front\ side} + G_{reflect,front\ side}\right) I_{diffuse}(t) \quad (18)$$

$$I_{0,back\ side}(t) = \left(G_{direct,back\ side}(t) + G_{reflect,back\ side}\right) I_{direct}(t) + \left(G_{diffuse,fback\ side} + G_{reflect,fback\ side}\right) I_{diffuse}(t) \quad (19)$$

Light distribution in parallel flatpanel photobioreactors

In large scale microalgae cultivation in photobioreactors often a series of reactors are placed parallel to each other. Such a configuration results in shading and significant part of the reactor surface is unable to receive direct solar irradiance. The height of shadow on vertical photobioreactor panels is given by the following equation:

$$h_{shadow}(t) = h - \tau tan(90 - \theta_z) \quad (20)$$

where, h (m) is the height of the reactor, τ (m) is the distance between the parallel reactor panels and θ_z is the solar zenith angle (in degrees). In order to perform the simulation, the panel is divided into two parts. The upper part of the panel receives both the direct and diffuse solar irradiance whereas the lower part receives only diffuse solar irradiance. The separation between these two parts depends on the solar zenith angle and it is computed for every time step during the day-time. Parallel positions of the photobioreactors also influence the penetration of diffuse solar irradiance in the space between the panels, where the intensity decreases from the top to the bottom. Thus, the geometric factors of diffuse solar irradiance for the front and back side of the reactor panels become a function of height and are given by the following equations:

$$G_{diffuse,front\ side,parallel}(y) = \frac{1 + \cos\left(\beta_{front\ side} + u\right)}{2} \qquad (21)$$

$$G_{diffuse,back\ side,parallel}(y) = \frac{1 + \cos(\beta_{back\ side} + u)}{2} \qquad (22)$$

$$u = \ tan^{-1}\left(\frac{y}{\tau}\right) \qquad (23)$$

In case of large-scale microalgae cultivation in photobioreactors, reflection from the ground is low for the parallel placed panels and is not considered in the present study. The incident irradiance on the front and back side of the photobioreactors are given by the following equation:

$$I_{0,front\ side}(y,t) = \left(G_{direct,front\ side}(t)\right) I_{direct}(t) + \left(G_{diffuse,front\ side,parallel}(y)\right) I_{diffuse} \qquad (24)$$

$$I_{0,back\ side}(y,t) = \left(G_{direct,back\ side}(t)\right) I_{direct}(t) + \left(G_{diffuse,back\ side,parallel}(y)\right) I_{diffuse}(t) \quad (25)$$

Transmission of light through wall of flat panel photobioreactor

In order to model the transmission of light through the reactor to the culture volume, two interfaces, namely, the interface between air and reactor wall outer surface as well as the interface between reactor wall and culture volume need to be considered. The amounts of solar radiation reflected from each of the interface depend on the refractive indices of the material as well as the angle of incidence. The amount of light refracted is obtained by Snell's Law from the following equation:

$$\frac{\sin(\theta_{air})}{\sin(\theta_{glass})} = \frac{\eta_{glass}}{\eta_{air}} \quad (26)$$

$$\frac{\sin(\theta_{glass})}{\sin(\theta_{culture\ volume})} = \frac{\eta_{gculture\ volume}}{\eta_{glass}} \quad (27)$$

The angle of incidence for the diffuse light is assumed to be 60^o as obtained in the literature [245]. Reflection of solar radiation from flat panels is determined by using Fresnel equations and is provided in the following equations:

$$R_s = \left[\frac{\eta_i \cos(\theta_i) - \eta_t \sqrt{1 - \left(\frac{\eta_i}{\eta_t}\sin(\theta_i)\right)^2}}{\eta_i \cos(\theta_i) + \eta_t \sqrt{1 - \left(\frac{\eta_i}{\eta_t}\sin(\theta_i)\right)^2}}\right]^2 \quad (28)$$

$$R_p = \left[\frac{\eta_i \sqrt{1 - \left(\frac{\eta_i}{\eta_t}\sin(\theta_i)\right)^2} - \eta_t \cos(\theta_i)}{\eta_i \sqrt{1 - \left(\frac{\eta_i}{\eta_t}\sin(\theta_i)\right)^2} + \eta_t \cos(\theta_i)}\right]^2 \quad (29)$$

where, R_s and R_p are the reflection of the s-polarized and p-polarized light respectively, and η_i and η_t are the refractive indices of the medium before and after the interface respectively.

Since, normal sunlight is non-polarized in nature, the overall co-efficient of reflection R, is the average of R_s and R_p.

$$R = \frac{R_s + R_p}{2} \qquad (30)$$

The overall reflection coefficient for the air and reactor wall interface ($R_{air,reactor\ wall}$) as well as reactor wall and culture volume interface ($R_{reactor\ wall,culture\ volume}$) is computed by the above equations for the different incidence angles and refractive indices of the respective media. Thus, the total amount of irradiance transmitted to microalgae culture medium from the front and back side of the panel is calculated by the following equation:

$$I_{i,front\ side}(t) = I_{o,front\ side}(t)\big(1 - R_{air,reactor\ wall} - R_{reactor\ wall,culture\ volume} + R_{air,reactor\ wall} * R_{reactor\ wall,culture\ volume}\big)T_m \qquad (31)$$

$$I_{i,back\ side}(t) = I_{o,back\ side}(t)\big(1 - R_{air,reactor\ wall} - R_{reactor\ wall,culture\ volume} + R_{air,reactor\ wall} * R_{reactor\ wall,culture\ volume}\big)T_m \qquad (32)$$

where, T_m is the factor incorporating the transparency of the medium.

Solar irradiance gradients within the culture volume

Two different light intensities need to be considered while modeling the light gradient inside the culture volume. The first light intensity is a function of height and penetration of diffuse radiation between the parallel plates of the photobioreactor and the second light intensity is the amount of radiation transmitted into the culture volume from the surface of

the reactor wall. For microalgae growth, only the photosynthetic active radiation (PAR) of the spectrum is utilized, which is about 43% [42]**.** The Beer-Lambart Law is used to assess the overall incident gradient in the culture volume.

$$I_{culture\ volume}(y,z,t) = 0.43\left[I_{i,front\ side}(t)e^{-(K1+K2C_x)z} + I_{i,black\ side}(t)e^{-(K1+K2C_x)(d-z)}\right] \quad (33)$$

To simplify the model, $I_{culture\ volume}(y,z,t)$ is integrated to obtain the mean value of irradiance for the entire culture volume ($I_{mean,culture\ volume}$) inside the photobioreactor at time t. Thus,

$$I_{mean,culture\ volume}(t) = \int_0^z \int_0^d I_{culture\ volume}(y,z,t)dydz \quad (34)$$

Heat and Mass Transfer Model for Flat Panel Photobioreactor

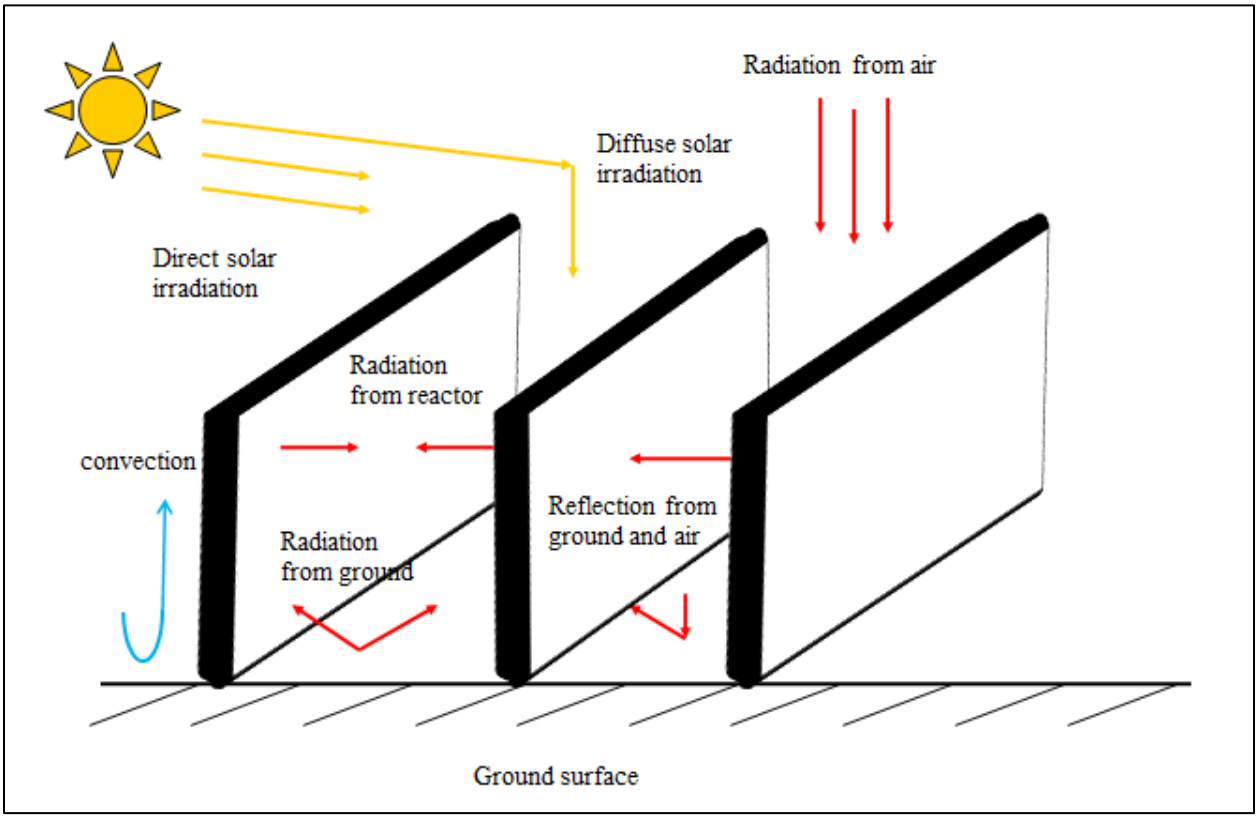

Figure S2. Fluxes considered to develop the combined heat and mass transfer model to quantify reactor temperature [169]

The temperature of the culture medium is determined by the formulating a heat transfer model for the photobioreactors. The governing equation is given by the following equation:

$$\boldsymbol{\rho_{water}} \mathrm{V} \boldsymbol{C_{p_{water}}} \frac{\boldsymbol{dT_{water}}}{\boldsymbol{dt}} = \boldsymbol{Q_{radiation,water}} + \boldsymbol{Q_{radiation,sun}} + \boldsymbol{Q_{radiation,air}} + \boldsymbol{Q_{radiation,ground}} + \boldsymbol{Q_{convection}} + \boldsymbol{Q_{reflection,ground,air}} + \boldsymbol{Q_{reflection,ground,sun}} \quad (35)$$

Where, T_{water} is the dynamic temperature of the culture volume (K), ρ_{water} is the density of water (kg m^{-3}), $C_{p_{water}}$ is the specific heat capacity of water (J kg^{-1} K^{-1}), V is the volume of photobioreactor (m^3), $Q_{radiation,water}$ is the radiation from the reactor surface (W), $Q_{radiation,sun}$ is the total solar radiation on the flat panel photobioreactor (W), $Q_{radiation,air}$ is the radiation from air (W), $Q_{convection}$ is the convective heat transfer from reactor surface (W), and $Q_{conduction}$ is the conductive heat transfer into the reactor.

For simplification, the temperature of the reactor wall and that of the culture volume is assumed identical. Hence, in the present study the different modes of heat transfer from the reactor surface is calculated in terms of the temperature of the culture medium.

Radiation from photobioreactor surface

The radiative heat flux from the reactor surface of the flat panel photobioreactor is computed by the following equation using the Stefen-Boltazmann law [168,240]:

$$Q_{radiation,water} = -2\tau\varepsilon_{water}\sigma S T_{water}^4 \quad (36)$$

where ε_{water} is the water emissivity ($\varepsilon_{water} = 0.97$), σ is the Stefan-Boltzmann constant (W m^{-2} K^{-4}), τ is the transmittance of the reactor wall, and S is the surface area of one side of the photobioreactor (m^2)

Solar irradiance on flat panel photobioreactor

Solar radiative flux received by the photobioreactor is computed on the basis of mean solar irradiance ($I_{mean,culture\ colume}$) on the reactor surface, which comprises of both direct and diffuse radiation. It is given by the following equation:

$$Q_{radiation,sun} = 2\tau I_{mean,culture\ colume} S\left(1 - \varepsilon_{photosynthesis}\right) \quad (37)$$

A part of the total incoming radiation is utilized by microalgae for their growth. This is determined by photosynthetic efficiency, given by $\varepsilon_{photosynthesis}$. The efficiency of photosynthesis in case of outdoor flat panel photobioreactor is assumed to be 3.8% [246].

Radiation from ambient air

The radiative heat flux from air is computed by the following equation:

$$Q_{radiation,air} = 2\tau\varepsilon_{water}\varepsilon_{air}\sigma S T_{air}^4 \quad (38)$$

where ε_{air} is air emissivity (=0.8) [133], T_{air} is the air temperature. Reflection from water is assumed to be negligible in the present study.

Convection from the reactor surface

The convective heat transfer coefficient from the reactor surface is given by the following equation:

$$Q_{convection} = -2h_{convection,air}(T_{water} - T_{air})S \quad (39)$$

Where, the convective heat transfer coefficient ($h_{convection,air}$) between reactor and air is given by the Nusselt number (*Nu*) as obtained in literature [169]

$$h_{convection,air} = \frac{Nu * \lambda_{air}}{L} \quad (40)$$

For flat panel photobioreactors, the characteristic length (L) equals its height (h).

The Nusselt number can be computed by the following equation:

$$Nu = [0.825 + 0.387(Ra * (f(Pr))^{1/6}]^2 \quad (41)$$

The Rayleigh number (Ra) and $f(Pr)$, which is a function of the Prandtl number is determined using the following equations:

$$Ra = \frac{g|T_{water} - T_{air}|L^3}{\alpha_{air}\nu_{air}T_{air}} \quad (42)$$

where, α_{air} is the diffusivity of air, g is the gravitational constant and ν_{air} is the kinematic viscosity of air

$$f(Pr) = [1 + (\frac{0.492}{Pr})^{9/16}]^{-16/9} \quad (43)$$

Reflected solar irradiation from ground

Direct and diffuse radiation reaching the ground surface are being reflected back into the photobioreactor surface. Solar radiation reflected from the ground is computed by the following equation

$$Q_{reflection,ground,sun} = 2\tau r_{ground}\varepsilon_{water}(I_{direct} + I_{diffuse})Sf_{reactor,\ ground} \quad (44)$$

where, r_{ground} is the ground reflectivity, $f_{reactor,ground}$ is the form factor from reactor surface to the ground. Assuming the ground is infinitely large, $f_{reactor,ground}$ is assumed to be 0.5 [168]

Reflected air radiation from ground

Part of the air radiation reaching the ground surface is being reflected back into the panels. The reflected air radiation from the ground is quantified by the equation

$$Q_{reflection,ground,air} = 2\tau r_{ground}\varepsilon_{water}\varepsilon_{air}\sigma ST_{air}^4 f_{reactor,\ ground} \quad (45)$$

Radiation from ground

The temperature of ground (T_g) often reaches high temperature due to varying solar irradiance and the ground radiates heat back to the atmosphere. The amount of radiation from the ground is given by the following equation

$$Q_{radiation,ground} = \tau\varepsilon_{water}\varepsilon_{ground}\sigma {T_g}^4 S \quad (46)$$

Determination of T_g

Heat balance on the surface of the ground is used to evaluate the temperature of the ground **(**T_g) as a function of time [168]:

$$\rho_g C_{p_g} V_g \frac{dT_g}{dt} = \left(Q_{in,g} - Q_{out,g}\right) S_g \quad (47)$$

Since, $\frac{V_g}{S_g} = l_g$ (thickness of the ground layer, since V_g is the ground volume and S_g is the ground surface area) the above equation can be written in the following way:

$$\rho_g C_{p_g} l_g \frac{dT_g}{dt} = \left(Q_{in,g} - Q_{out,g}\right) \quad (48)$$

The different heat fluxes in the above equation can be computed in the following way:

$$Q_{in,g} = \varepsilon_{air}\varepsilon_{ground}\sigma T_{air}^4 + \varepsilon_{ground}\left(I_{direct}(t) + I_{diffuse}(t)\right) \quad (49)$$

$$Q_{out,g} = \varepsilon_{ground}\sigma {T_g}^4 + h_{convection,g}\left(T_g - T_{air}\right) + Q_{conduction,g} \quad (50)$$

The convective heat transfer coefficient between the ground and air, $h_{convection,g}$ can be computed by the following equation, as obtained in literature [168]

$$h_{convection,g} = \lambda_{air}\left(0.664Re_c + 0.037\left({Re_L}^{0.8} - {Re_c}^{0.8}\right)\right)Pr^{0.333} \quad (51)$$

$$Re_c = 5 * 10^5 \quad (52)$$

$$Pr = 0.7 \quad (53)$$

$$Re_L = \frac{\rho_{air} L v_w}{\mu_{air}} \quad (54)$$

where, ρ_{air} is the density of air, the wind velocity is v_w and the viscosity of air is given by μ_{air}.

The conduction from the ground ($Q_{conduction,g}$) is calculated as referenced in [168].

$$Q_{conduction,g} = -k_{ground}\frac{T_g - T_{g,ref}}{l_{conduction,g}} \quad (55)$$

where, $l_{conduction,g} = 0.2$m from literature [168]

The temperature factor (f_T) which affects the specific growth rate of microalgae is given by the following equation as reported in literature [41]:

$$f_T = \left(\frac{T_{lethal} - T_{water}}{T_{lethal} - T_{optimal}}\right)^{\beta_T} \exp\left(-\beta_T\left(\frac{T_{lethal} - T_{water}}{T_{lethal} - T_{optimal}} - 1\right)\right) \quad (56)$$

where, T_{lethal} (°C), $T_{optimal}$ (°C) and T_{water} (°C) are the lethal temperature of microalgae growth, optimal temperature of microalgae growth and water temperature of the culture medium, respectively.

Microalgae growth kinetics model

The following describes a generalized mircoalage growth kinetics model considering various biological processes involved. Following previous studies, *Nannochloropsis sp.* was selected as the suitable algal species for the current work and appropriate growth

kinetics parameters were used [48,131]. The approach presented here can be applied to other microalgal species if relevant growth kinetic parameters are available.

Nitrogen Uptake Modeling

The uptake of nitrogen by the microalgae was computed by solving the following set of equations [48,135]:

$$\frac{dN_{biomass}}{dt} = \left(\frac{N_{calculated\ specific\ uptake\ rate}}{N_{biomass}} - RR_N\right) N_{biomass} = R_{nitrogen\ uptake} \quad (57)$$

where $N_{biomass}$ was the cell quota of nitrogen in algal biomass (kg kg^{-1}), $N_{calculated\ specific\ uptake\ rate}$ was the calculated specific uptake rate of nitrogen (kg kg^{-1} day^{-1}), RR_N was respiration constant of nitrogen (day^{-1}) and $R_{nitrogen\ uptake}$ was the specific uptake rate of nitrogen (day^{-1}). The $N_{calculated\ specific\ uptake\ rate}$ was related to the maximum specific uptake $N_{max\ specific\ uptake\ rate}$ (kg kg^{-1} day^{-1}), uptake of internal nitrogen concentration efficiency ($\eta_{nitrogen,internal}$) and uptake of external nitrogen concentration efficiency ($\eta_{nitrogen,external}$) by the following equation:

$$N_{calculated\ specific\ uptake\ rate} = N_{max\ specific\ uptake\ rate} * \eta_{nitrogen,internal} * \eta_{nitrogen,external} \quad (58)$$

The $\eta_{nitrogen,internal}$ was defined by the following equation where $N_{biomass,minimum}$ was the minimum level of nitrogen present internally below which the cells do not grow (kg/kg).

$$\eta_{nitrogen,internal} = 1 - \frac{N_{biomass,minimum}}{N_{biomass}} \quad (59)$$

The $\eta_{nitrogen,external}$ was treated as a Michaelis-Menten kinetic function and was computed according to the following equation [143,243,244]:

$$\eta_{nitrogen,external} = \frac{N_{medium}}{N_{medium} + HSC_{nitrogen\ uptake}} \quad (60)$$

where N_{medium} was the concentration of nitrogen in the medium (kg m^{-3}) and $HSC_{nitrogen\ uptake}$ was the half-saturation constant of uptake of nitrogen (kg m^{-3}).

Phosphorus Uptake Modeling

The uptake of phosphorus by the microalgae was evaluated similarly to the nitrogen uptake. The governing equations are as follows:

$$\frac{dP_{biomass}}{dt} = \left(\frac{P_{calculated\ specific\ uptake\ rate}}{P_{biomass}} - RR_P\right) P_{biomass} = R_{phosphorus\ uptake} \quad (61)$$

where $P_{biomass}$ was the cell quota of nitrogen in algal biomass (kg kg^{-1}), $P_{calculated\ specific\ uptake\ rate}$ was the calculated specific uptake rate of nitrogen (kg kg^{-1} day^{-1}), RR_P was respiration constant of nitrogen (day^{-1}) and $R_{phosphorus\ uptake}$ was the specific uptake rate of nitrogen (day^{-1}). The $P_{calculated\ specific\ uptake\ rate}$ was related to the maximum specific uptake $P_{max\ specific\ uptake\ rate}$ (kg kg^{-1} day^{-1}), uptake of internal nitrogen concentration efficiency ($\eta_{phosphorus,internal}$) and uptake of external nitrogen concentration efficiency ($\eta_{phosphorus,external}$) by the following equation:

$$P_{calculated\ specific\ uptake\ rate} = P_{max\ specific\ uptake\ rate} * \eta_{phosphorus,internal} * \eta_{phosphorus,\ external} \quad (62)$$

The $\eta_{phosphorus,internal}$ was defined by the following equation where $P_{biomass,minimum}$ was the minimum level of nitrogen present internally below which the cells do not grow (kg kg^{-1}).

$$\eta_{phosphorus,internal} = 1 - \frac{P_{biomass,minimum}}{P_{biomass}} \quad (63)$$

The $\eta_{phosphorous,external}$ was treated as a Michaelis-Menten kinetics function and was computed according to the following equation:

$$\eta_{phosphorus,\ external} = \frac{P_{medium}}{P_{medium}+HSC_{phosphorus\ uptake}} \qquad (64)$$

where P_{medium} was phosphorous concentration in the medium (kg m^{-3}) and $HSC_{phosphorous\ uptake}$ was the half-saturation constant of uptake of phosphorous (kg m^{-3}).

Carbon dioxide uptake modeling

The transfer and uptake of CO_2 by microalgae is a complex process and was modeled by coupling of two separate phenomena, CO_2 transfer by sparging from gas phase to liquid phase (bulk culture medium) and uptake by microalgae during the growth phase. The following set of equations describing carbon dioxide uptake used in the model was obtained from literature [130,134,135,141].

CO_2 transfer from gas phase to bulk culture medium

The mass transfer of CO_2 from the sparging phase to the bulk culture medium was obtained by solving the following equations as obtained in literature [134–136].

An elemental height dz of the reactor depth was assumed and transfer of CO_2 within the element was expressed by the following equation:

$$\frac{d}{dt}\left[\left(\frac{p\varepsilon_{gas\ holdup}A_{cs}dz}{RT_{water}}\right)y\right] = M_{in} - M_{out} - dM_t$$

$$= G_{molar\ flow}y - G_{molar\ flow}(y+dy) - dM_t \qquad (65)$$

The rate of transfer of CO_2 from the gas phase to the bulk culture medium (dM_t) was estimated by the following equation:

$$dM_t = K_{CO2}(1 - \varepsilon_{gas\ holdup})A_{cs}(C_{CO_2}{}^{*} - C_{CO2,dissolved})dz \qquad (66)$$

where, K_{CO2} was the mass transfer coefficient from the gas phase to the liquid phase, and ${C_{CO2}}^*$ was the concentration of dissolved CO_2 in the liquid phase which was in equilibrium with the concentration of CO_2 in the gas phase. K_{CO2} was estimated by the following equation:

$$\frac{K_{CO2}}{K_{O2}} = \sqrt{\frac{D_{CO2}}{D_{O2}}} \qquad (67)$$

As the residence times of the gas in the culture medium was small, pseudo steady state conditions were assumed. Thus, the following equation was obtained by combining equation the above equations:

$$\frac{dy}{dz} = -\left(\frac{K_{CO2}\left(1 - \varepsilon_{gas\ holdup}\right)A_{cs}}{G_{molar\ flow}}\right)\left({C_{CO2}}^* - C_{CO2,dissolved}\right) \qquad (68)$$

The saturation concentration of CO_2 (${C_{CO2}}^*$) was computed using Henry's Law according to the following:

$${C_{CO2}}^* = \frac{py}{RT_{water}H} \qquad (69)$$

where, H was the Henry's constant and p was the partial pressure of CO_2 in the atmosphere.

Combining equations 68 and 69 and then integrating within the proper limits, the following equation was obtained:

$$y_{out} = \frac{RT_{water}H}{p}\left(C_{CO2,dissolved} + \left(\frac{y_{in}p}{RT_{water}H} - C_{CO2,dissolved}\right)\exp\left(\frac{-K_{CO2}\left(1-\varepsilon_{gas\ holdup}\right)A_{cs}z*p*1000}{G_{molar\ flow}RT_{water}H}\right)\right) \qquad (70)$$

Thus, the moles of CO_2 transferred from the gas phase to the culture medium ($M_{CO2,transfer}$) was given by the following equation:

$$M_{CO2,transfer} = G_{molar\ flow}(y_{in} - y_{out}) = G_{molar\ flow}(y_{in} - \frac{RT_{water}H}{p}(C_{CO2,dissolved} +$$

$$(\frac{y_{in}p}{RT_{water}H} - C_{CO2,dissolved})\exp(\frac{-K_{CO2}(1-\varepsilon_{gas\ holdup})A_{cs}z*p*1000}{G_{molar\ flow}RT_{water}H}))) \quad (71)$$

Uptake of Carbon by microalgae

The bio uptake of carbon by microalgae during the growth phase was modeled using an approach described in the literature [134,136]. The dissociation of CO_2 in water was given by the following equations:

$$CO_{2,gas} + H_2O \leftrightarrow H_2CO_3{}^* \overset{K_1}{\Leftrightarrow} HCO_3{}^- + H^+ \quad (72)$$

$$HCO_3{}^- \overset{K_2}{\Leftrightarrow} CO_3{}^{2-} + H^+ \quad (73)$$

where, K_1 and K_2 were the dissociation constants of $H_2CO_3{}^*$ and HCO_3 respectively. The total dissolved concentration of carbon in the medium could be obtained by adding the concentration of [H_2CO_3], [$HCO_3{}^-$], and [$CO_3{}^{2-}$], respectively. Several studies considered the total dissolved concentration of carbon species in water to determine the carbon uptake by microalgae [130,134]. In this study, it was assumed that the pH of the solution was between 7.67-6.83 where the dominant species was bicarbonate [136]. Thus, the bio uptake of carbon by microalgae was assumed to take place only in the form of bicarbonate and the concentration of dissolved CO_2 ($C_{CO2,dissolved}$) was essentially the concentration of bicarbonate in the solution.

Assuming that the culture medium was thoroughly mixed, molar balance of dissolved carbon in the culture medium provided the following equation:

$$(1 - \varepsilon_{gas\ holdup})V\frac{dC_{CO2,dissolved}}{dt} = M_{CO2,transfer} - M_{carbon\ uptake,algae} \quad (74)$$

The carbon uptake rate by microalgae ($M_{carbon\ uptake,algae}$) was estimated utilizing the following equation:

$$M_{carbon\ uptake,algae} = \left(1 - \varepsilon_{gas\ holdup}\right)V\left(\frac{1}{Y_{algae}}\right)\left(\frac{dX}{dt}\right)\left(\frac{1}{MW_{bicarbonate\ ion}}\right) \quad (75)$$

Thus, combining the above equations, the main governing equation was obtained as follows:

$$\left(1 - \varepsilon_{gas\ holdup}\right)V\frac{dC_{CO2,dissolved}}{dt} = G_{molar\ flow}\left(y_{in} - \frac{RT_{water}H}{p}\left(C_{CO2,dissolved} + \left(\frac{y_{in}p}{RT_{water}H} - C_{CO2,dissolved}\right)\exp\left(\frac{-K_{CO2}\left(1-\varepsilon_{gas\ holdup}\right)A_{cs}z*p*1000}{G_{molar\ flow}RT_{water}H}\right)\right)\right) - \left(1 - \varepsilon_{gas\ holdup}\right)V\left(\frac{1}{Y_{algae}}\right)\left(\frac{dX}{dt}\right)\left(\frac{1}{MW_{bicarbonate\ ion}}\right) \quad (76)$$

Modeling carbon uptake by microalgae in the growth phase was provided in greater detail in literature [130,134–136,141].